GEOLOGICAL SURVEY OF CANADA
OPEN FILE 7142

Assessment of Telluric Activity in the Area of Proposed Alaska Highway Pipeline

L. Trichtchenko, P. Fernberg and M. Harrison

2012

Natural Resources Canada | Ressources naturelles Canada

Canada

GEOLOGICAL SURVEY OF CANADA
OPEN FILE 7142

Assessment of Telluric Activity in the Area of Proposed Alaska Highway Pipeline

L. Trichtchenko, P. Fernberg and M. Harrison

2012

doi:10.4095/291561

This publication is available from the Geological Survey of Canada Bookstore (http://gsc.nrcan.gc.ca/bookstore_e.php).
It can also be downloaded free of charge from GeoPub (http://geopub.nrcan.gc.ca/).

Recommended citation:
Trichtchenko, L., Fernberg, P., and Harrison, M., 2012. Assessment of Telluric Activity in the Area of Proposed Alaska Highway Pipeline, Geological Survey of Canada, Open File 7142, 111 p. doi:10.4095/291561

Publications in this series have not been edited; they are released as submitted by the authors.

For more information related to this document please contact

Larisa Trichtchenko
Research Scientist
Geomagnetic Laboratory
2617 Anderson Road
Ottawa, ON
K1A 0E7

Tel: 613-837-9452
Fax: 613-824-9803
Email: ltrichtc@nrcan.gc.ca

Table of Contents

E. Executive Summary …….. E1
Introduction …… E2
Geomagnetic Climatology…….. E3
Earth Resistivity…….. E4
Telluric Electric Fields …….. E6
Telluric Activity Assessment ……..... E8
Possible Application to Cathodic Protection Design……. E8
Chapter 1 Causes of Enhanced Telluric Activity…..……..…… 1.0
1.0 Introduction…….. 1.0
1.1 Sun-Earth Connections…. 1.1
1.2 Geomagnetic Induction in Pipelines…. 1.3
1.3 Proposed Pipeline Route…… 1.4
Chapter 2 Geomagnetic Climatology…….. 2.1
2.1 Introduction…… 2.3
2.2 Geomagnetic Data…….. 2.2
2.3. Geomagnetic Variations in Pipeline Area…… 2.4
2.4 Statistical Properties of Geomagnetic Variations for 1995-2007…….. 2.8
Chapter 3 Review of Earth Resistivity Structure…… 3.1
3.1 Introduction…… 3.1
3.2 Physical and Geological Settings along the Pipeline Route…….. 3.7
3.3 One-Dimensional Resistivity Models along the Pipeline Route..……..... 3.15
3.4 References…….. 3.28
Appendix Tables A 3.1-A-3.8…… A1
Table A3.1…… A1
Table A3.2…… A3
Table A3.3…… A5
Table A3.4…… A7
Table A3.5…… A11
Table A3.6…… A13
Table A3.7…… A15
Table A3.8…… A17
Chapter 4 Assessment of Telluric Activity…….. 4.1
4.1 Introduction……... 4.1
4.2 Theoretical Background…… 4.2
4.3 Surface Impedance Models……..... 4.5
4.4 Daily Variations of Geo-Electric Field…….. 4.7
4.5 Indices of Telluric Activity…… 4.19
4.6 Statistical Properties of the Geo-electric Field Variations…… 4.20
4.7 Long-Term (solar cycle) Variations of Telluric Activity……... 4.22
4.8 Possible Application to Cathodic Protection Design……. 4.26
4.9. Conclusions and References…… 4.27

Executive Summary

Introduction

The proposed Alaska Highway gas pipeline is more vulnerable to telluric effects because of its position in the auroral zone (Figure E.1). In this region the strong geomagnetic activity associated with the aurora means that northern pipelines experience larger telluric currents compared to those further south.

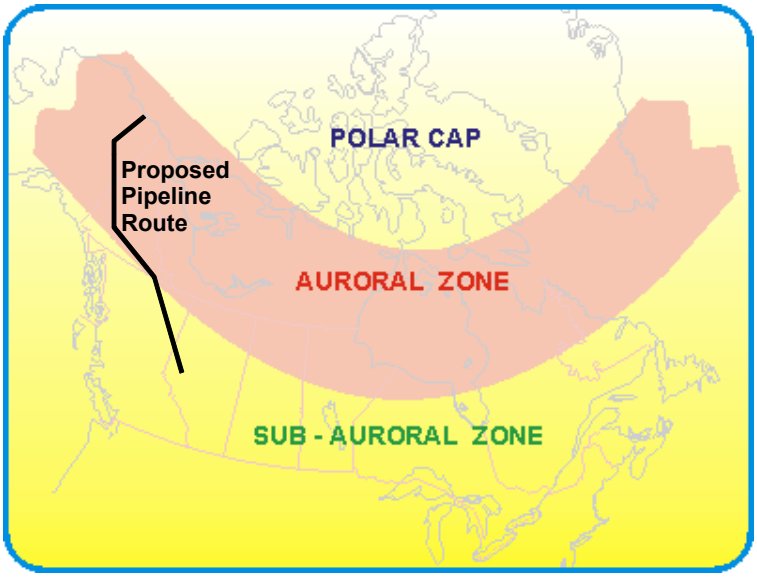

Figure E.1. Position of pipeline in the auroral zone.

Construction of the Trans-Alaska Pipeline in the 1970s prompted increased research on telluric effects on northern pipelines. Since then our understanding of the factors affecting telluric effects on pipelines has increased considerably and can be used to make a comprehensive assessment of the telluric hazard to the Alaska Highway pipeline.

This study uses data from magnetic observatories in Alaska and northern Canada to determine the occurrence of geomagnetic activity in these regions. A review of geological information has been made and used to produce 1D Earth resistivity models for 8 zones along the pipeline route. These models were then used with the geomagnetic field data to determine the telluric electric fields that would be experienced by the pipeline. The statistical analysis on the occurrence of telluric activity have been done which may be used for cathodic protection design to properly withstand the higher telluric activity of the Alaska area

Geomagnetic Climatology

To determine the occurrence of geomagnetic activity in the regions crossed by the pipeline route, data from the Alaska and Canadian magnetic observatories: Barrow (BRW), College (CMO), Sitka (SIT), Yellowknife (YKC) and Meanook (MEA) were used. Data from the Ottawa magnetic observatory (OTT) were also used to provide a comparison with activity at a mid-latitude site away from the auroral zone.

A statistical analysis was made of 33 years of data from 1975 to 2007. The evaluation of the geomagnetic activity was based on the hourly range (HRX, HRY, HRZ) of the northwards (X), eastward (Y), and vertical (Z) geomagnetic field components. Figure E.2. shows that the average percentage of hours during which the range value, HRX, exceeded 40nT varies from about 15% at Sitka to about 30% at Meanook, ~50% at College , ~60% at Yellowknife and up to ~80% at Barrow. Extreme geomagnetic activity above the level of 600 nT occurred about 0.3% of the time at Sitka (~1 day/year) and up to 3% of the time (~11 days/year) at Barrow.

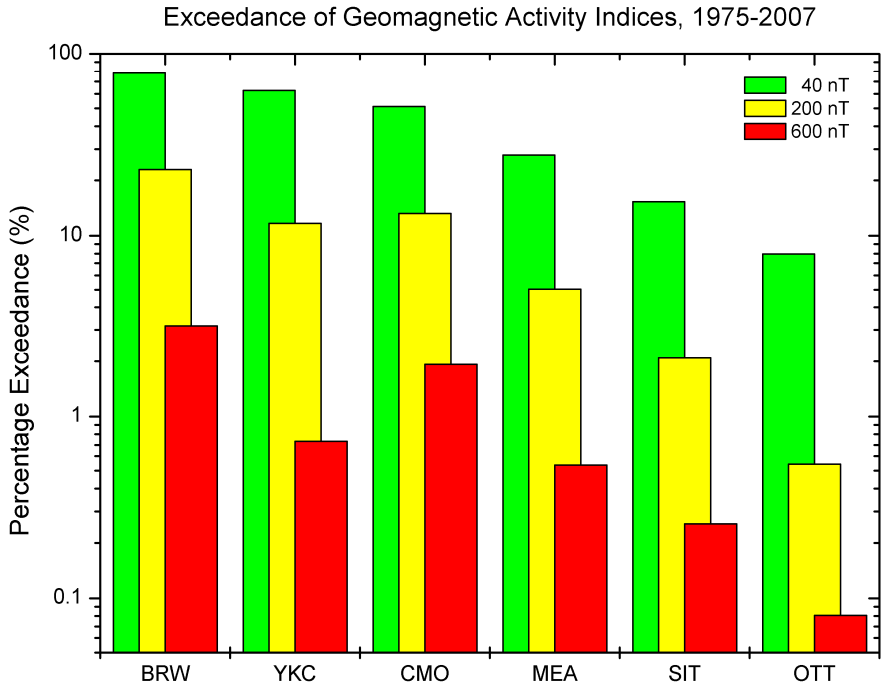

Figure E.2. Occurrence of geomagnetic activity in the vicinity of the pipeline. Results for Ottawa show mid-latitude activitv levels.

Figures E.3 and E.4 show examples of the distribution of geomagnetic activity throughout a year (in this example, 2004). The strongest activity occurred during major magnetic storms on July 24-28 and November 8-11. However there was plenty of magnetic activity throughout the year. Considerable magnetic activity occurred during all years studied and did not show the variation with the 11-year solar cycle seen at lower latitudes.

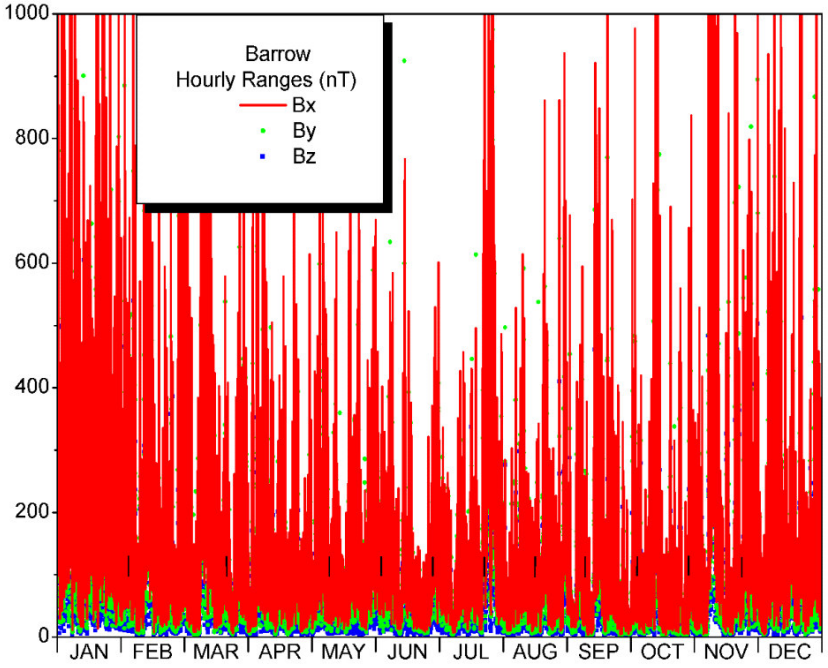

Figure E.3. Geomagnetic activity at Barrow in 2004.

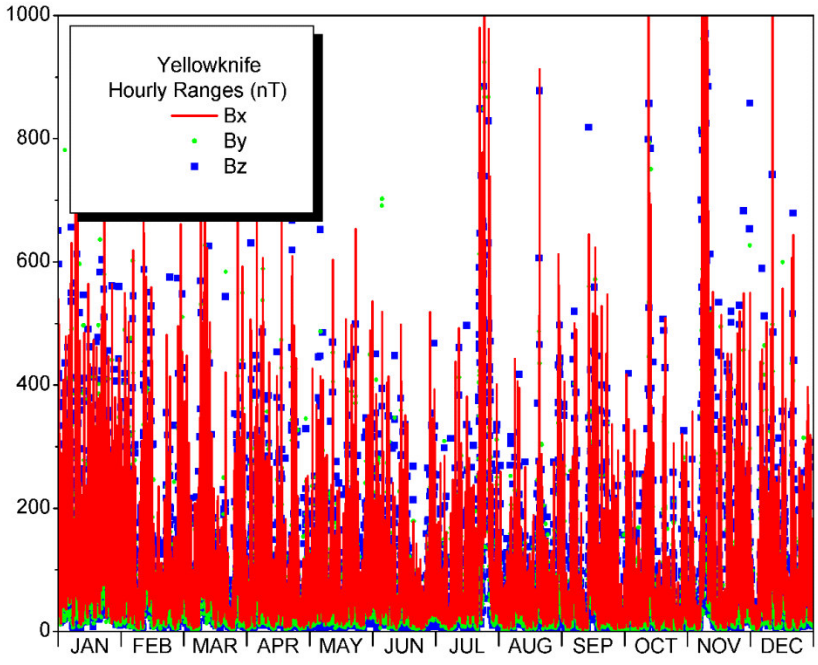

Figure E.4 Geomagnetic activity at Yellowknife during 2004.

Earth Resistivity

The size of the telluric electric fields produced by geomagnetic disturbances depends on the Earth resistivity down to the depth of penetration of the geomagnetic disturbances. We are concerned with geomagnetic field variations with periods from minutes to hours with penetration depths ranging from a few kilometres to hundreds of kilometres. Thus we need information about the resistivity, not just of the surface rock layers but also deeper into the Earth.

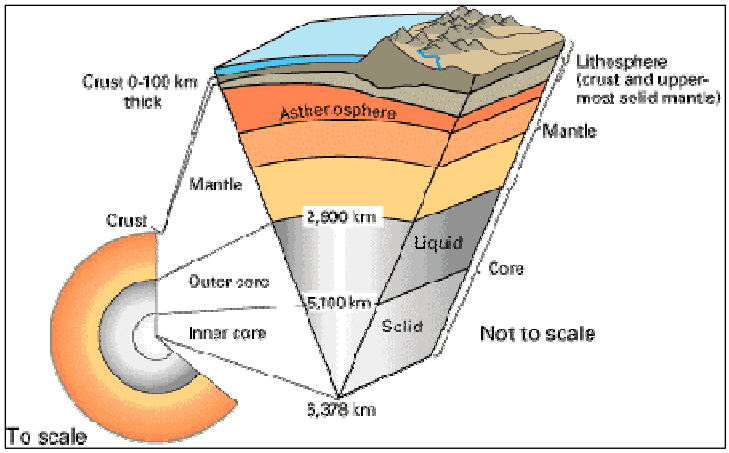

Figure E.5. Earth's internal structure

On the large scale, Earth's interior structure is divisible into four main layers: crust, mantle, outer core, and inner core (Figure E.5). Each layer can be further subdivided based on unique physical differences. The outermost, thin, rigid crust is underlain by the dense, hot layer of semi-solid rock of the mantle. Changes with depth of temperature and pressure, changes to abundance and distribution of conductive minerals, and pore volume and fluid composition all change the resistivity, going from higher resistivities in the crust to low resistivity in the mantle.

At the Earth's surface the pipeline route crosses a variety of structural features from flat sedimentary layers to the folded rock layers in the mountain belts. For our analysis of the earth resistivity structure we have divided the pipeline route into 8 zones (see Figure E.6). Zone 1 consists of the sedimentary basin around Prudhoe Bay. Zone 2 is the Brooks Range mountains. Zones 3, 4 and 5 cover the central and southeastern region of Alaska, with Zones 3 and 5 containing more resistive rocks. Zone 6 comprises much of southern Yukon. Zone 7 is the mountain belt in northeastern British Columbia. Zone 8 is part of the Western Canada Sedimentary Basin that covers most of the Canadian prairies.

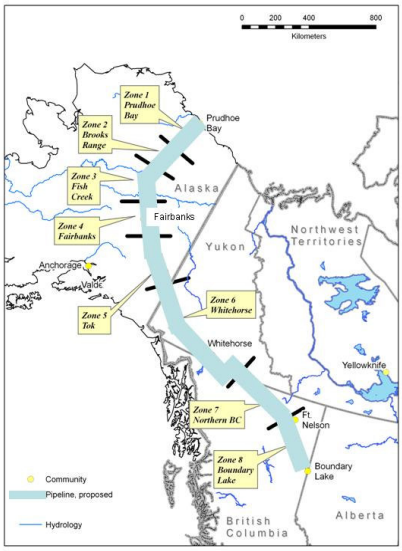

Figure E.6. Earth resistivity zones along the pipeline route

To determine the resistivities in each zone an extensive review was made of publically-available information, including government geological reports and maps, on-line resources, soil-engineering studies of the Trans-Alaska Pipeline, and scientific journals. Where they were available, petroleum exploration well measurements provide resistivity values for the near surface rocks, while magnetotelluric surveys provide remote sensing of the resistivities of the deeper layers. In other areas the geologic structure and knowledge about typical rock resistivities was used to provide resistivity values. These were used to determine one-dimensional (i.e variation only with depth) models of the Earth resistivity for each zone (Figure E.7).

Comparison of the models shows that there are significant differences in the resistivities of the crust in the different zones. There is also a major difference with Zones 1 and 8 compared to the other zones, in that these two zones have a sedimentary basin layer which gives lower resistivity at shallower depths.

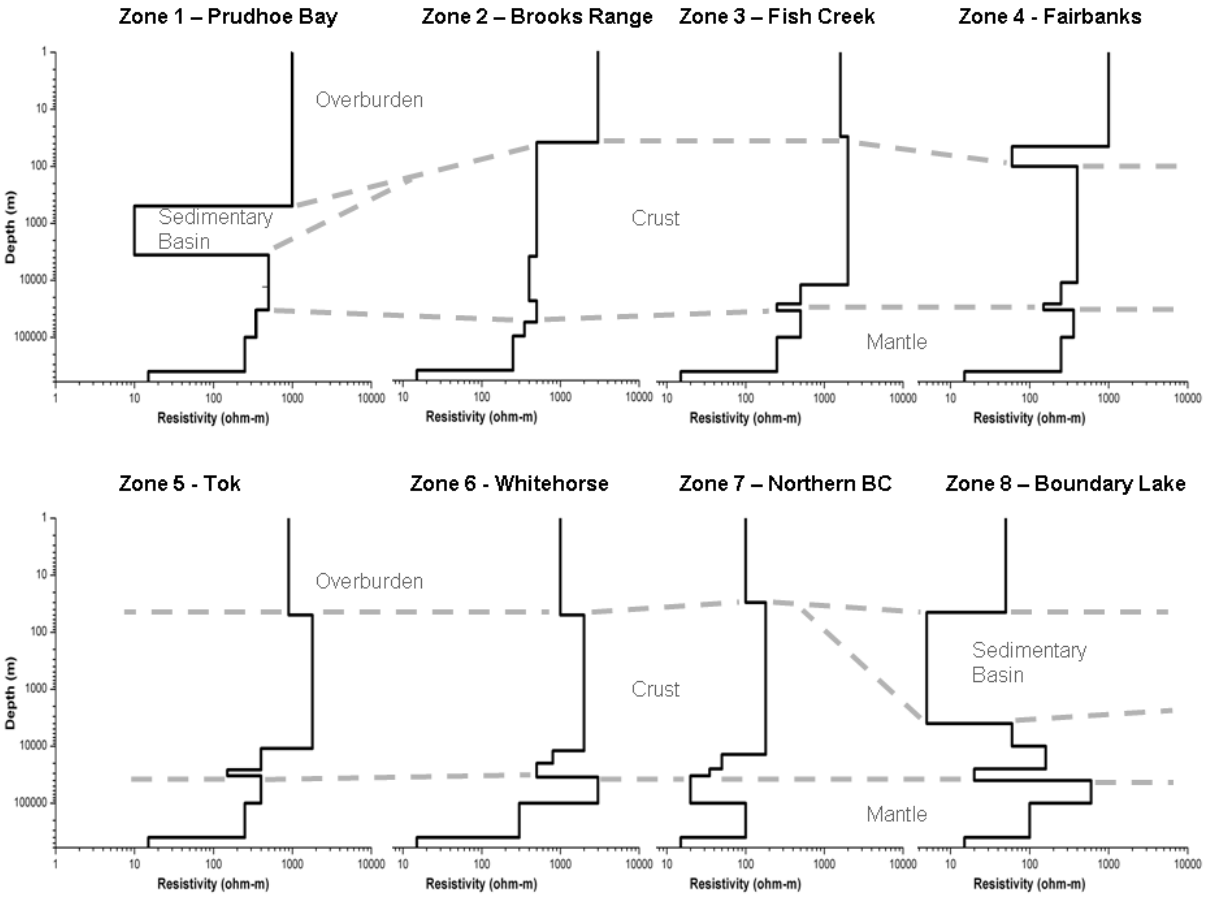

Figure E.7. 1-D resistivity models for the eight zones along the pipeline route. Note the use of logarithmic scales on the axes

Telluric Electric Fields

The 1-D resistivity models for the different zones were used to determine the "surface impedance" for the eight zones along the pipeline route (Figure E.8). The surface impedance represents the transfer function between geomagnetic variations and geo-electric (telluric) field at the Earth's surface. To calculate electric fields we use recordings of the magnetic field and the surface impedance. As the surface impedance varies with frequency it is easier to transform the magnetic data to the frequency domain, multiply by the surface impedance to obtain the electric field spectrum and then use an inverse transform to obtain the electric field in the time domain (Figure E.9). Calculations were made of the northwards and eastwards components of the electric field. An example of the electric fields calculated for a storm day (November 8, 2004) are shown in Figure E.10. This shows that the largest electric fields, on that day, occurred in zones 2 to 6.

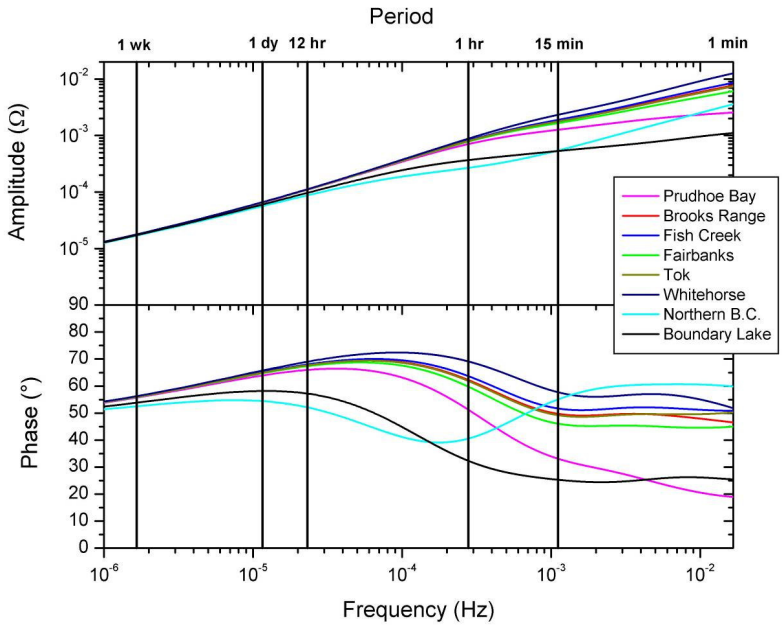

Figure E.8 Surface impedances for each zone

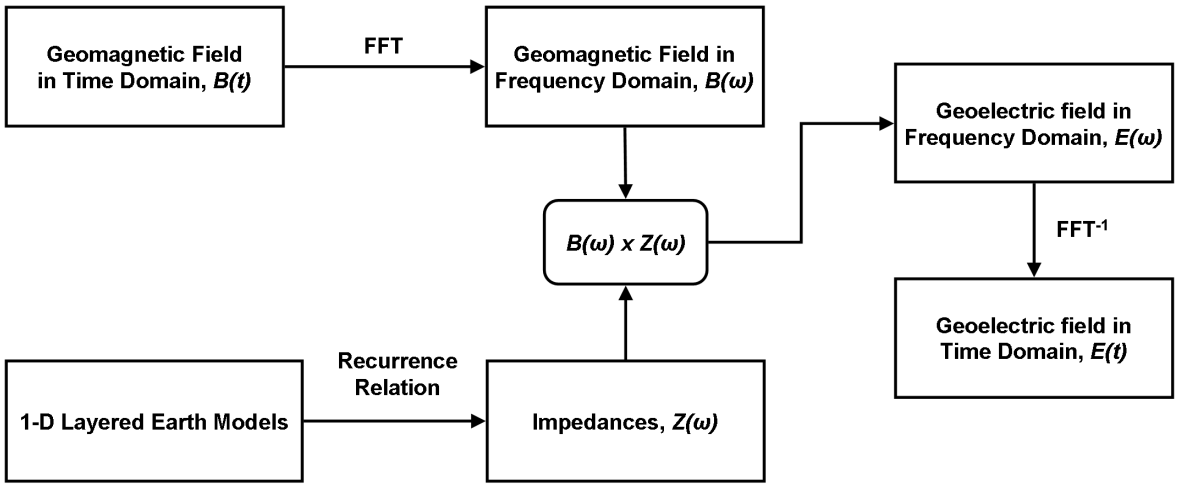

Figure E.9 Schematic for calculation of electric fields

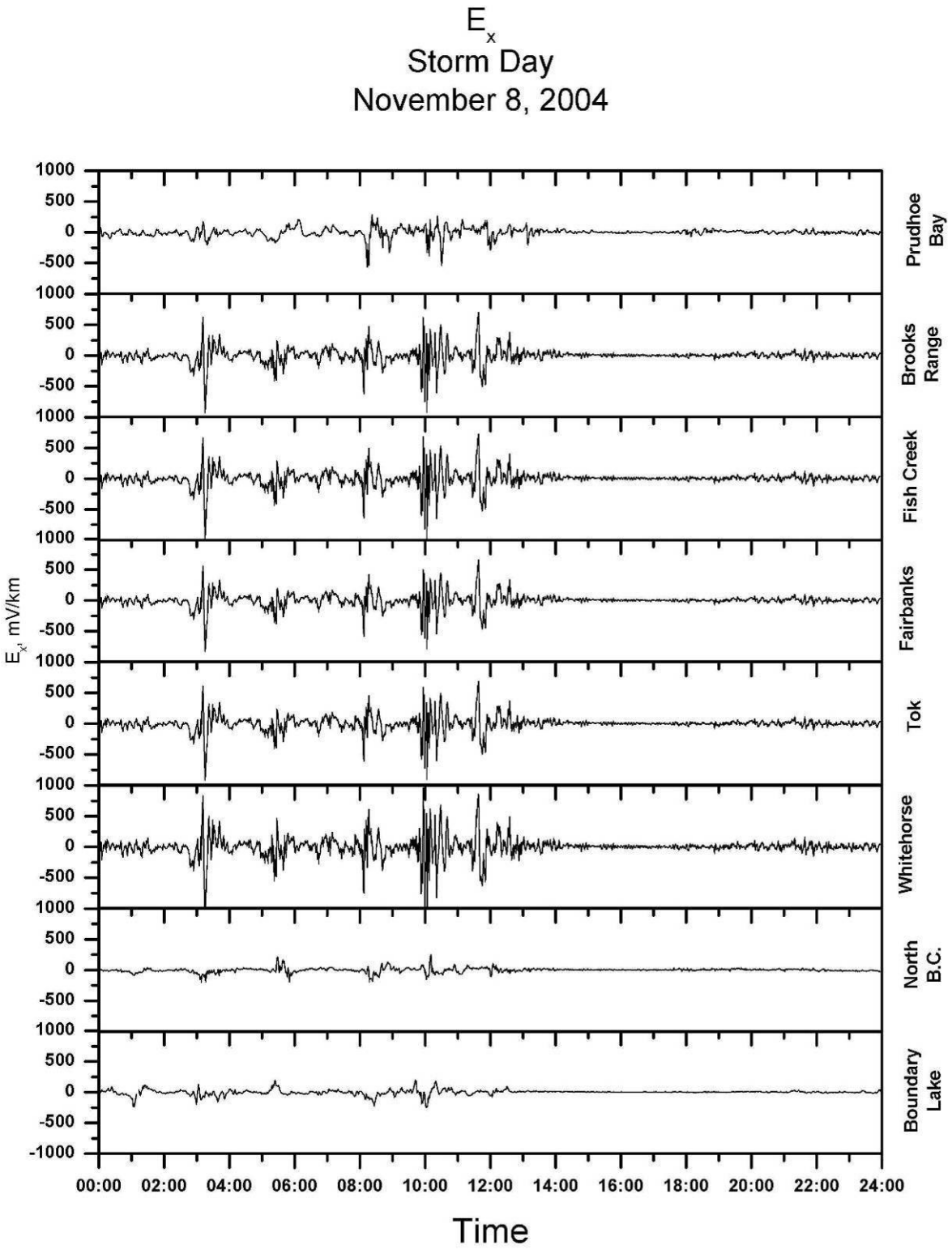

Figure E.10 Electric fields calculated using the 1-D models

Telluric Activity Assessment

The route of the planned Alaska Highway pipeline lies in the auroral zone where geomagnetic activity is higher so making the pipeline more at risk from telluric current activity. To assess the risk from telluric activity we have considered (1) the occurrence of geomagnetic activity, (2) the Earth resistivity structure and were used to determine the statistical occurrences of the different levels of telluric activity along the pipeline route.

Geomagnetic activity is more frequent at the Prudhoe Bay end of the pipeline, so that even on days characterised as "quiet" at stations further south, Prudhoe Bay still experienced significant magnetic activity. During disturbed times the geomagnetic activity expands southward to encompass the entire pipeline.

Electric fields produced by the geomagnetic variations are dependent on the Earth resistivity from the surface down into the crust and mantle, with higher resistivities leading to larger electric fields. The sedimentary basins at the northern and southern ends of the pipeline route have lower resistivitiy than elsewhere and this gives lower electric fields than on other parts of the route.

Possible Application to Cathodic Protection Design

The effect of electric fields induced in pipelines can be modelled using distributed-source transmission line (DSTL) theory. This was first used for modelling AC induction in pipelines and was subsequently applied to geomagnetic induction in pipelines. In the DSTL approach the pipeline is represented by a transmission line with a series impedance, *Z*, given by the resistance of the pipeline steel and a parallel conductance, *Y*, given by the conductance through the pipeline coating. The induced electric field is represented by voltage sources distributed along the transmission line (Figure E.11). The modelling can include multiple pipeline sections connected together. Each pipeline section can have different material characteristics, pipeline direction and size of electric field. This enables model calculations to be made for realistic pipelines including features such as bends, insulating flanges and ground connections.

Assuming the pipeline is “electrically

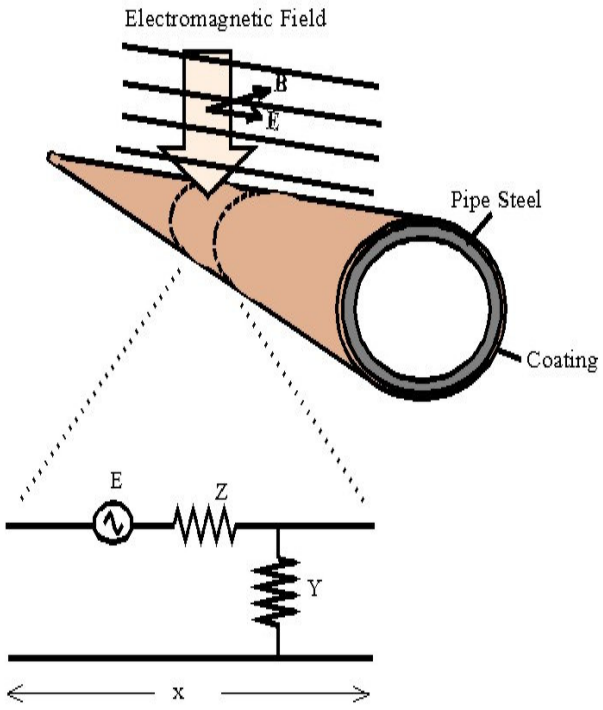

Figure E.11 Transmission line model of pipeline including distributed voltage sources representing induced electric field.

long", and is running in the east-west direction (i.e. $E_p=E_y$), the terminating impedances are the same at both ends and equals Z_T, for any end of the pipeline (at $x=x_1$ or $x=x_2$) and using typical values for pipelines parameters as $1/\gamma$=60 km, Z_c=1.67 Ohms, Z_T =0.1 Ohms, the estimation of pipe-to-soil variations for cathodic design considerations can be done as (see Chapter 4 for details)

$$PSP_T(mV) = 3.4(km) \cdot E_y(mV/km) \tag{E1}$$

Thus, Fig E.2 can also present the statistics of the hourly maximum PSP with following changes: the low level of telluric activity of 20 mV/km is equivalent to hourly maximum PSP of 0.068 V; medium level of 160mV/km is equivalent to 0.544 V and high level of 420 mV/km is equivalent to1.428 V.

It can be estimated now, that if pipeline has a life time is 60 years, then in "active" zone PSP will exceed 544 mV during10% of this time, i.e. 6 years.

The analysis of more than 30 years of data from geomagnetic observatories in Alaska and Northern Canada shows that geomagnetic activity in the area of proposed pipeline is 80% higher than in southern locations. Thus, estimation of telluric activity in the area has been done to further clarify the effects the effects which might be not significant in lower latitudes. In order to do that, telluric activity indices and levels were statistically established. Results of analysis show that as in the case of the geomagnetic activity, 80% of the time telluric activity in the pipeline area is above "normal" level. In regard to PSP evaluations, the simplified approach shows how developed assessment can be used for estimation of PSP variations for design considerations.

Proper estimation of the telluric current effects on pipelines corrosion protection system will improve the design considerations for new pipelines in the Northern areas and operations of the corrosion protection systems for existing pipelines.

Chapter 1 Causes of Enhanced Telluric Activity

1. Introduction

A natural gas pipeline is proposed to extend from Prudhoe Bay in Alaska to Boundary Lake on the British Columbia / Alberta provincial boundary, a distance of 2760 km (1715 miles). (http://www.emc.gov.yk.ca/oilandgas/ahpp.html), continuing from the international border the pipeline route runs parallel to most of the Alaska Highway.
The location of the proposed pipeline means that it will be exposed to large geomagnetic disturbance more frequently than at lower latitudes in Canada and USA. The geomagnetic field variations induce electric fields in the Earth and in electrical conductors at the Earth's surface such as pipelines. These "telluric" electric currents produce variations in pipe-to-soil potential causing problems for pipeline monitoring and reducing the effectiveness of the cathodic protection.

To make a complete assessment of the impact of telluric currents on a pipeline it is necessary to determine the rate of occurrence of geomagnetic disturbances, review the information on Earth conductivity structure and use this to calculate the telluric electric fields that would be produced. We have compiled statistics on the occurrence of the different telluric electric field levels along the pipeline route. Produced estimations can serve as an input to the numerical simulation of the pipeline with regard to design of cathodic protection system.

The detailed work to assess the telluric impact on the proposed pipeline is described in the following chapters. In the rest of the Introduction some more background information about the Sun-Earth connection that leads to geomagnetic activity, the process of geomagnetic induction in pipelines, and the relation of the pipeline route to the zone of increased telluric activity associated with the aurora is provided.

1.1. Sun - Earth Connection

The geomagnetic and telluric activity on the Earth originates from activity on the Sun. One of the principle indicators of activity on the Sun is the number of sunspots. Daily counts of the sunspots have been made for many years and their number shows a cycle with a period of approximately 11 years (Figure 1.1). Figure 1.2 shows examples of solar images taken near the maximum of the solar cycle and near the minimum of the solar cycle.

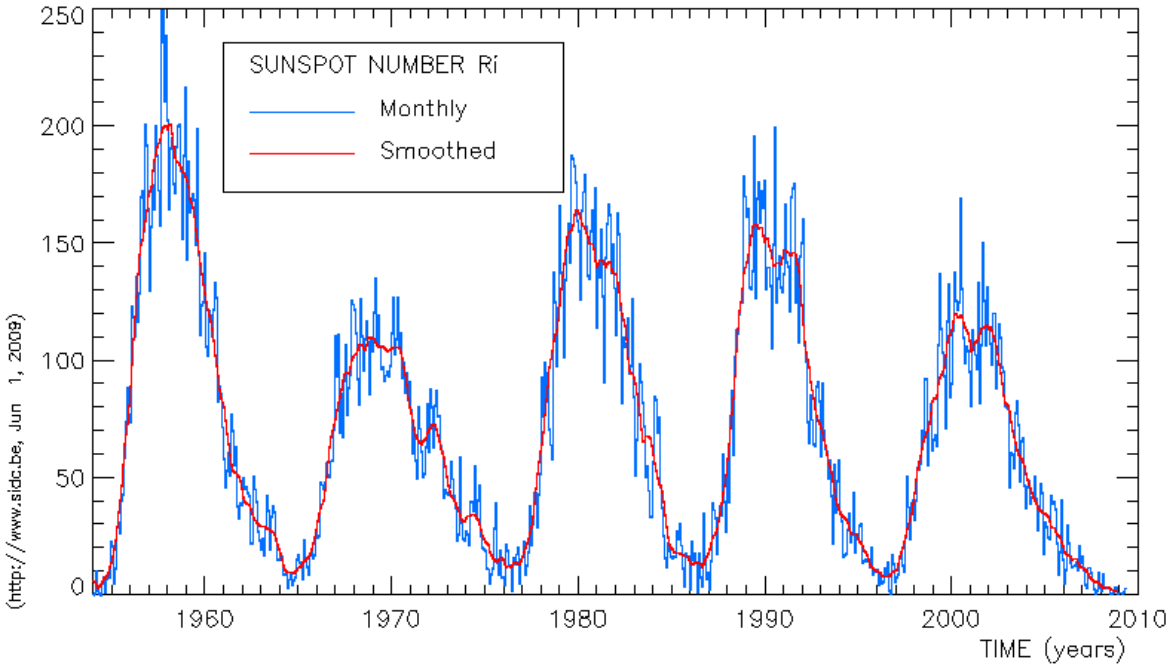

Figure 1.1. The 11-year cycle in the number of sunspots

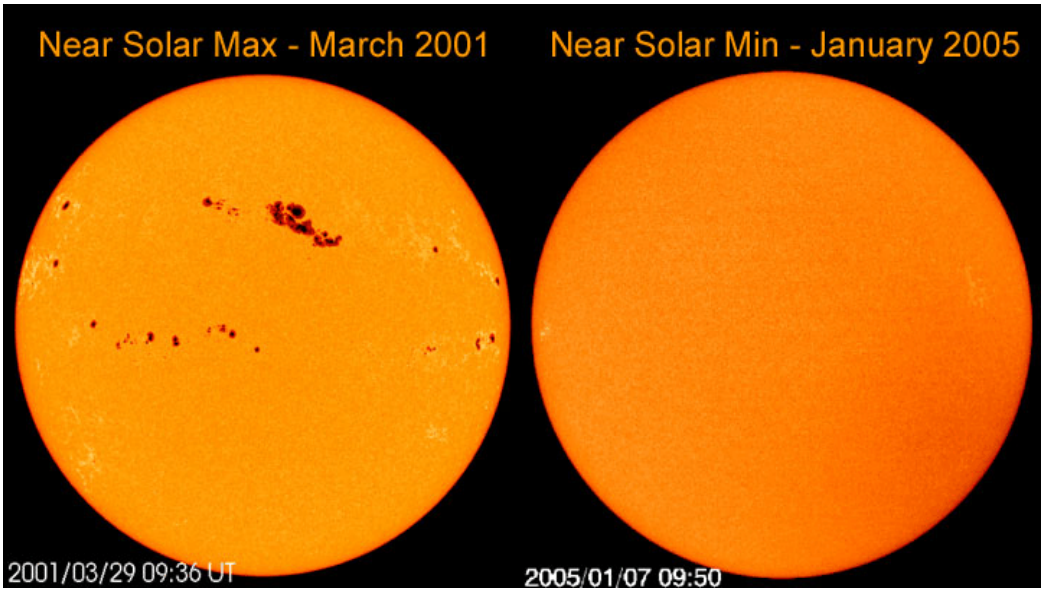

Figure 1.2. Examples of solar images showing sunspots at solar maximum and the absence of sunspots at solar minimum.

The Sun constantly radiates particles out into space. This "solar wind" compresses the Earth`s magnetic field on the day-side and draws it out into a tail on the night-side forming a region, the magnetosphere, where the geomagnetic field shields the Earth from the solar particles (Figure 1.3). However, solar particles can penetrate this shield in a narrow region around the magnetic poles. The particles are guided down the magnetic field lines into the upper atmosphere where they create the aurora (northern lights). The aurora occurs in a ring around the geomagnetic pole as shown by the images from the Polar satellite (Figure 1.4). During quiet times the auroral oval contracts as shown in Figure 1.4a but during disturbed times the auoral oval expands as shown in

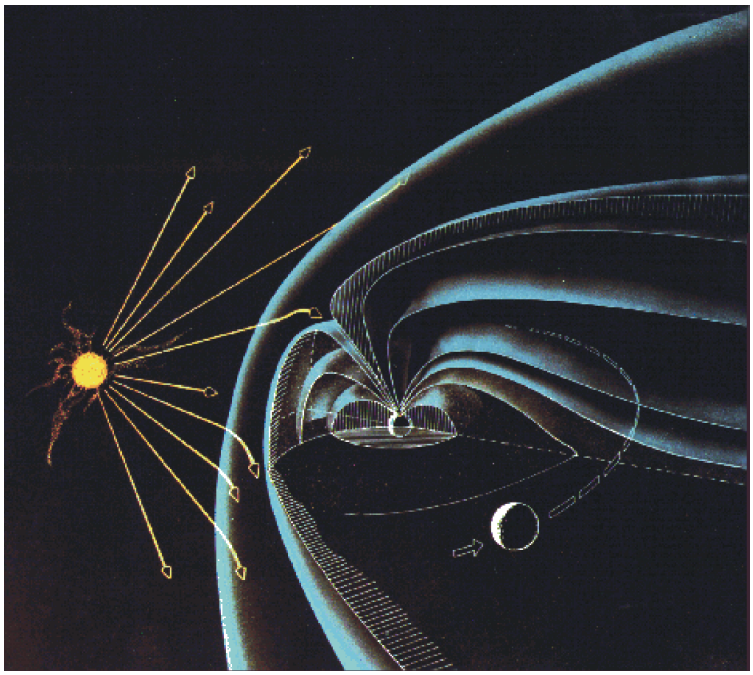

Figure 1.3. Interaction of the Solar Wind with the Earth`s Magnetosphere

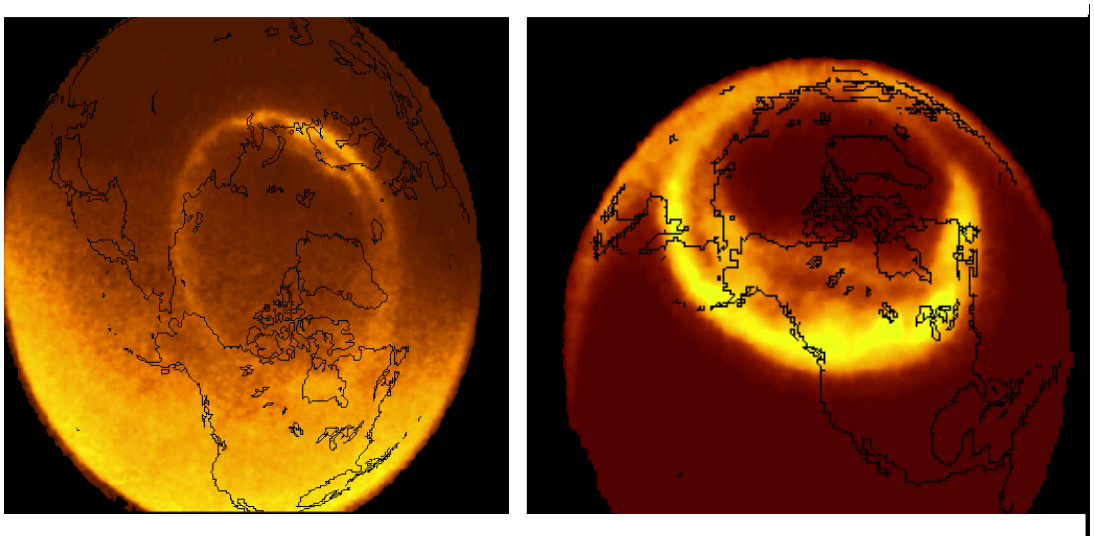

Figure 1.4 Images of the aurora taken from the Polar satellite during (a) quiet times (b) active times.

1.2. Geomagnetic Induction in Pipelines

Strong electric currents in the ionosphere, called the auroral electrojets, accompany the aurora The magnetic disturbances observed at high latitudes are the magnetic fields produced by these auroral electrojets. The variations of the magnetic field, in turn, induce electric currents in the Earth and in long conductors such as pipelines. These telluric currents have been an ongoing problem for engineers setting up cathodic protection systems and the variations in pipe-to-soil potential (PSP) produced by telluric currents often make pipeline surveys. Construction of the Trans-Alaska Pipeline in the auroral zone prompted considerable work on the currents that might be induced (Figure 1.5) and has required special monitoring techniques to be developed.

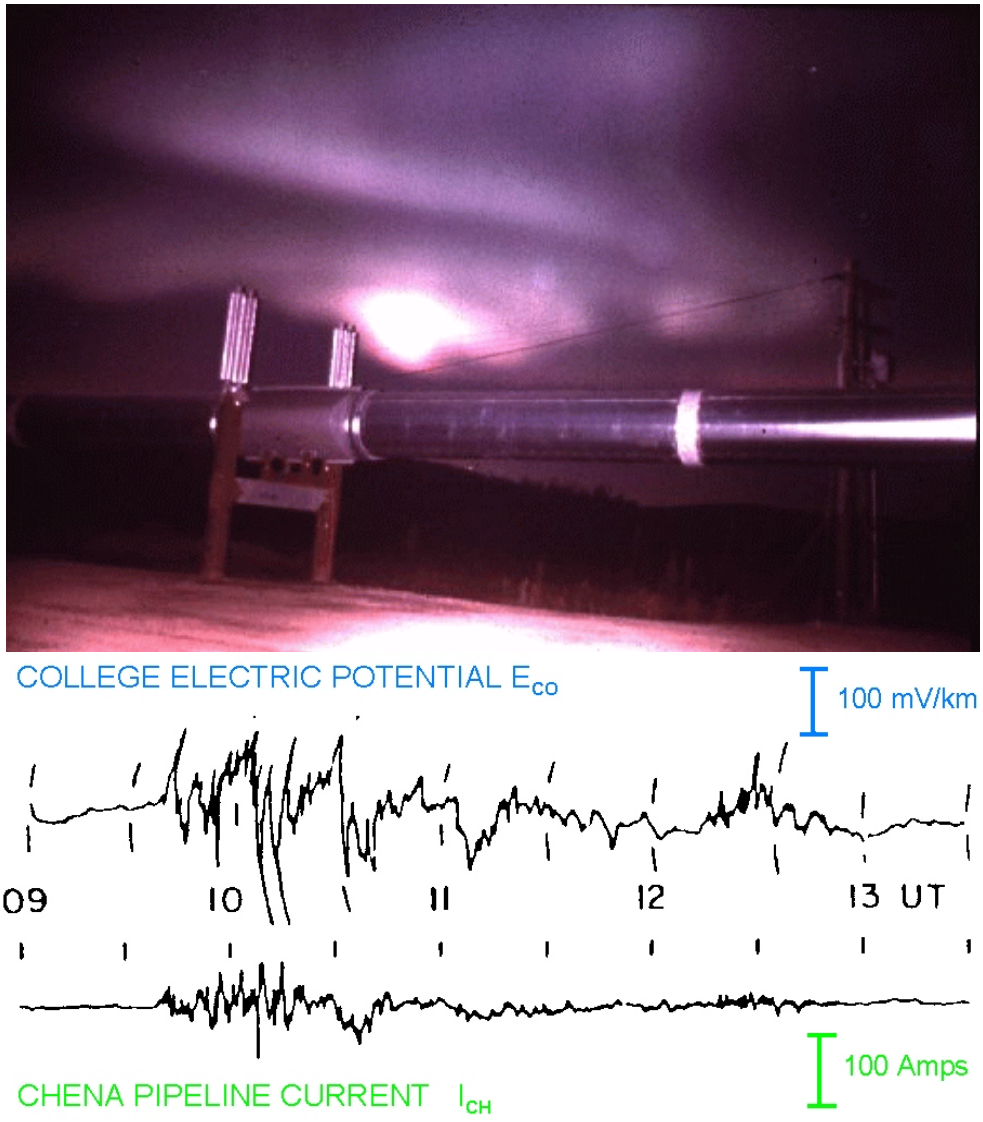

Figure 1.5. a) Aurora above the Alaska pipeline
b) Example of electric fields and telluric currents in the pipeline.

1.3. Proposed Pipeline Route

The proposed route for the pipeline takes it through the geomagnetically active auroral zone. During "quieter" times the auroral zone over the northern part of the pipeline route as shown in Figure 1.6. When the geomagnetic activity increases the auroral oval expands, extending down over the whole pipeline route (Figure 1.7). Thus the pipeline will be exposed to the intense geomagnetic activity along the auroral zone and considerable telluric activity can be expected in the pipeline.

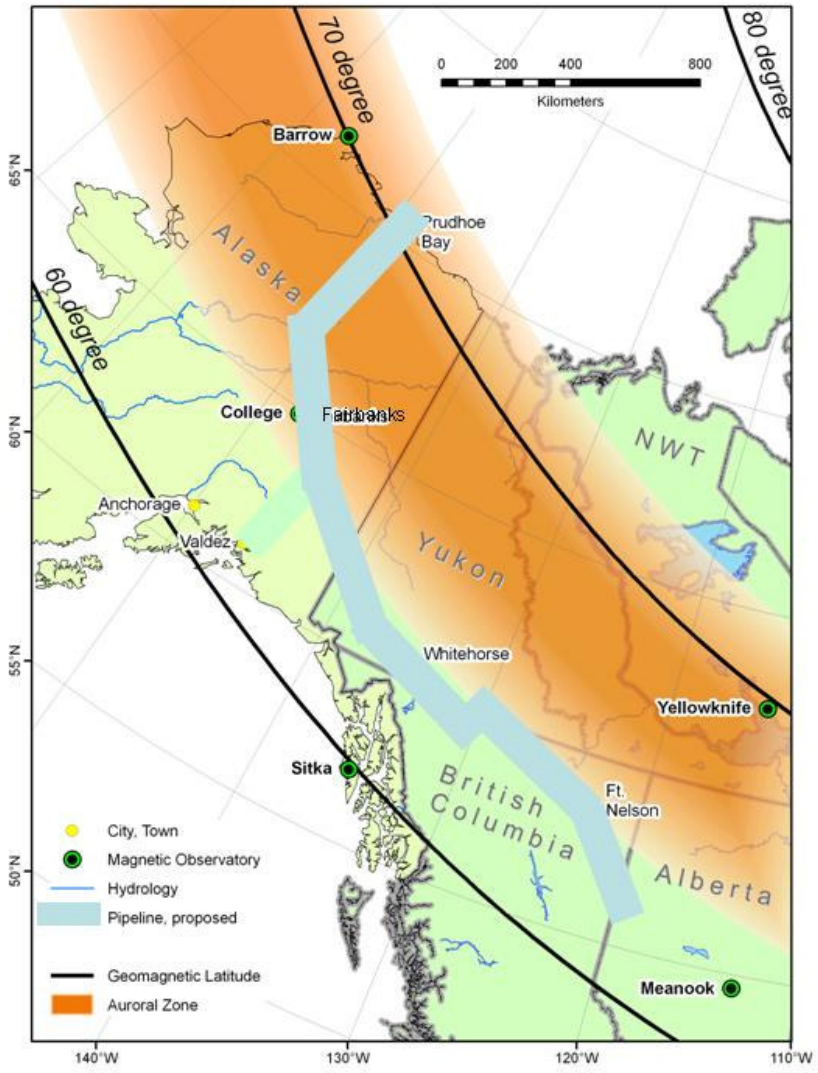

Figure 1.6 Route of the proposed pipeline in relation to the quiet-time auroral zone.

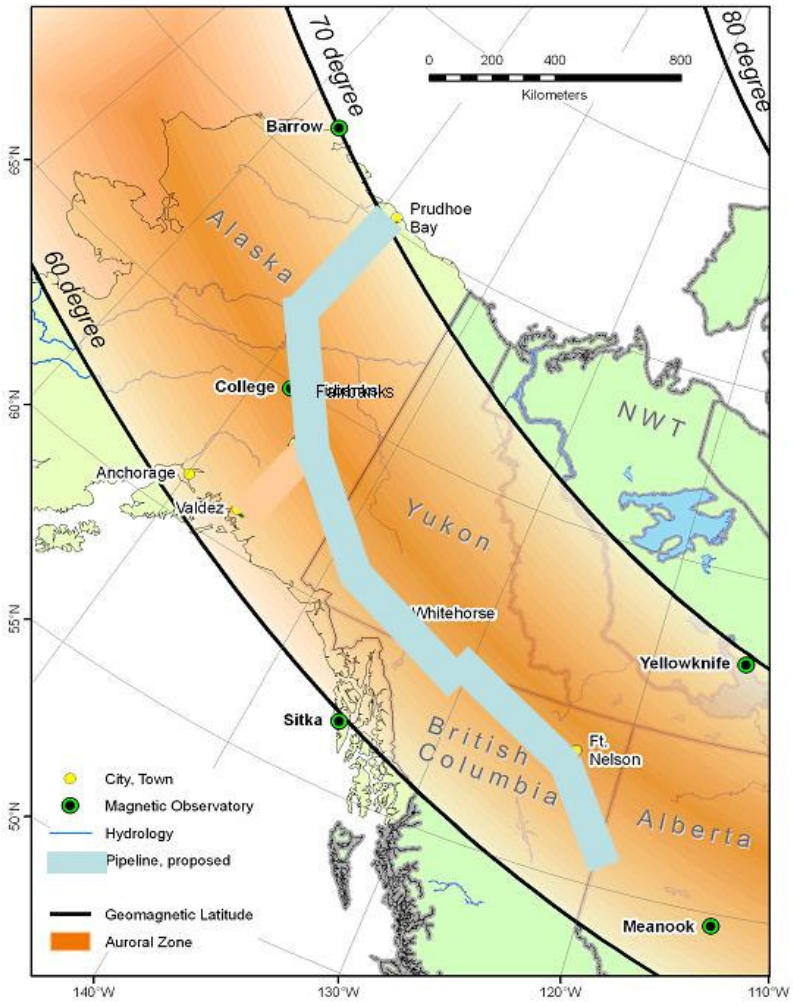

Figure 1.7 Route of the proposed pipeline in relation to the active-time auroral zone.

Chapter 2 Geomagnetic Climatology

2.1. Introduction

Analysis of the geomagnetic activity in the pipeline area was made using data from five American and Canadian geomagnetic observatories in the pipeline area. Because the pipeline route is located in the areas of the high geomagnetic and telluric activity, comparisons with usual levels of activity from the Ottawa geomagnetic observatory were made. The locations of the geomagnetic observatories are presented in Table 2.1.

Station	Code	Co-Latitude	Longitude
USA			
Barrow	BRW	18.7	203.4
College	CMO	25.1	212.2
Sitka	SIT	32.9	224.7
Canada			
Yellowknife	YKC	27.5	245.5
Meanook	MEA	35.4	246.7
Ottawa	OTT	44.6	284.5

Table 2.1. Locations of Geomagnetic Observatories

To demonstrate the specifics of the geomagnetic activity in the pipeline area, we compared hourly geomagnetic activity indices at the five observatories mentioned above with geomagnetic indices at the Ottawa (low latitude) observatory for the same representative year (2004). This year was chosen as it has good data coverage (very few missing hours) and has periods with both geomagnetic storms and quiet levels of activity. We have done a statistical description of 30 years of geomagnetic activity in pipeline area which evaluates the occurrence of the different activity levels and set the possible lowest and highest limits for the geomagnetic “climate” in the area of the proposed pipeline route.

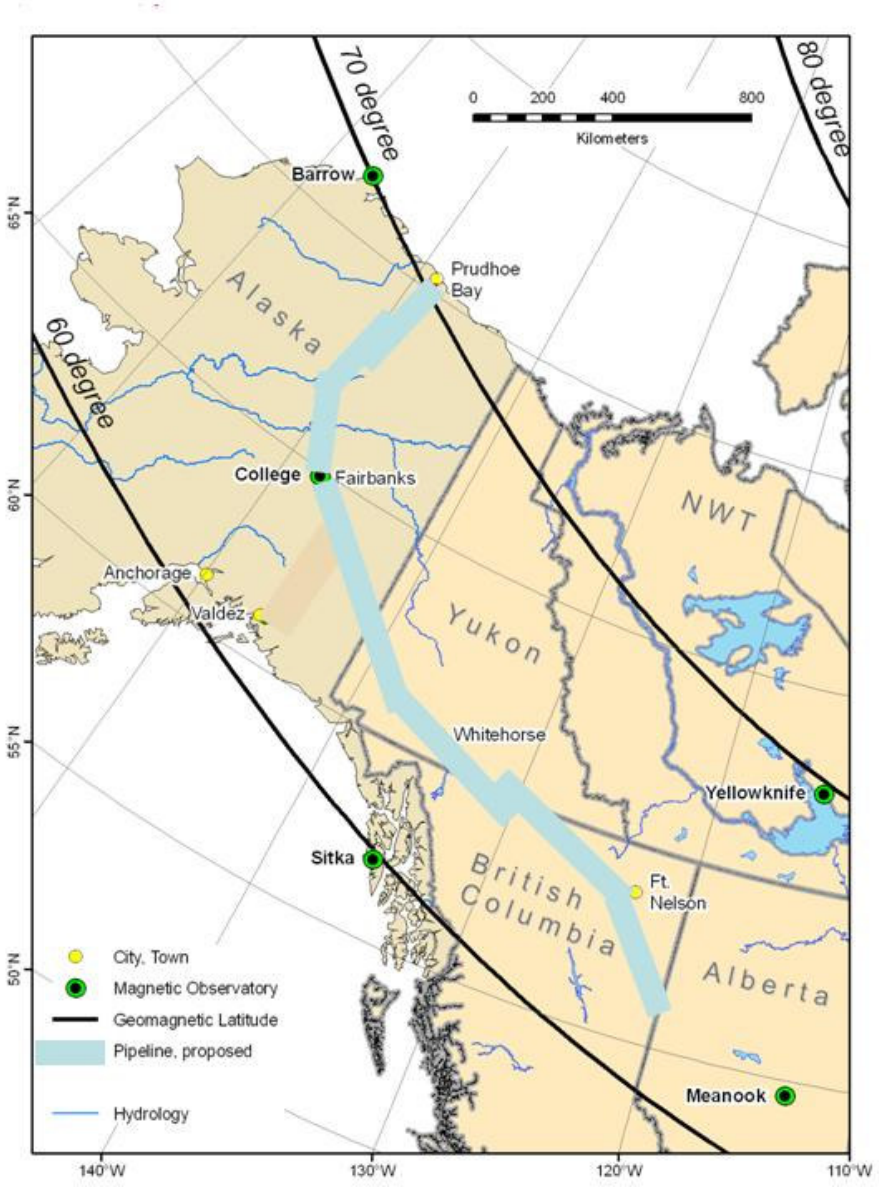

Figure 2.1. Location of geomagnetic observatories with respect to pipeline and lines of geomagnetic latitude

2.2. Geomagnetic Data

Data sampling rate was 1 minute, which is the standard rate for digitally filtered samples of data for the INTERMAGNET consortium of the geomagnetic observatories. Recordings consist of three components of the magnetic field, X (directed northward), Y (directed eastward) and Z (directed vertically down) and cover more than 30 years, from 1975 to 2007.

The data were processed to determine the maximum hourly range (*i.e.* the absolute difference between the lowest and highest 1-minute values within a particular hour) for both horizontal components for each hour of each day of each year. Therefore, for further study of the geomagnetic activity, we use hourly index, rather than minute-by-minute variation. The approach of utilizing indices is widely used in the geomagnetic field study (Mayaud, 1980).

The hourly range indices in X and Y components, HRX and HRY were examined to identify and remove those hours when; (1) no data was available due to various causes at the observatory that resulted in no measurements being made, and, (2) there were less than 48 minutes of data available for a particular hour. The amount of "data loss" from year to year was variable as shown in Figure 2.2, ranging from zero to total losses during 1975-1977 and 1983 for Sitka and 1975 for College. This was due to digital recording systems not being available at College as of January 1976 and January 1978 at Sitka. Also the data for 1983 at Sitka are in a format not compatible or readable with the modern programs and systems, and thus could not be used.

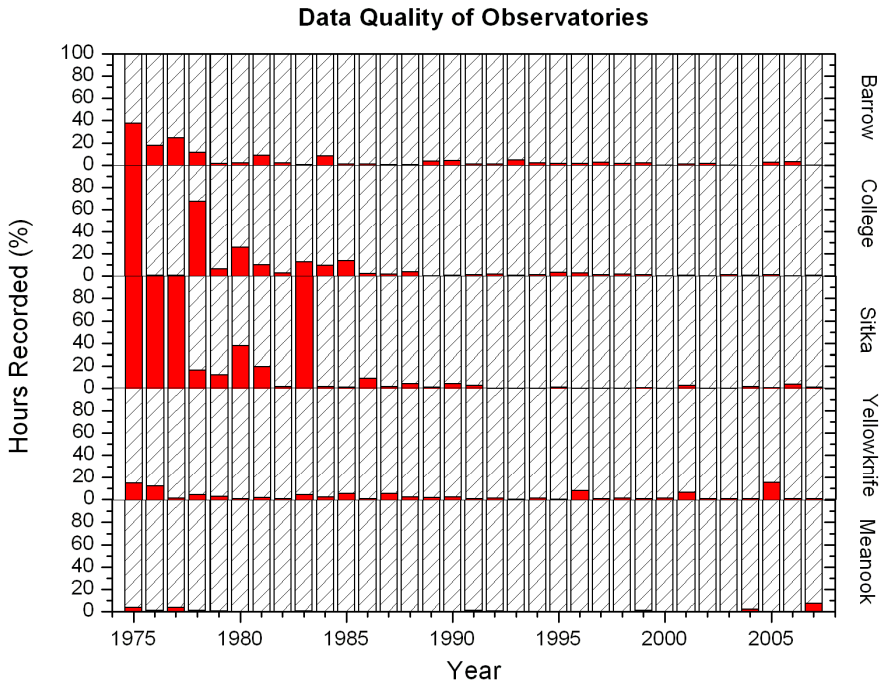

Figure 2.2. Data availability at the observatories in the pipeline area

2.3. Geomagnetic Variations in Pipeline Area

For an initial examination of the geomagnetic activity in pipeline area, a typical year was chosen. The year 2004 is in the declining phase of the solar cycle, with two large geomagnetic storms in July and November, and is a representative of the average annual geomagnetic situation. The evaluation of the geomagnetic activity was based on the hourly range of the geomagnetic field (all three components, HRX, HRY, HRZ). These are shown in Figures 2.3-2.5.

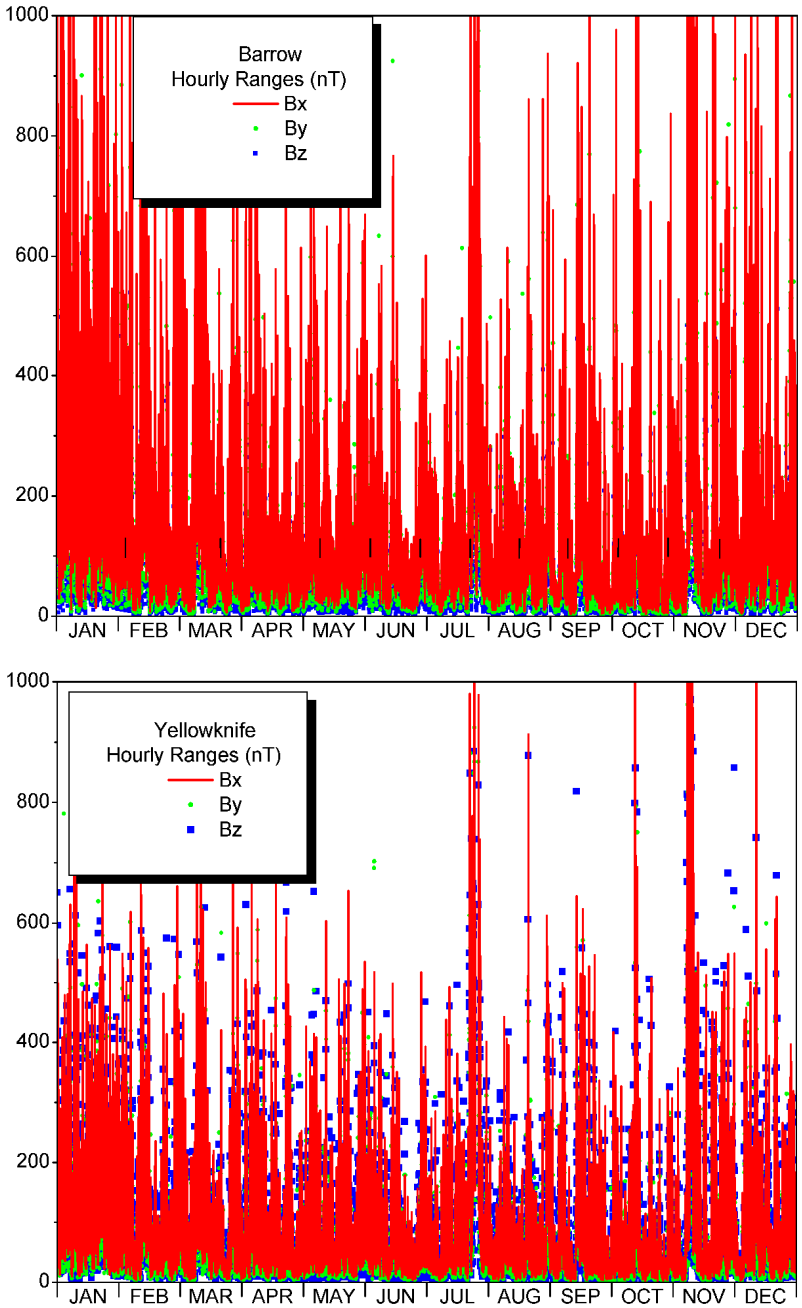

Figure 2.3. Geomagnetic activity of 2004 in hourly range index. Top:Barrow Bottom:Yellowknife

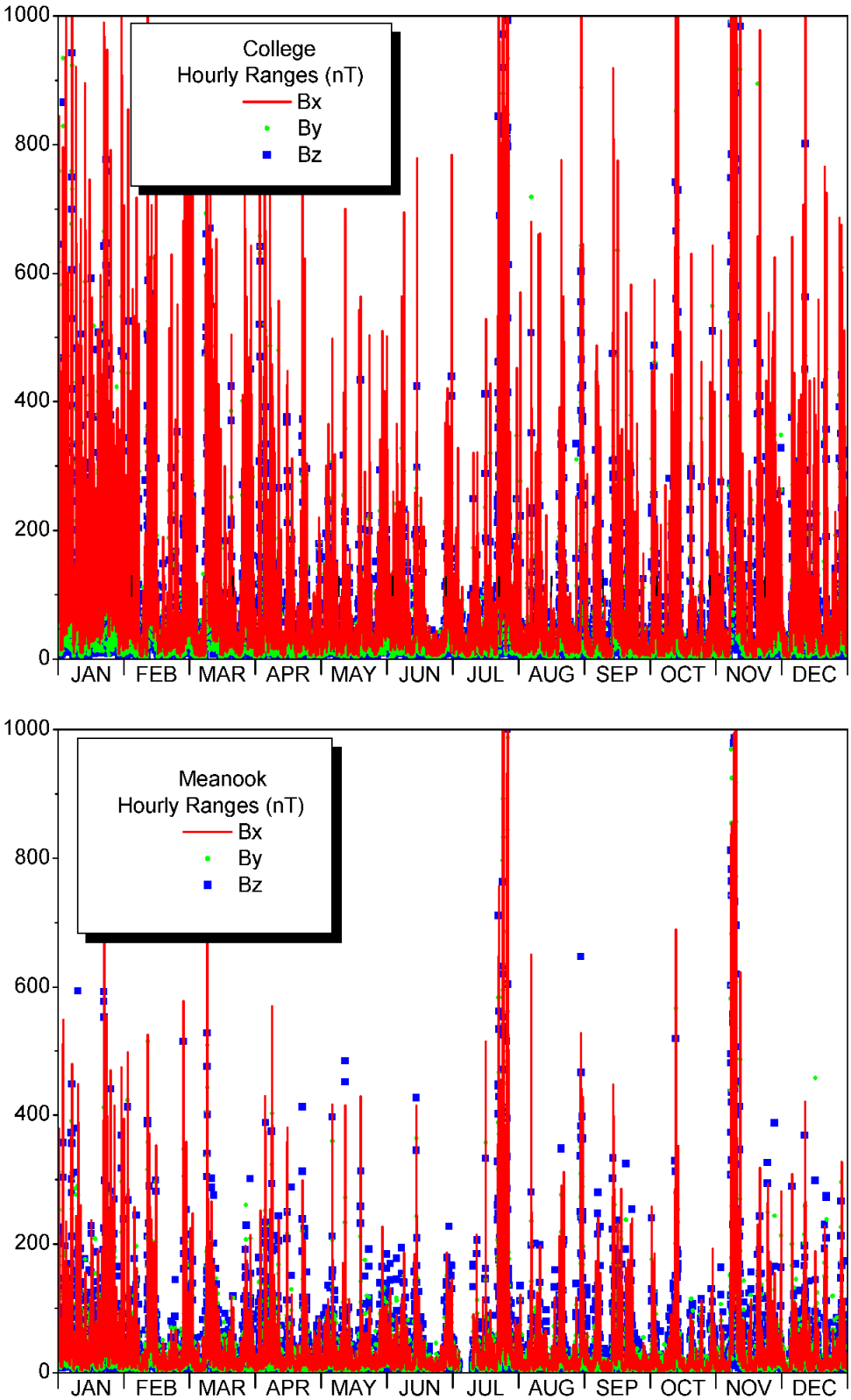

Figure 2.4. Geomagnetic activity of 2004 in hourly range index. Top:College Bottom:Meanook

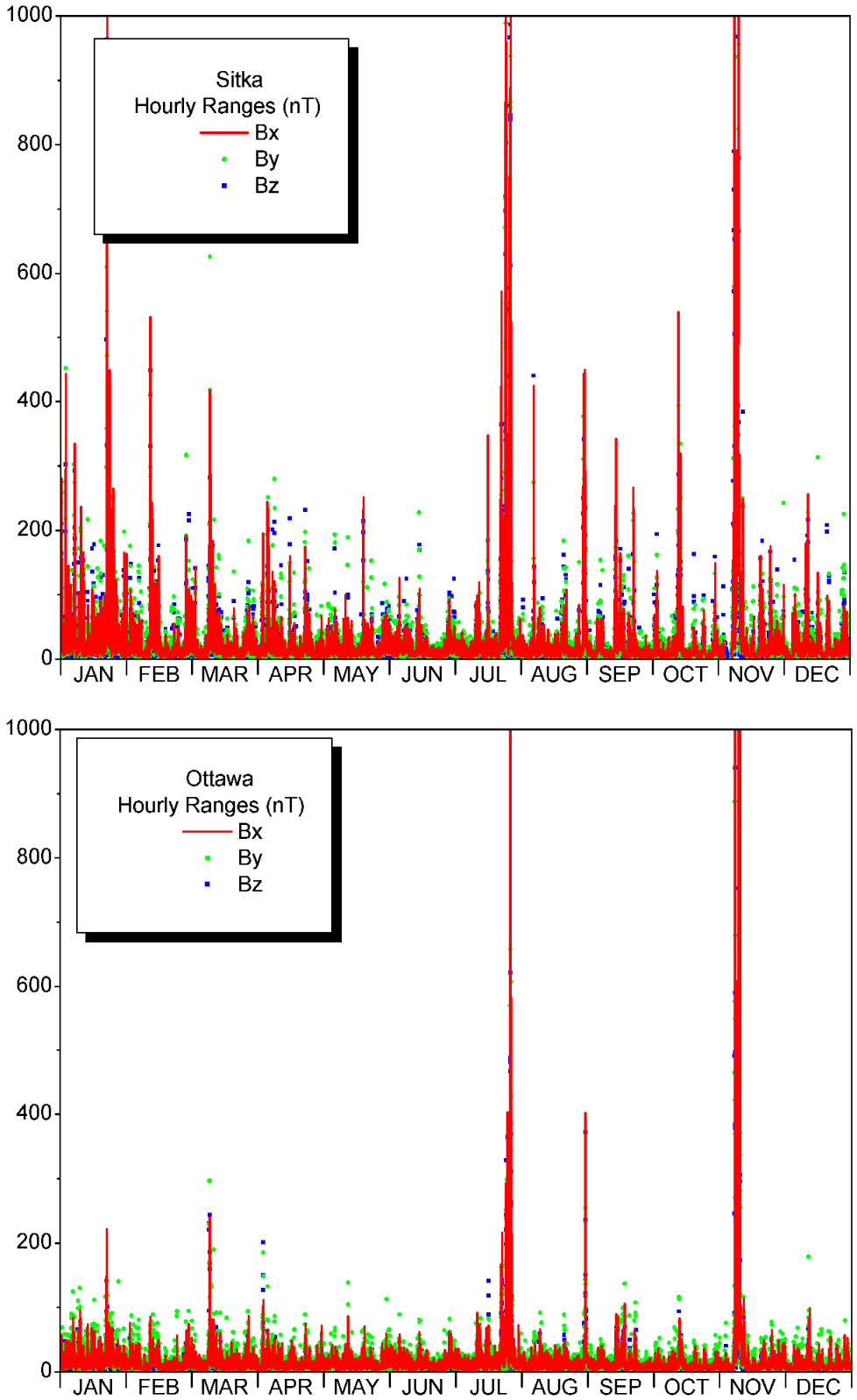

Figure 2.5. Geomagnetic activity of 2004 in hourly range index. Top:Sitka Bottom:Ottawa

Visual examination of the plots shows that the area close to Prudhoe Bay (represented by geomagnetic data from Barrow magnetic observatory) experiences the largest geomagnetic fluctuations, while near Fairbanks (College geomagnetic observatory) and south of it (represented by Yellowknife geomagnetic observatory) experience more typical of auroral zone variations. Meanook geomagnetic observatory shows low auroral zone activity. Geomagnetic activity at Sitka area is less than at Meanook due to its lower geomagnetic latitude location (see map, Figure 2.1). Normal geomagnetic activity experienced by the pipeline in low latitudes can be represented by the Ottawa geomagnetic observatory.

The pipeline area has been subdivided into three geomagnetic zones according to the levels of activity: the "high auroral zone" represented by observatories Barrow, College and Yellowknife, the "low auroral zone" represented by Meanook and Sitka, and the "normal" low latitude zone represented by the Ottawa geomagnetic observatory data.

As a statistical characteristic of activity, the 95% occurrence level during the representative year has been chosen. Figure 2.5 shows the HRX index values at different observatories for 95% occurrence during 2004. Three different indices were chosen based on these values, 40 nT as "absolute quiet level", *i.e.* 95% of the year geomagnetic activity is below 40 nT at low latitude locations; 200 nT as low-auroral zone activity level, *i.e.* 95% of the year the geomagnetic activity is below this level at "low-auroral" zone; and 600 nT as the high "auroral zone" activity level.

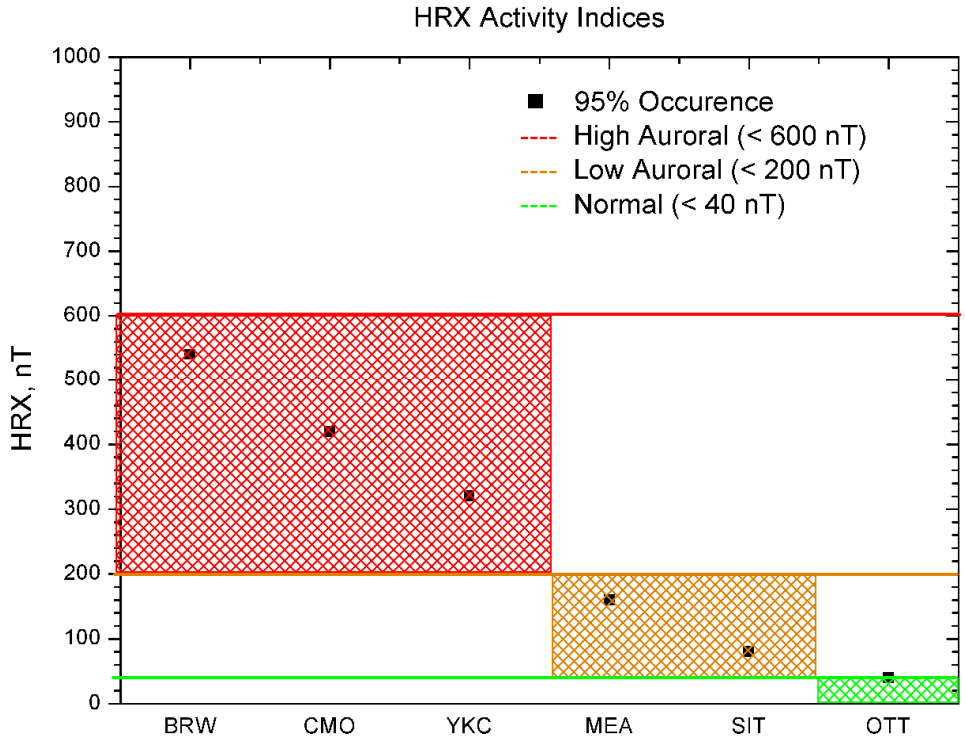

Figure 2.6. Activity indices as derived from 95% occurrence levels of HRX

2.4 Statistical Properties of Geomagnetic Variations for 1995-2007

In order to produce statistically valuable results, data from a period of time comparable to the pipeline lifetime (tens of years) need be used. Thus, geomagnetic data covering period of time from 1975 to 2007 were analyzed.

Figure 2.6 illustrates the qualitative differences between the amounts of geomagnetic activity experienced in auroral, sub-auroral and low latitude areas considered over the whole time period. It shows the percentage of hours for which the HRX index exceeded the three levels of activity, 40, 200 and 600 nT.

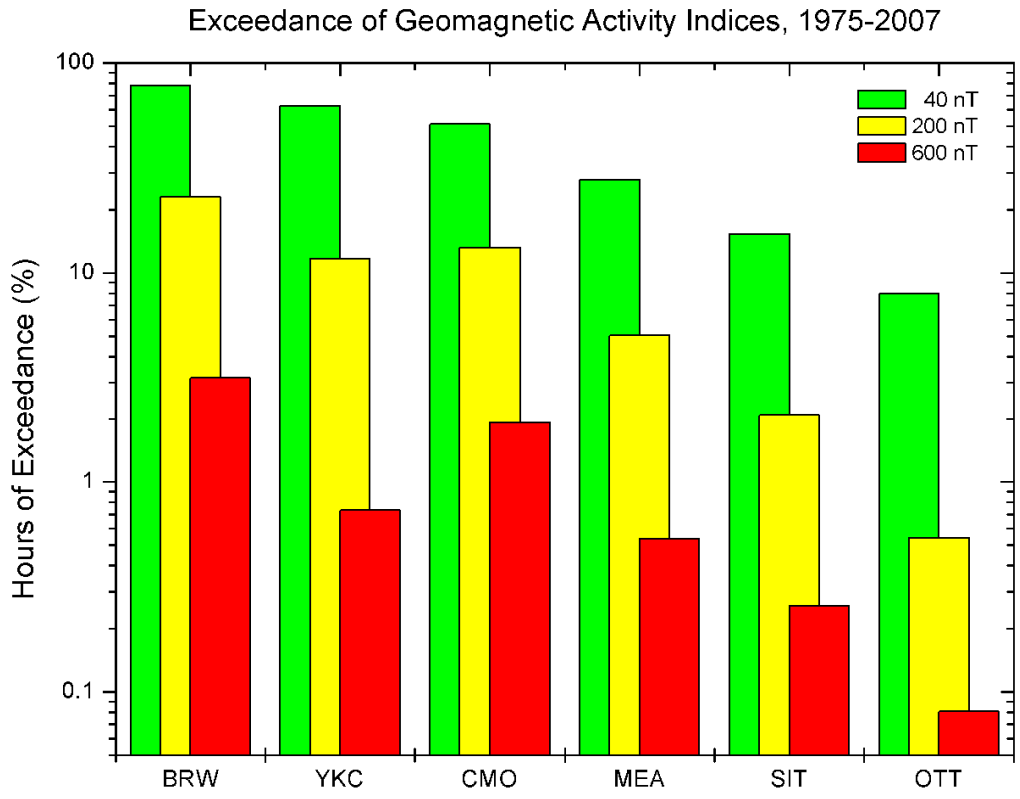

Figure 2.7. Total exceedance of geomagnetic activity indices for entire time period studied

By examining the figure it can be seen that the average exceedance of geomagnetic activity at a 40 nT level varies from about 15% at Sitka to about 30% at Meanook, ~50% at College , ~60% at Yellowknife and up to ~80% at Barrow. Extreme geomagnetic activity above the level of 600 nT was exceeded from about 0.3% of the time at Sitka (~1 day), to up to 3% of the time (~11 days) in Barrow.

More detailed plots for each observatory are presented in Figures 2.8-2.10, with annual sunspot number (shaded areas) by which solar activity variations are characterized.

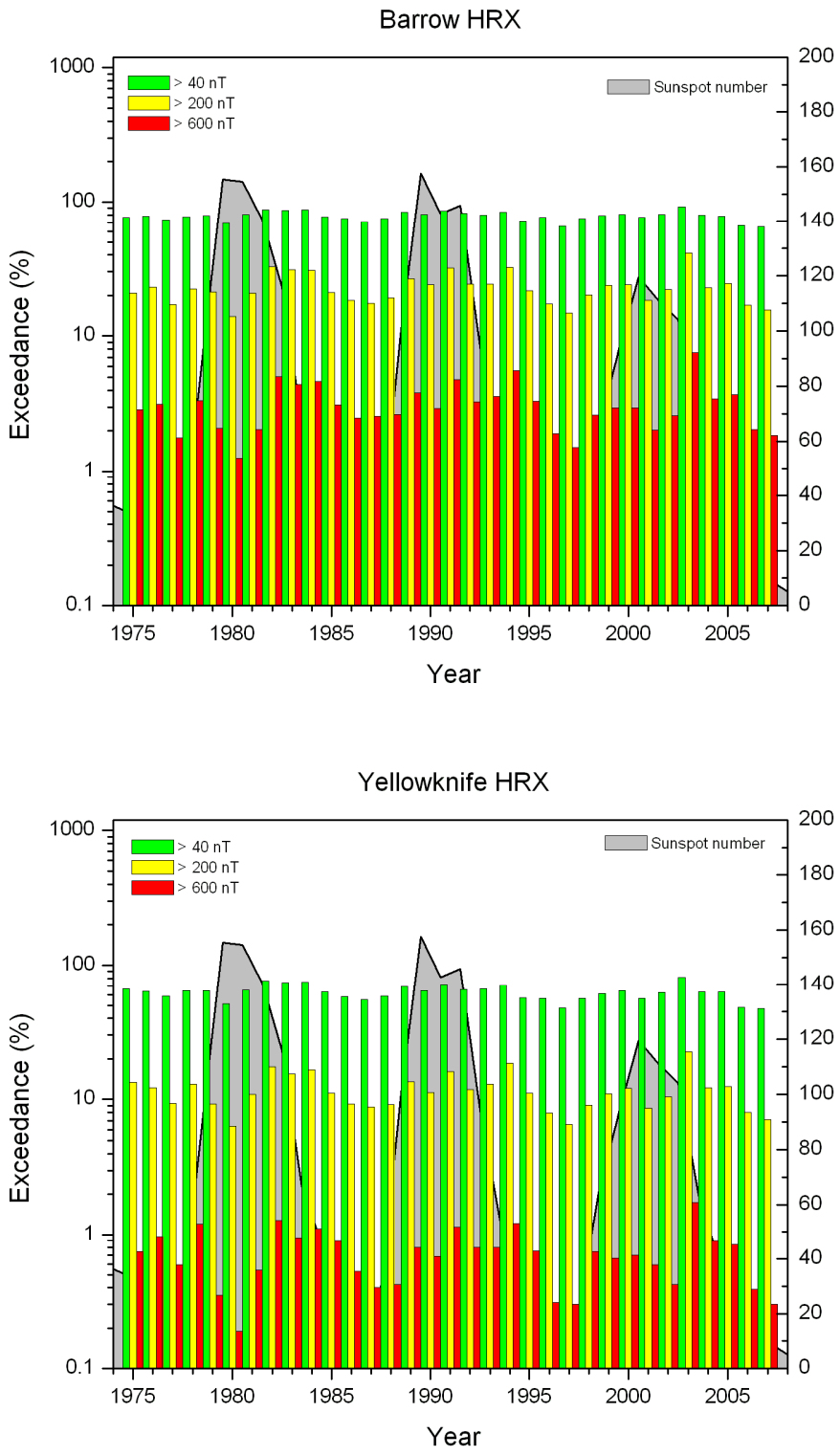

Figure 2.8. Percentage of exceedance of activity indices for geomagnetic observatories plotted over the yearly average sunspot number, Top: Barrow Bottom: Yellowknife

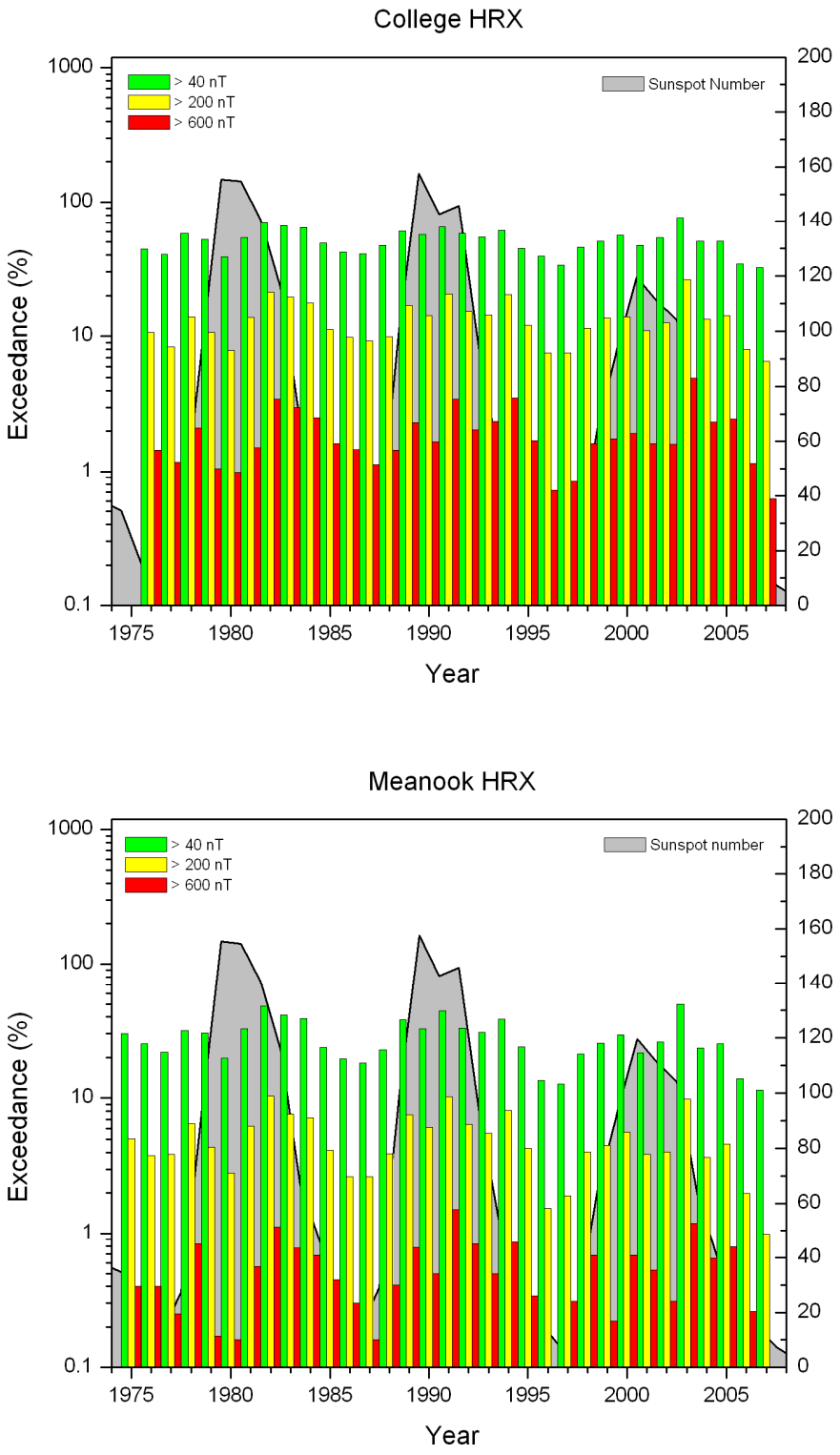

Figure 2.9. Percentage of exceedance of activity indices for geomagnetic observatories plotted over the yearly average sunspot number, Top: College Bottom: Meanook

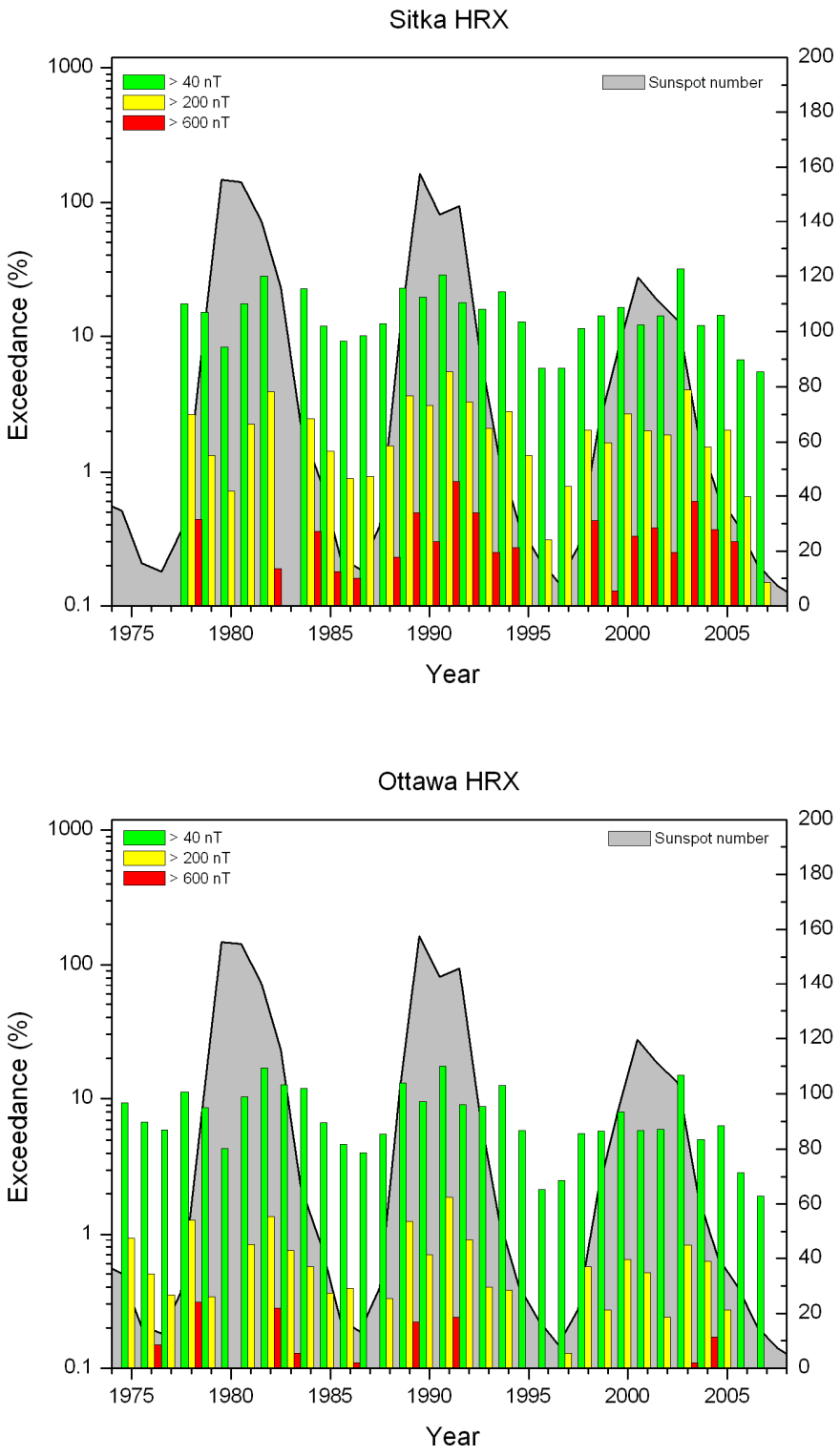

Figure 2.10. Percentage of exceedance of activity indices for geomagnetic observatories plotted over the yearly average sunspot number, Top: Sitka Bottom: Ottawa

As can be seen from the figures, there is no well-pronounced correspondence between solar cycle maxima and geomagnetic activity maxima. The explanation is that the former are expressed in sunspot number which has greater correlation with eruptive solar events such as solar flares and coronal mass ejections. These coronal mass ejections are responsible for the large but rare geomagnetic storms which have less significant statistical effects than other types of solar activity, such as recurrent coronal holes. This type of activity manifests itself in high speed solar wind streams which are continuous for many days, producing recurrent geomagnetic activity in the auroral zone. These high speed streams are very well pronounced during the declining parts of solar cycle, and also have effects during the uprising part of solar cycle, but are less influential during sunspot maxima. Geomagnetic activity is stronger during the declining phases at all auroral stations (Barrow, College and Yellowknife).

References:

Mayaud, P.N., 1980, *Derivation, Meaning and Use of the Geomagnetic Indices*, Geophysical Monograph 22, AGU, Washington, DC, pp.40-52.

Chapter 3. Review of Earth Resistivity Structure

3.1 Introduction

In order to assess the variations of pipe-to-soil potential (PSP) along the proposed Alaska Project Pipeline route, the resistivity structure of the underlying Earth needs to be determined because it affects the intensity of the geoelectric field experienced by the pipeline. This chapter describes how geological and geophysical information was used to prepare one-dimensional (1D) models of the Earth resistivity for use as inputs into the modelling of the geoelectric field and pipeline pipe-to-soil potential (PSP).

A review of publically-available information was undertaken, and included government geological reports and maps including on-line resources, soil-engineering studies of the Trans-Alaska Pipeline, and scientific journals. The focus was on the identification of previous geophysical surveys, undertaken as part of crustal investigations, which provide measurements of subsurface electrical resistivity, and to obtain thickness of the crust. No re-calculation of available geophysical data was undertaken.

Based on the review results, the pipeline route was divided into a series of zones that reflect significantly different geological realms which in turn would manifest themselves as zones of differing resistivity. The identification of a zone was based on the concept of geological terranes where a terrane represents a region of the Earth's crust characterized by a distinctive assemblage of rock that is different from its neighbours. Terranes are typically fault bounded. For each zone we produced an Earth model in which the resistivity changed in only one direction: vertically. This one-dimensional (1D) models does not include lateral changes of resistivity within each zone. However lateral resistivity changes are taken into account by the changes in the resistivity models from zone to zone.

Each 1D model is comprised of a series of layers, showing the thickness and resistivity, extending from Earth's surface through the crust and into the mantle. Determination of resistivity into deep Earth is necessary because the low frequency magnetic field variations penetrate several hundred kilometres through the entire crust and into the mantle. Hence, the resulting surface geoelectric field is influenced by the combined response through several hundred km into the Earth's interior.

This chapter first provides a background of Earth's internal structure and how variable the electrical resistivity of Earth materials can be, as well as how resistivity is measured. Secondly, the geological setting of the pipeline route is briefly described, including a review of past geophysical surveys undertaken in the study area to measure Earth resistivity. Finally, a description is provided on how 1D models were developed for the eight different resistivity zones identified along the pipeline route, the sources of information that were used, ending with a presentation of the eight 1D models. An appendix provides tables detailing the information sources and justifications for resistivity values and thickness for layers shown in each of the models.

3.1.1 Interior Structure of Earth

The Earth's electrical resistivity varies with depth as a function of temperature and pressure, changes to abundance and distribution of conductive minerals, and pore volume and fluid composition (Ferguson, 2008). For the purpose of modelling the geoelectric field, Earth can be divided into large and small scale structures in which the electrical resistivity is affected by different factors.

On the large scale, Earth's interior structure is divisible into four main layers: crust, mantle, outer core, and inner core (Figure 3.1). Each layer can be further subdivided based on unique physical differences. The outermost, thin, rigid crust is underlain by the dense, hot layer of semi-solid rock of the mantle.

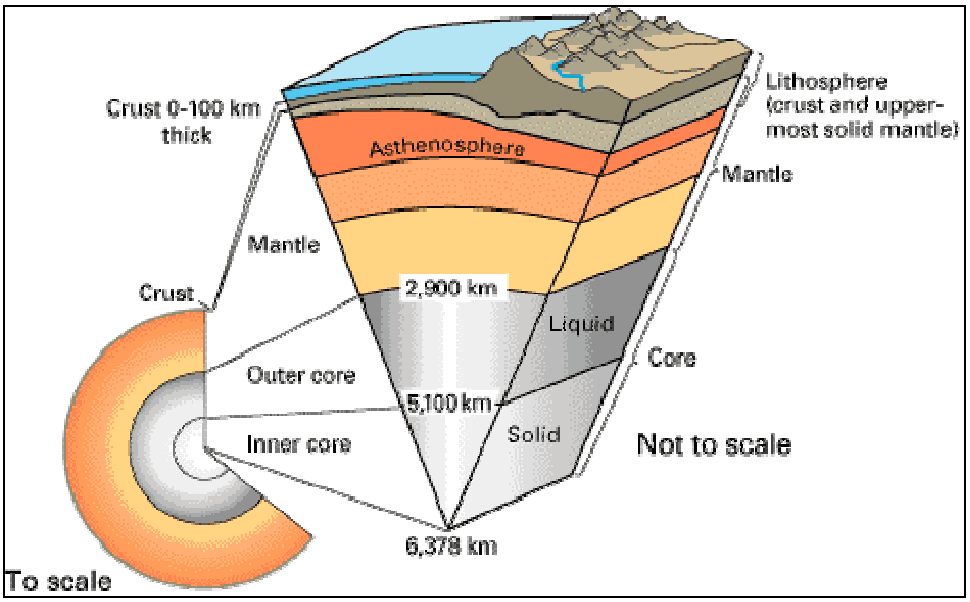

Figure 3.1. Earth's internal layers. (source: http://pubs.usgs.gov/gip/dynamic/inside.html)

Layers within the crust (upper, middle and lower) and mantle (upper and lower) are defined by transitional boundaries where increasing pressure and temperature changes the physical and electric properties of minerals with ever increasing depth. Starting at the depth of about 100-km is the Low-Velocity Zone where partial melting of the uppermost portion of the mantle starts to occur. A discontinuity in resistivity at the depth of 400 km occurs because of a mineral phase change where the dominant minerals (olivine and pyroxene) comprising the mantle at this depth transform to a more compact form (Mussett and Khan, 2000). At a depth of about 600 km, the boundary between upper and lower mantle, a mineral phase change occurs as minerals become evermore dense. These changes influence the electrical resistivity and result in the mantle having a much lower resistivity than the overlying crust.

Small scale Earth structure is considered to be changes in soil and near surface bedrock. Within 500m of the ground surface properties such as soil/rock lithology, groundwater content and

salinity, fracture distribution, clay content and presence of permafrost can all influence the near-surface resistivity (Ferguson, 2005). The effect on induced geoelectric fields (from geomagnetic disturbances) is low, but more importantly the near surface resistivity may influence the placement of ground beds used in pipeline corrosion protection systems.

3.1.2 Electrical Resistivity of Earth Materials

The resistivity of Earth materials varies widely, as shown in Figure 3.2, with a considerable overlap of range between different materials. Common rocks show a resistivity range from 10 to 100,000 Ohm meters (Ω.m), with values for various rock types provided in Tables 3.1 and 3.2. Geologic age of the rock, particularly for sedimentary rocks, also has an effect on resistivity values as shown in Table 3.2, whereby compaction associated with increasing thickness of overlying rock reduces pore space and amount of inter-pore water thereby increasing the rock resistivity. World-wide surveys have shown that near-surface sedimentary rock has a much lower resistivity than underlying crystalline and metamorphic and igneous rock (Ferguson and Odwar, 1997). Resistivity will vary among different types of sedimentary rock, being high where there is proportionally more limestone than shale and sandstone, and least for shale dominant rock especially if carbonaceous-rich. Local variations, such as presence of inter-connected sulphide minerals and graphite, are always a possibility that can further modify the resistivity values.

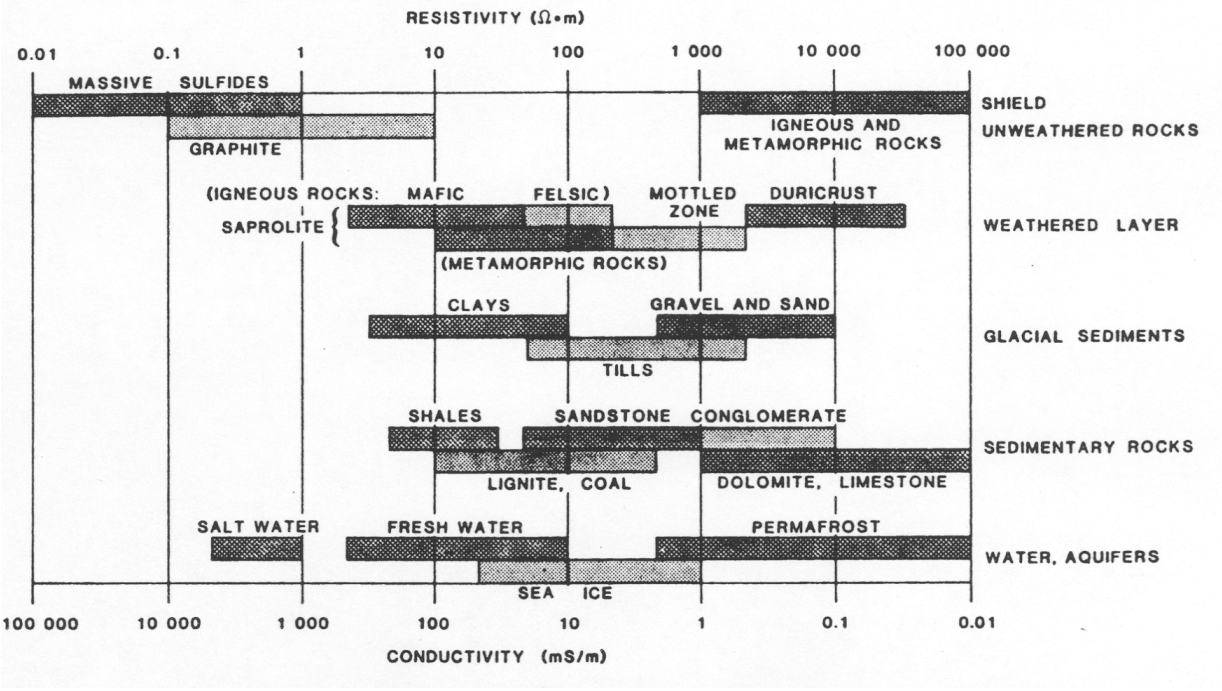

Figure 3.2. Range of resistivities for common Earth materials (from Sheriff, 2002).

Worldwide, the mid-to-lower crust exhibits lower resistivity compared to the upper crust (typically crystalline rock several km thick) due to temperature and pressure increasing with depth. However the entire crust has a higher resistivity than the underlying mantle. In the

mantle the ever increasing pressure and temperature cause the olivine and pyroxene minerals to undergo a phase change to a more dense form that greatly decreases the electrical resistivity.

Consolidated Sedimentary Rock	**Range (Ω.m)**	**Volcanic Rock (extrusive)**	**In situ (Ω.m)**
Argillite	74-840	Basalt	800
Conglomerate	2,000-13,000	Diabase	450
Dolomite	700-2,500	Diabase	450
Greywacke	400-1,200	**Plutonic (intrusive) Rock**	**In situ (Ω.m)**
Limestone	350-6,000	Gabbro	490
Sandstone	1,000-4,000	Diorite	7,000
Shale	20-2,000	Syenite	2,400
Slate	340-1,600	Granite	4,300

Table 3.1. Resistivity values for some common rocks (modified from Palacky, 1988)

Geologic age	**Marine sand, shale, greywacke**	**Terrestrial sands, claystone, arkose**	**Volcanic Rocks (basalt, rhyolite, tuffs)**	**Intrusive Rocks (granite, gabbro)**	**Sedimentary Rock (limestone, dolomite, salt)**
Quaternary, Tertiary	1 - 10	15 – 20	10 – 200	500 – 2000	50 – 5000
Mesozoic	5 – 20	25 – 100	20 – 500	500 – 2000	100 – 10000
Carboniferous	10 – 40	50 – 300	50 – 1000	1000 – 5000	200 – 100000
Pre-Carboniferous Paleozoic	40 - 200	100 – 500	100 – 2000	1000 – 5000	10000 – 100000
Precambrian	100 - 2000	300 - 5000	200 - 5000	5000 - 20000	10000 - 100000

Table 3.2. Resistivity values for water-bearing rocks of various types
(from Dobrin and Savit, 1988)

Both the crust and mantle can exhibit lateral variations of electrical resistivity on scales of tens to hundred kilometres due to effects from deep-seated geological structure, tectonic mechanisms, and changes in pressure, temperature and mineralogy, such that regional resistivities are either higher or lower than globally averaged values (Jones, 1992).

Mechanisms that can alter resistivity of crustal rocks and mantle, include: changes to amount of minor constituents (such as graphite and sulphides) and their degree of interconnection; presence of partial melt fluids and aqueous fluids; and enhanced electronic conduction at grain-boundary films of carbon (Wu et al, 2005, Plover, 1996).

Subduction can drag down to crustal depths water saturated and carbonaceous and/or sulphidic rich sediments which are more conductive than surrounding deep crust or mantle (Ledo et al, 2004).

Overburden also exhibits a wide resistivity range from < 10 Ω.m to about 10,000 Ω.m depending on the porosity, groundwater conductivity, and clay content (Ferguson and Odwar, 1997). For glacially deposited sediments resistivity values are lowest in clays, mid-range for till, and highest in gravel and sand (Palacky, 1988). In permafrost terrain, the resistivity of ice-bearing soils and rock is a function of the unfrozen water content. Ice has a higher resistivity than water and if present in sufficient quantity it will increase the resistivity of an otherwise unfrozen material (Assoc. Mining, 2004). When frozen, the resistivity generally doubles in fine sized sediments such as clay and silt, and increases by a half an order of magnitude for coarser sands and gravels. Frozen rock exhibits a varying resistivity depending on its water content, porosity, salinity of the pore water, and grain size of the rock (Parkhomenko and Keller, 1967). At -12^{o}C, the resistivity of a rock is about 10 to 100 times larger than when measured at 18^{o}C (Mackay, 1970). However, if the rock is relatively impermeable to water, then the resistivity when frozen may not differ significantly from the unfrozen condition. Table 3.3 provides a compilation showing the difference in resistivity between unfrozen and frozen overburden in northern Canada.

Soil Materials	**Apparent Resistivity** (ohm-m)
Thawed	
Fine lake bottom sediments	2 – 20
Saturated peat	4 – 10
Sandy or gravely, silt	4 – 60
Sand and gravel beach	15 – 80
Moist gravel	80 – 200
Ice muddy silt	120 – 300
Moist peat	800 – 1000
Frozen	
Silt	1000 – 1200
Old high level beach gravel	900 – 1500
Icy Peat	3300 – 6100
Fine cross-bedded sands with thin beds of peat	3600 – 4000
Muddy gravel	4500 – 6000
Segregated ice	6000 +
Sand, silt and gravel mix with ice lenses, pipes and dikes	9500 +
Silty peat	13000 +
Sand with gravel lenses	15000 – 20000
Gravel and sand ridge	20000 – 22000

Table 3.3. Apparent resistivity of thawed and frozen materials (Mackay, 1970)

3.1.3 Measuring Earth Resistivity

Geophysical surveys using electromagnetic (EM) methods are typically used to measure variations of the Earth resistivity. Most ground and airborne EM survey systems use an electrical generator to transmit a magnetic field to induce a current into the subsurface and then measure the response. Such techniques are limited to detecting resistivity changes between tens to a few hundred metres deep because of the higher frequencies that are produced by the relatively low-powered transmitter.

The magnetotelluric (MT) method is the only geophysical technique with the ability to provide an image of the Earth's electrical structure over a depth range from near surface to the deep mantle because it utilizes powerful naturally induced currents that globally penetrate Earth. The ratio of the electrical and magnetic field strengths, as a function of frequency, provides a measurement of electrical impedance which in turn is used to calculate the apparent resistivity at various depths. The depth to which resistivity structures can be imaged depends on the depth of penetration of the EM fields. This is dependent on the presence of local near-surface structures of low-resistivity (that can impede penetration by EM fields) and the periodicity and intensity of the EM wave (Wennberg and Ferguson, 2002). As common to other EM methods, the MT technique measures a "bulk" apparent resistivity of the Earth material over a large area at a range of depths.

In-situ measurement of resistivity in oil and gas exploration wells is accomplished by the use of probes lowered into a well, often to a depth of thousands of meters. An induction tool, similar to a surface EM method, measures resistivity up to 5m or more from the borehole and provides a good representation of resistivity through the surrounding rock (Mussett and Kahn, 2000). Comparison of petroleum-well induction logs has shown a very good match with resistivity derived from MT soundings (Boerner et al, 2000; Wu, 2001).

Laboratory measurements of the resistivity exhibited by samples of different rock types also provides information whereby the resistivity of an area can be inferred if the geology of the area is known.

3.2 Physical and Geological Settings along the Pipeline Route.

3.2.1 Physiography

The proposed pipeline route follows the Trans-Alaska pipeline from Prudhow Bay to RFairbanks and then follows the Alaska Highway corridor. This route goes through lowlands, river and fault valleys and mountain passes that penetrate through much of the rugged terrain. Both in the Alaska and Canada portions, the pipeline route crosses the same three major North American physiographic systems (Figure 3.3). Each system is divisible into a number of physiographic subdivisions that generally reflect topography and underlying geology.

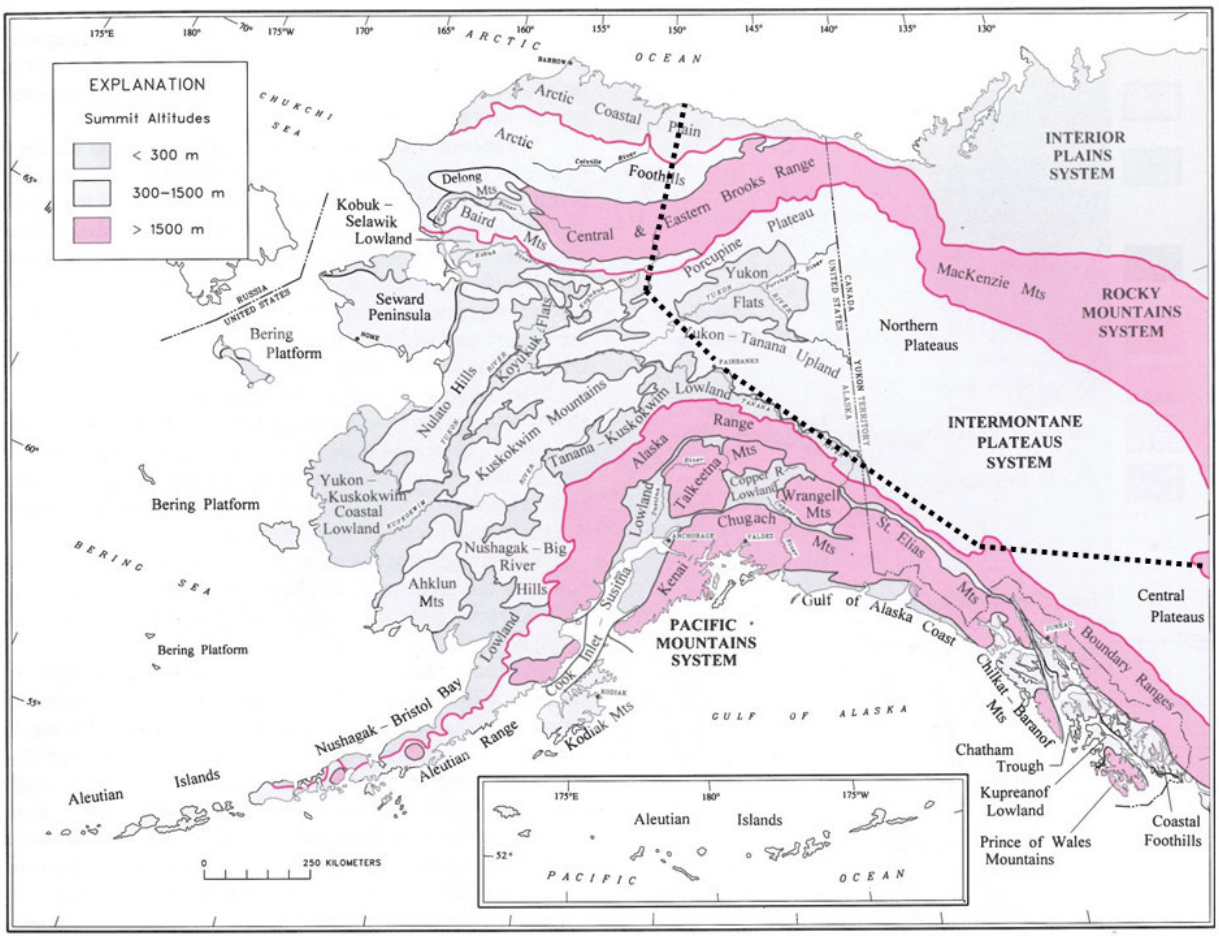

Figure 3.3. Physiography of Alaska and adjacent parts of Canada (from Plafker and Berg, 1994). Heavy red lines bound major North American physiographic systems. Approximate pipeline route indicated by dashed line.

3.2.2 Tectonic Framework, Bedrock Geology and Major Faults

Most of the pipeline route crosses the geologically complex, mountainous Cordilleran region of Alaska and northwestern Canada. To identify approximately uniform resistivity zones that are on the scale of tens to a few hundred kilometers long, the concept of terranes or superterranes (referred to as realms in Nelson and Colpron (2007)) was used. Terranes are regions of the Earth's crust characterized by a distinctive assemblage of rock that is markedly different from its neighbors, often fault-bounded, and as such the gross geology would be reflected in the overall electrical resistivity for a particular terrane, and which can be different from the other terranes.

The pipeline route crosses the following three superterranes (Figure. 3.4):

(a) Ancestral North America (ANA) includes ancient basement rocks and deformed continental margins;
(b) The Intermontane Superterrane represents a collection of individual terranes made up of offshore rifted continental fragments, volcanic island arcs and ocean basins; and,
(c) The Arctic Superterrane, which is divided into several terranes and subterranes, the largest two being the Arctic Alaska Terrane and the Angayucham/Tozitna terrane (www.geo.arizona.edu, 2009).

Sedimentary bedrock is the predominant rock type underlying much of the pipeline route in Alaska. The foothills and coastal plain of the North Slope are underlain by a laterally extensive and thick succession of marine and non-marine sedimentary rocks that form the Colville sedimentary basin, deepening to 9 km in front of the Brooks Range mountains. Beneath the Colville Basin is the Arctic Alaska Terrane, a mix of metamorphosed sedimentary, volcanic and intrusive rocks more deformed closer in to the Brooks Range. Thrust faulting has resulted in a series of steeply dipping slices of sedimentary rock that make up the Brooks Range, including metamorphosed sedimentary and volcanic rocks in the central part of the range. The pipeline also passes over clusters of intrusive igneous rocks that are widespread in central and southeastern Alaska (including eastern Yukon-Tanana Lowland). Extensive exposures of younger volcanic rocks occur in the Porcupine Plateau and westernmost Yukon-Tanana Upland. Metamorphosed rocks are common beneath the route in southeastern Alaska.

In Canada folded and faulted sedimentary bedrock also underlies much of the pipeline route. Substantial exposure of intrusive igneous rock and undivided metamorphic rock occurs west and northwest of Whitehorse. Up to 4 km thick flat-lying sedimentary bedrock of the Interior Platform (Figure. 3.4) underlies the southeastern end of the route in northeastern British Columbia. Buried beneath the Interior Platform are ancient basement crystalline rocks, part of ancestral North America, which have been-subdivided into numerous domains that reflect origin and dominant rock type. Of particular interest to the determination of a resistivity profile are the Ksituan, Kiskatinaw, Nova and Fort Simpson domains comprised of metamorphosed granitic rocks and gneisses exhibiting linear zones of low-resistivity (Ross and Eaton, 2002, Turkoglu et al, 2009).

Major faults that cross the pipeline route in Alaska are highlighted in Figure 3.4. These faults, from north to south are as follows: Kobuk, Tintina, Teslin and Great Slave Lake Shear Zone. The Denali fault runs parallel along part of the pipeline corridor.

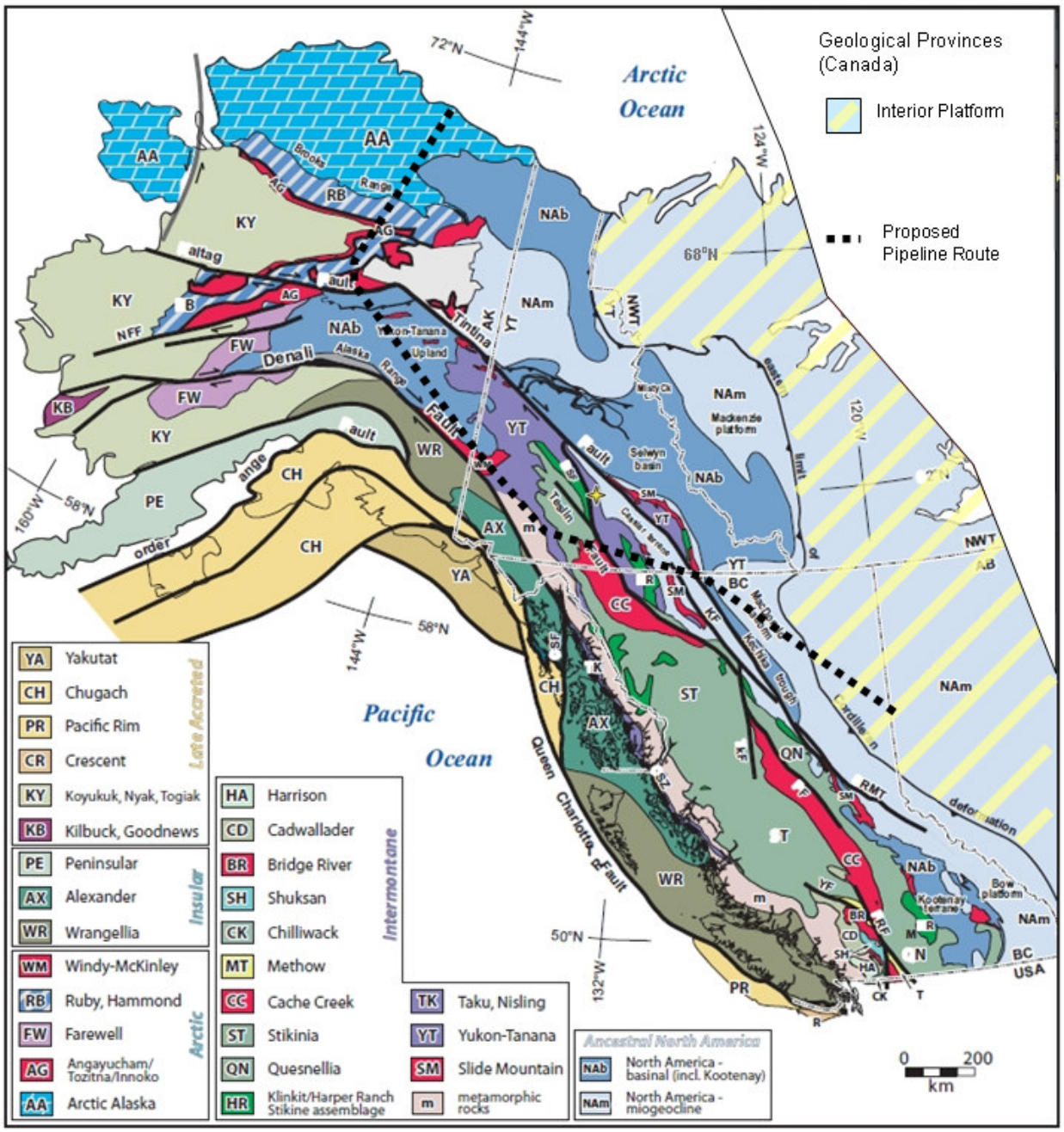

Figure 3.4. Terranes and tectonic realms of the Canadian – Alaskan Cordillera (from Nelson and Colpron, 2007). General route of proposed pipeline marked by dashed line. Abbreviations of interest: AB-Alberta, AK-Alaska, BC-British Columbia, NWT-Northwest Territories, RMT-Rocky Mountain Trench, YK-Yukon Territory.

3.2.3 Surficial Deposits (Overburden)

Overburden (e.g., silt, sand, gravel, broken rock) of differing kinds is present along the pipeline route in varying depths. Since the pipeline route normally follows river and mountain valleys in northern Alaska and elsewhere, the surficial deposits are typically a combination of fluvial-deposited gravels and sands in the river valley bottom flanked by terrace gravels. Glacially deposited moraine-till underlies the mountain valleys cutting though the Brooks Range. Colluvium (unsorted rock fragments) is common along the higher mountain slopes. From the south side of Brooks Range to Fairbanks the route crosses an expanse of alluvium, eolian deposits (wind-blown silt) and colluvium. Along the Tanana River valley from Fairbanks to the Alaska-Yukon boundary, the route is underlain by a rapidly varying mix of surficial material, including river flood-plain alluvium, valley bottom eolian deposits of silt and sand, glacio-fluvial outwash gravels, glacial till moraine, and alluvial fan deposits of sand and gravel. Within the Canada portion there is an extensive cover of glacial moraine deposits forming a till blanket and/or till veneer, although the route tends to follow valleys where glaciofluvial sands and gravels and glaciolucustrine silts and clays are predominant.

3.2.4 Permafrost Distribution and Depth

Permafrost of varying continuity underlies about three-quarters of the pipeline route, as shown in Figure 3.5, being thicker and of greater lateral extent in the north and diminishing evermore southward. A number of local factors, such as type of surficial geology, topography, topographic relief, slope angle, snow and vegetative cover, and presence of lakes and rivers and flowing groundwater, all combine to influence the presence and thickness of permafrost (Miller and Whitehead, 1999).

Thickness and areal continuity is greatest in the continuous permafrost zone of northern Alaska, beneath the Arctic Coastal Plain and Brooks Range, covering about 20% of the pipeline route. At Prudhoe Bay local permafrost extends to depths of about 600 m, but shallows toward the Brooks Range where it varies in depth from about 27 to 111m. Extensive discontinuous permafrost (50-90% frozen) underlies the remaining portion of the pipeline route in Alaska, from the Yukon Flats across the Yukon-Tanana Upland to the Alaska-Yukon Territory border. However, from Fairbanks southeastward to Tok and the international border, much of the pipeline route follows a river valley where permafrost is sporadic (10-50% frozen) to isolated (>0-10% frozen), with permafrost depths varying irregularly between 10 and about 100 m.

Much of the Canadian portion of the pipeline route, from the Alaska border to Fort Nelson, lies within a sporadic discontinuous (10-50% frozen) permafrost zone with a depth of less than 10 m. Southeast of Fort Nelson, permafrost only occurs as isolated patches (0-10% frozen) and then ceases to exist halfway to Boundary Lake, the end of the route.

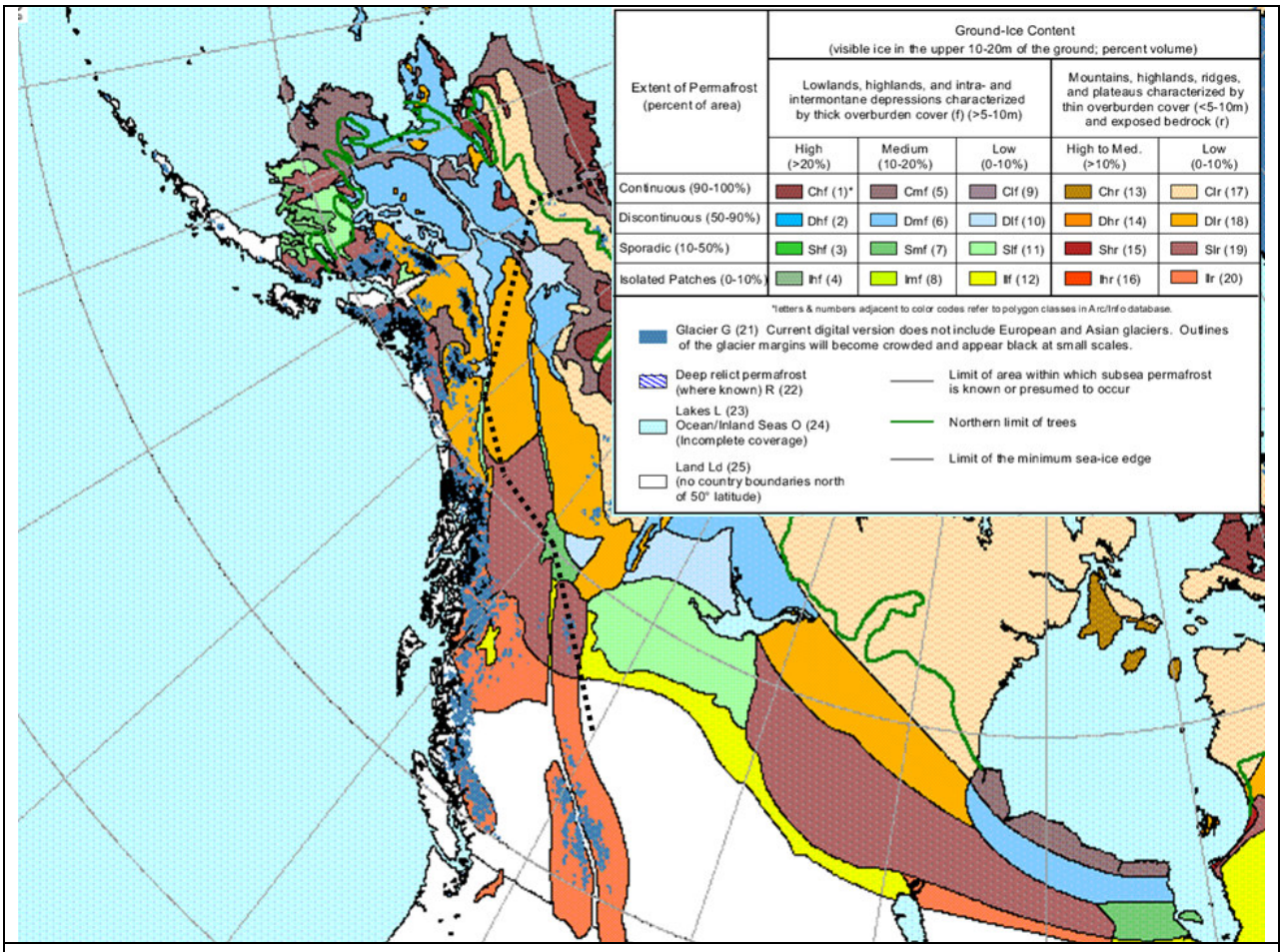

Figure 3.5. Map of permafrost for Alaska and northwestern Canada (from Brown et al, 1998). Proposed pipeline route is shown as dotted line.

3.2.5. MT Surveys in study area

A program of MT soundings in Alaska was undertaken by the U.S Geological Survey during 1985-1992 for the Trans-Alaska Crustal Transect (TACT). As shown in Figure 3.6 the TACT-MT survey covered the entire Alaska portion of the proposed pipeline route. About half of these MT soundings underwent a preliminary 1D interpretation of the resistivity by Campbell et al (2001) but most interpretations were limited to a tabulation of the layer thickness and its resistivity for the upper few kilometres of Earth's crust; results which were incorporated in the development of 1D resistivity models for the Alaska portion of the pipeline route. No interpretations were available for that portion of pipeline north of Brooks Range, across the North Slope.

In 1985, Stanley et al (1990) completed three transects (Figure 3.6) across the Denali fault and Alaska Range, focusing on the shallow crust. The results were presented using a stitched 1D model to represent a 2D version of the subsurface. Later MT surveying completed in 2002 (Fisher et al, 2004a) has identified low-resistivity structures immediately below and lateral to the Denali Fault, however, this particular survey stopped short 30 km of the proposed pipeline corridor.

During the 1990s and early 2000s, the Geological Survey of Canada, as part of the Lithoprobe SNORCLE (Slave-Northern Cordillera Lithospheric Evolution) program, completed three regional-scale crustal transects (Figure 3.6) crossing the main geological structures in the Yukon, Northwest Territories and British Columbia. The crust was imaged using both seismic and MT methods. Comprehensive 2D interpretations have been published by several authors, the results of which have been applied to the preparation of 1D models presented in this report. Figure 3.7 presents 2D inversion models along SNORCLE Corridors 2 and 3, and Figure 3.8 provides maps of average resistivity of the crust and upper mantle at various depths.

A recently published geophysical study of the upper mantle structure in northern Alberta (Turkoglu et al, 2009) incorporated both new MT (using 3D interpretation) and previous 2D MT surveys, the results of which were also incorporated in the preparation of a 1D resistivity model for the southeastern part of the pipeline route.

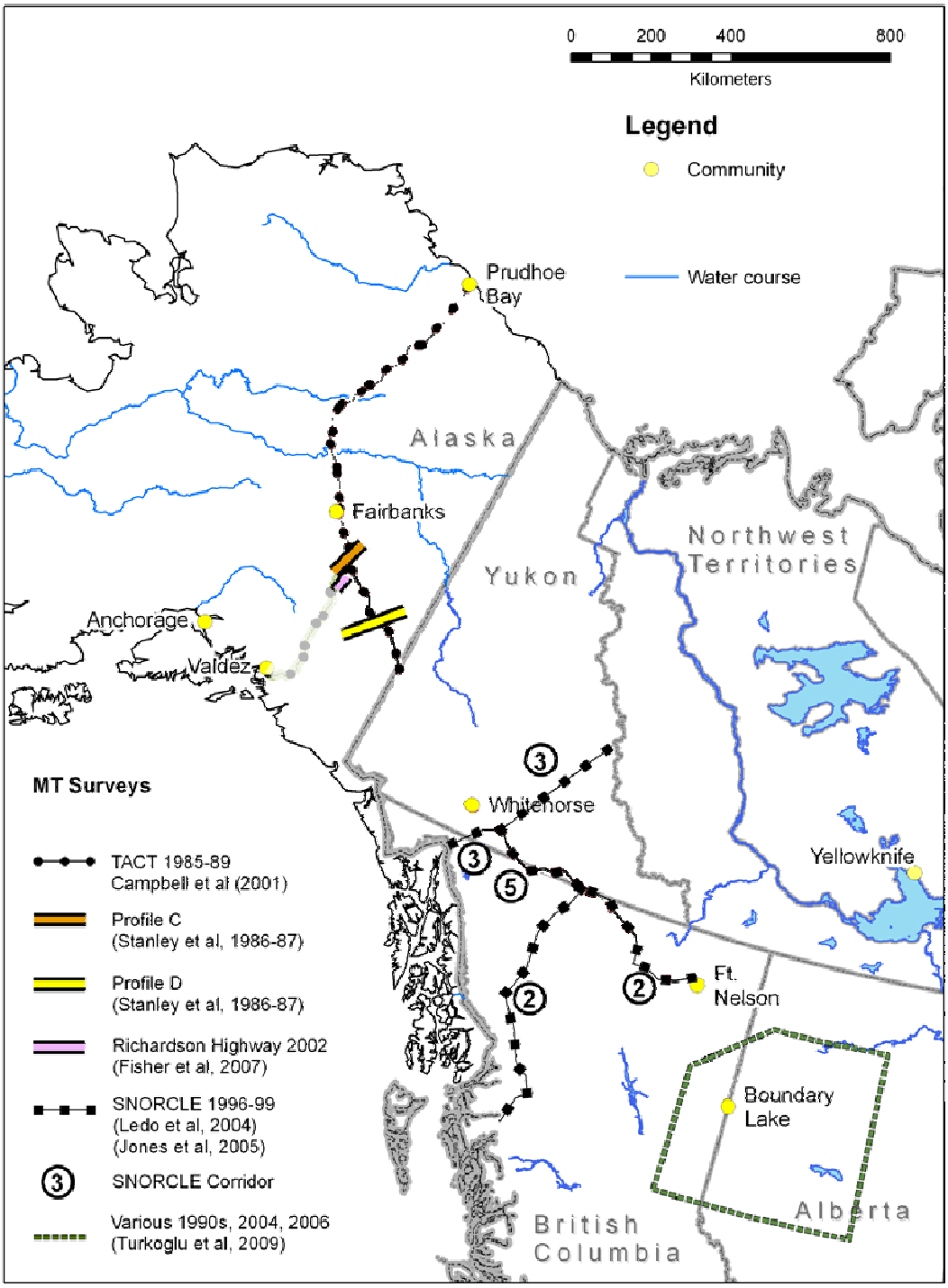

Figure 3.6. Location of MT surveys along or crossing the proposed pipeline corridor, and which are sources of Earth resistivity measurements

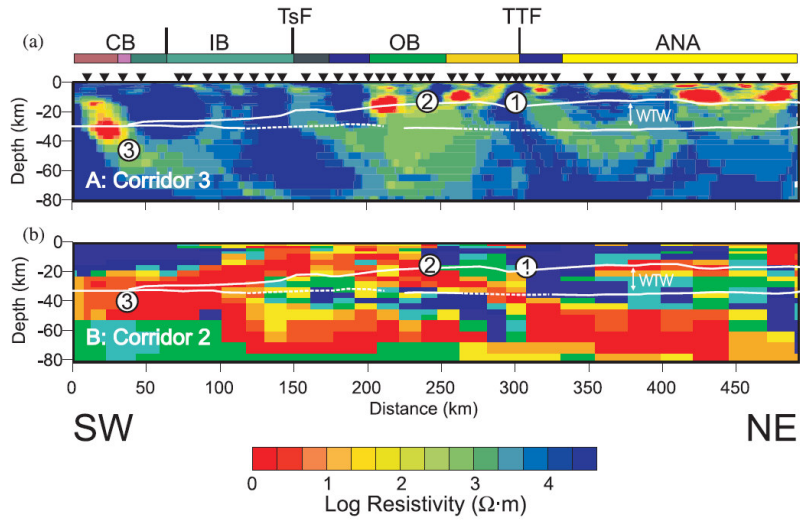

Figure 3.7. 2D resistivity models along SNORCLE Corridors 2 and 3. See Figure 3.6 for location of SNORCLE corridors (from Jones et al, 2005). Arrows indicate where the proposed pipeline crosses each corridor.

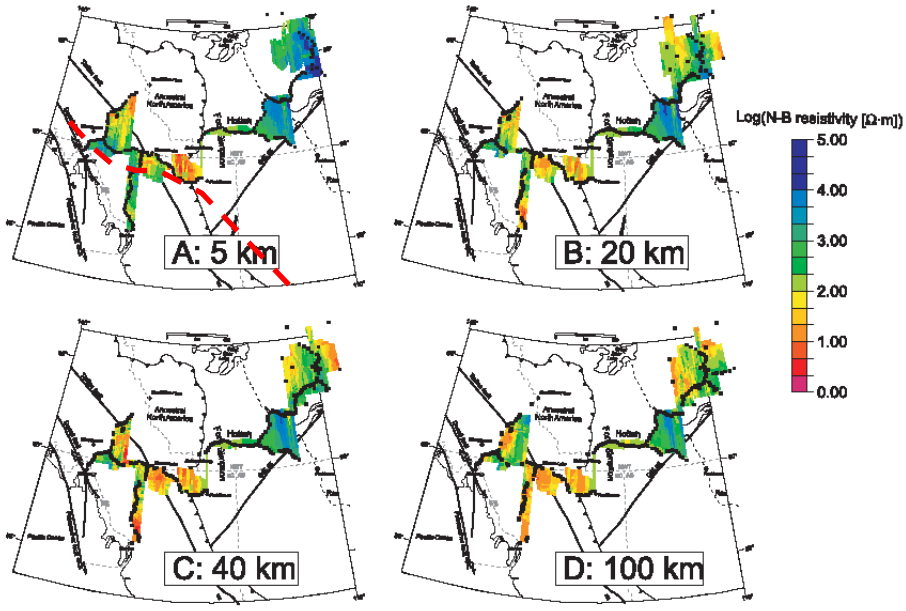

Figure 3.8. Maps of the averaged resistivity at various crustal and mantle depths (A to D) as determined by MT transects along highways in part of northwestern Canada (from Jones et al, 2005). General pipeline route is shown as red dashed line.

3.3. One-Dimensional Resistivity Models Along Pipeline Route

3.3.1. One-Dimensional Modelling of Earth Resistivity

As a first approximation to determine the Earth resistivity structure along the pipeline route, a one dimensional (1D) representation (i.e. layered structures) was chosen as it contains the least complication of geological structure and is the simplest way to broadly assign resistivity values to any particular depth. From the surface downward the layers of a 1D model are as follows: overburden; sedimentary rocks accumulated in a depositional basin (not always present); basement complex (sedimentary, volcanic and intrusive igneous, and metamorphosed rocks) that is considered to be the upper crust; middle and lower crust (sometimes combined into a single layer); and, mantle divisions based on changes of its seismic velocity.

The earliest 1D models, pertaining to pipeline telluric current effects in Alaska, were 2 and 3 layer models prepared by Campbell (1978) for depths to 1200 km (Figure 3.9). These models were used for calculating the geoelectric field for geomagnetic field variations with periods between 5 minutes and 4 hours, penetrating to crustal and mantle depths. Furthermore, Campbell remarked that he used a relatively low resistivity value (500 Ω.m), common to tectonically active mountain belts, to represent the upper crust layer for mountainous Alaska.

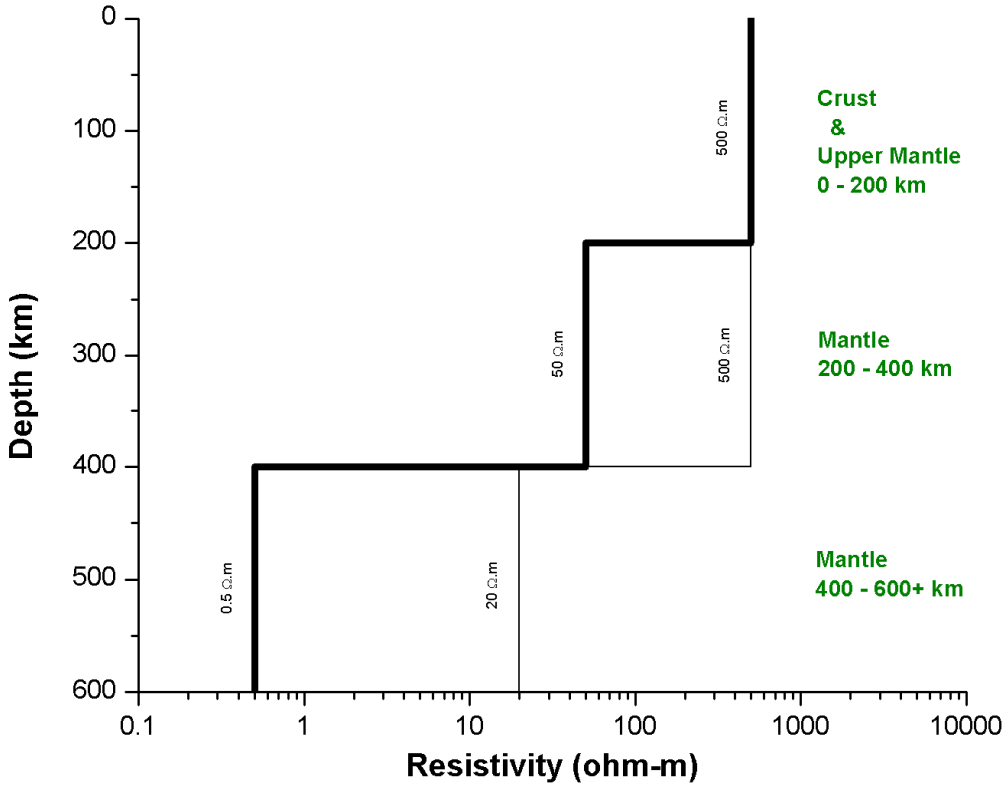

Figure 3.9. Representation of Earth resistivity in Alaska as 2- and 3-layer models shown as light and heavy lines, respectively (modified from Campbell, 1978).

Electrical resistivity values used in the preparation of the pipeline route 1D models were obtained from published reports. An emphasis was placed on using apparent resistivity values obtained from MT surveys, conducted as part of crustal investigations, since such a value would represent the "bulk" resistivity of the Earth material over a large area. However, due to a greater variability of geological conditions for the upper crust layer there is a corresponding larger variance of resistivity than for the lower layers of the crust and mantle where the resistivity is expected to be more uniform

Often the reported resistivity values for a particular layer were conflicting. The approach used was to be consistent in applying the same resistivity value for the same material (type of overburden, a particular sedimentary rock formation or lithotectonic assemblage) or mantle divisions. Selection of a resistivity value for the upper crust layer proved to be most problematic since overall resistivity is dependent on majority of rock type present, degree of metamorphism and structural complexity, and availability of interpreted MT survey data. Another complicating factor for selection of resistivity values is that the MT surveying (as part of crustal transects) was focused on areas of geological interest such as the Denali and Tintina Faults, where conceivably the resistivity of surrounding upper crust could be greatly modified by the formation of or the fault itself. Furthermore, some of the earlier MT survey results show a much higher resistivity than subsequent MT surveying and interpretation have shown.

Results from the TACT-MT survey were used to provide a constraint on the assignment of resistivity values to the upper crust layer for 1D Earth resistivity models covering the Alaska portion of the proposed pipeline route. To obtain an approximate cross-sectional representation of resistivity changes along part of the pipeline route using TACT-MT data, the preliminary interpreted depth and resistivity of the layers for each sounding site were stitched together and then contoured.

Induction logs from oil and gas exploration wells were used to assign resistivity values to sedimentary basin rock (part of the upper crust layer) for that part of the pipeline crossing the Alaska North Slope because no preliminary 1D interpretations prepared from the TACT MT survey have been published. For some zones, airborne EM surveys were available and provided measured resistivity values for the overburden.

Depth of overburden, as well as permafrost thickness, was obtained from examination of surficial geology maps and reports, national atlases, plus landform studies completed for the Trans-Alaska Pipeline (TAPS) pipeline route. Permafrost depths were also presented on some stratigraphic compilation maps of the North Slope. Sedimentary basin depths were obtained from stratigraphic cross-sections (compiled from exploration well logs) and general basin thickness maps. Crustal and mantle layer thickness were obtained from published results of crustal transects done in Alaska, and northwestern Canada. For the 100, 400 and 600 km depths of each mantle division shown in the 1D resistivity models, these are the generally accepted depths in the geological literature.

3.3.2. Earth Resistivity Modelling for Proposed Pipeline

For our analysis of the earth resistivity structure the pipeline route was divided into 8 zones on the basis of lithostratigraphic terranes or subterranes, the concept previously described in section 3.2.2. Those areas of the pipeline underlain by sedimentary basins, which exhibit considerably lower resistivity, were considered as distinct zones although the Superterrane in which they occur was of wider extent. In addition, areas with extensive amounts of intrusive rocks were considered as distinct zones since such rock is usually more resistive. It is also important to realize that for each zone, the resistivity assigned to the layers has been extrapolated from a portion of the zone where a MT survey follows the pipeline route or crosses it at a single location. The assumption is made that the underlying resistivity and layer thickness, as determined by the MT survey, is the same over the entire zone.

Areal extent of each of the eight zones is shown in Figure 3.10. Zone 1 covers the Alaska North Slope and includes the Colville sedimentary basin underlying Prudhoe Bay to the Brooks Range. Zone 2 crosses the Brooks Range mountains. Zones 3, 4 and 5 cover the central and southeastern region of Alaska, with Zones 3 and 5 containing more resistive rocks. Zone 6 comprises much of southern Yukon. Zone 7 crosses part of northeastern British Columbia. Zone 8 is within part of the Western Canada Sedimentary Basin that covers most of the Canadian prairies.

Figures 3.11 to 3.18 present the layered 1D models for each of the eight resistivity zones along the proposed pipeline corridor. For each model an accompanying table (Tables A3.1 to A3.8) is found in Appendix 3A and provides background information on the justification and source(s) of the assigned thickness and resistivity. Notes and abbreviations common to these tables are included at the end of Table A3.8.

Figure 3.19 is a compilation of all the zones and provides a visual comparison of the differences of layer and resistivity between the eight zones. A major difference exists with Zones 1 and 8 compared to the other zones, in that these two zones have a sedimentary basin layer.

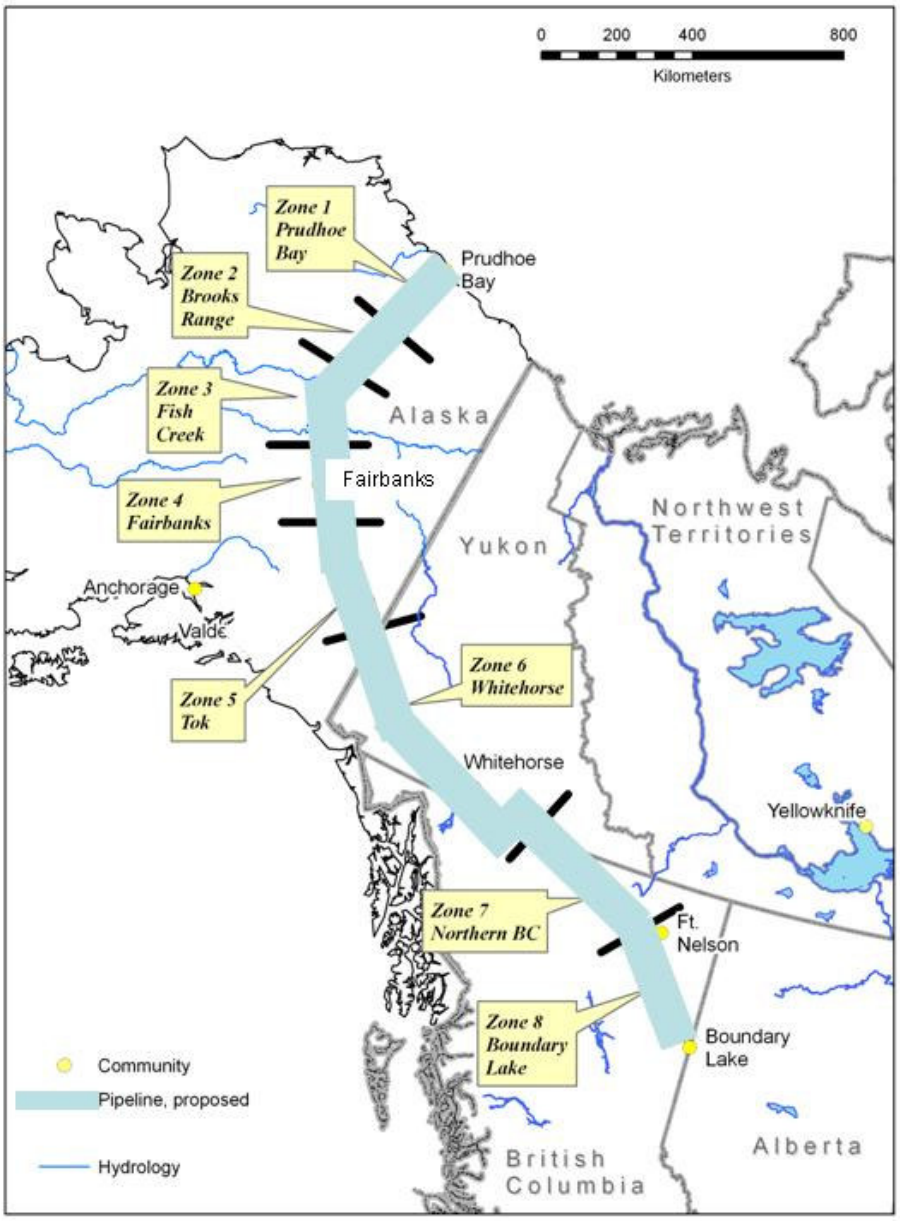

Figure 3.10. Zones along the pipeline route used to produce 1D Earth resistivity models.

3.3.3 Zone 1 - Prudhoe

Zone 1 extends 225 km from Prudhoe Bay (at mileage point AMP-0) to Galbraith Lake (AMP-140) on the north side of the Brooks Range mountains, crossing the Arctic Coastal Plain and Arctic Foothills. Continuous permafrost is about 600m thick at the coast, thinning southward to about 240 m. Overburden is predominantly modern flood-plain alluvium along the Sagvanirktok River which parallels the pipeline route. Underlying crustal rocks of the North Slope subterrane (part of the Arctic Alaska Terrane in the Arctic Superterrane) include a 3.6 km thick sedimentary basin succession of shale, siltstone, sandstone and some limestone over more deformed and metamorphosed sediments. Upper crustal resistivity was obtained by extrapolation from deep-well induction logs completed in the region because interpreted TACT MT survey data was lacking.

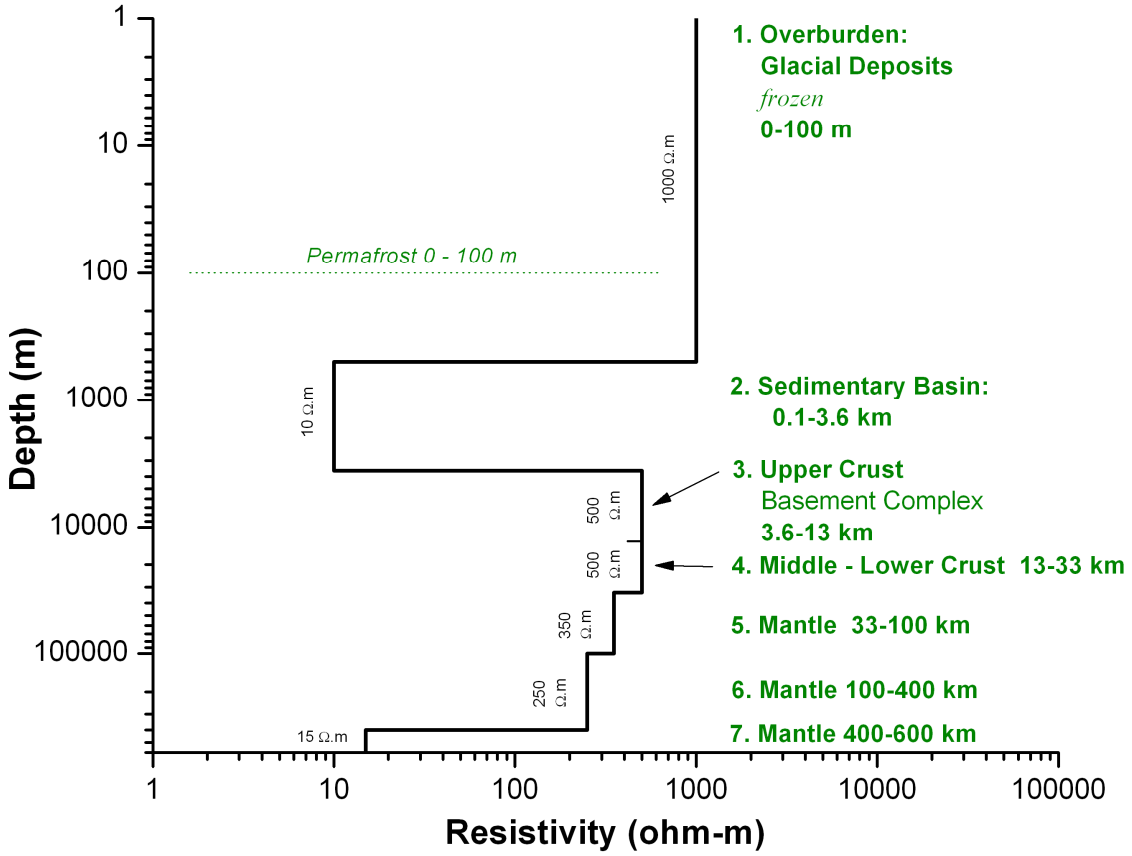

Figure is to be read in conjunction with accompanying table. Resistivity values and depths have been interpreted from published geological reports and maps, and may differ from actual conditions measured by a geophysical survey and/or borehole.

Figure 3.11: 1D Earth resistivity model for Zone 1. Refer to Table A3.1 for additional details.

3.3.4 Zone 2 – Brooks Range

Zone 2 extends 177 km across the Brooks Range from Galbraith Lake (at AMP-140) on the north flank to Middle Fork-Koyukok River (at AMP-250) on the south flank of the mountains. Continuous permafrost reaches a depth of at least 70m. Overburden is predominately coarse colluvium and glacial moraine on the slopes with alluvium on the mountain valley floors. Bedrock is an extensive thrust-faulted thick assemblage of sedimentary and metamorphosed sediments; belonging to a variety of sub-terranes of the Arctic Alaska Terrane. Upper crustal resistivity was obtained from a combination of extrapolation from deep-well logs on the North slope and values from previous preliminary interpretations of the TACT MT soundings.

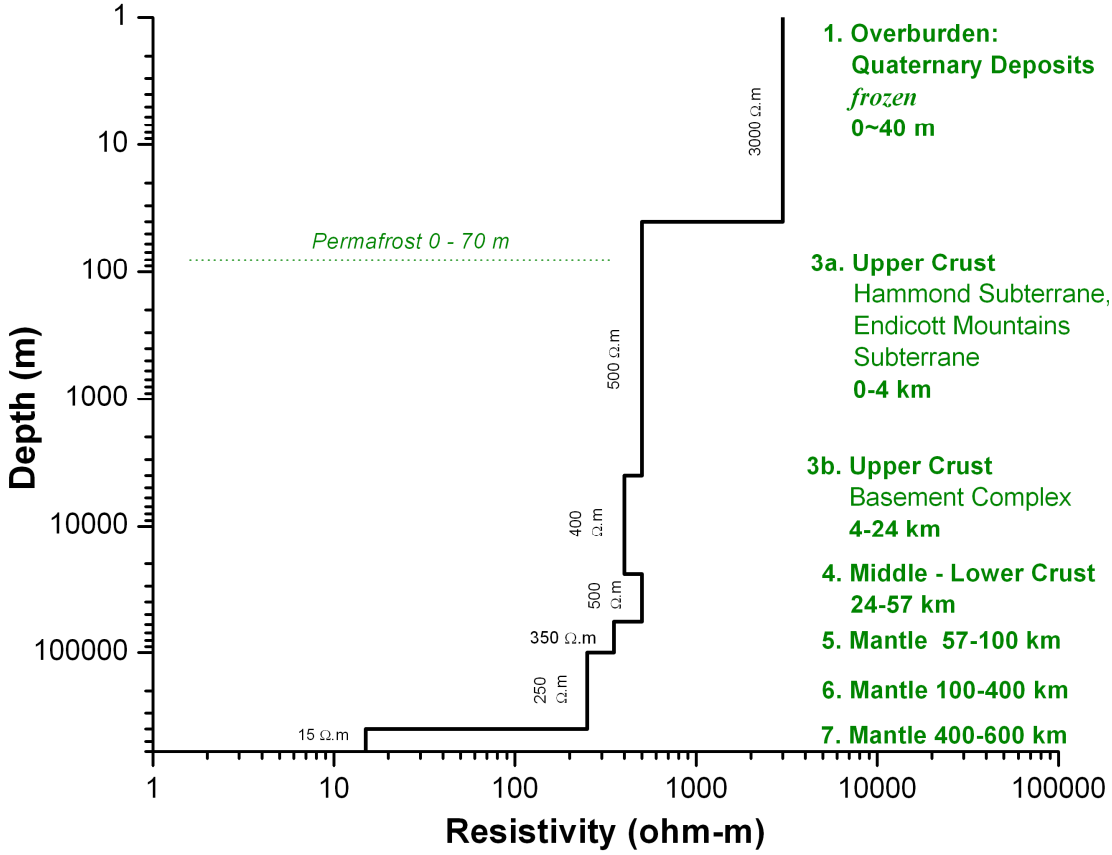

Figure is to be read in conjunction with accompanying table. Resistivity values and depths have been interpreted from published geological reports and maps, and may differ from actual conditions measured by a geophysical survey and/or borehole.

Figure 3.12: 1D Earth resistivity model for Zone 2. Refer to Table A3.2 for additional details.

3.3.5 Zone 3 – Fish Creek

Zone 3 extends 210 km from the south flank of Brooks Range (AMP-250) to the Livengood area (AMP-380), crossing the Porcupine Plateau into the beginning of the Yukon-Tanana Uplands. Permafrost is mostly continuous with depth varying anywhere from less than 25m to over 100m. Overburden is variable, with glacial till in the north, colluvium along hill slopes, and silts in the south. Bedrock is a mix of sedimentary, volcanic and intrusive rocks; belonging to a variety of terranes and sub-terranes of the Arctic Superterrane. The Kaltag – Tintina fault system marks the southern margin of Zone 3. Crustal resistivity was based on average of TACT MT preliminary 1D interpretations.

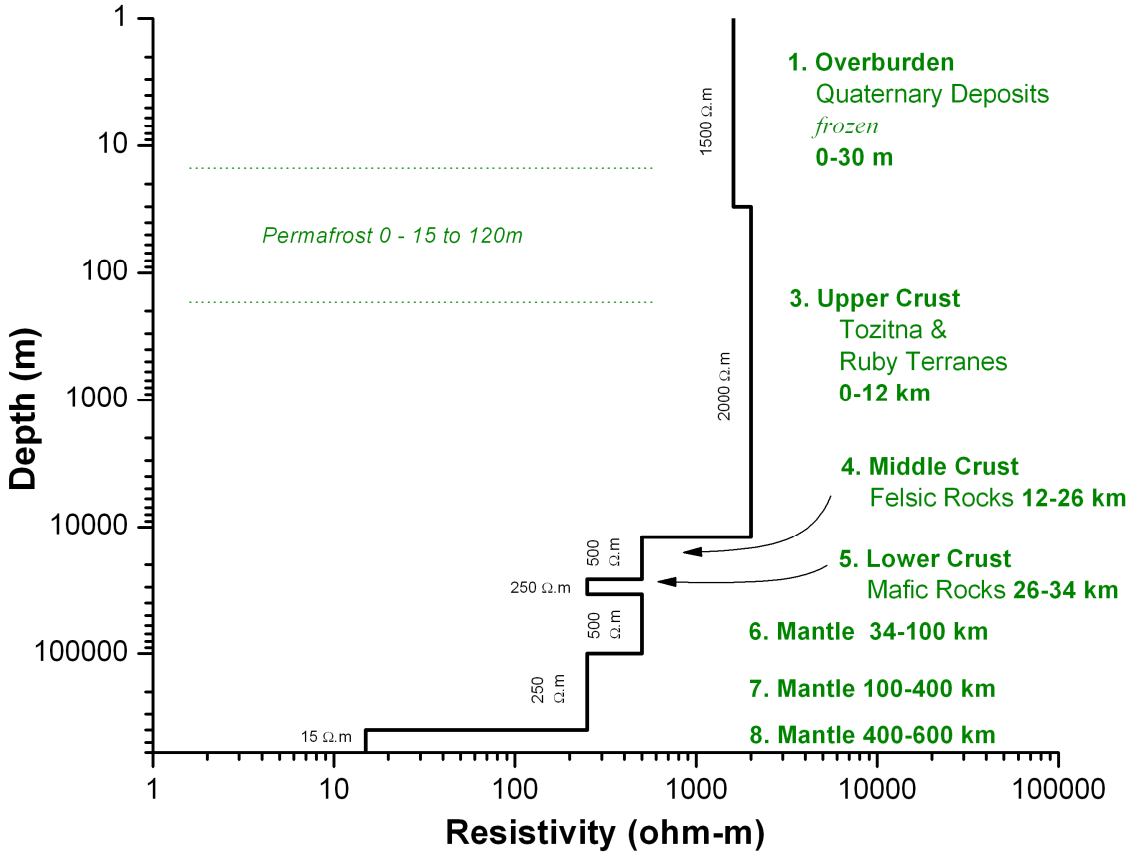

Figure is to be read in conjunction with accompanying table. Resistivity values and depths have been interpreted from published geological reports and maps, and may differ from actual conditions measured by a geophysical survey and/or borehole.

Figure 3.13: 1D Earth resistivity model for Zone 3. Refer to Table A3.3 for additional details.

3.3.6 Zone 4 – Fairbanks

Zone 4 extends 225 km from the Livengood area (AMP-380) to near Big Delta (AMP-520), across the Yukon-Tanana Uplands. Isolated permafrost (discontinuous elsewhere) occurs along Tanana River valley - which parallels much of the pipeline route and highway - with depths ranging from about 30 to 100 m. Overburden is mainly windblown silt with colluvium on hill slopes. Bedrock is comprised of metasediments, undivided metamorphosed rock and minor metavolcanics; belonging to the ancestral North America tectonic realm. The Kaltag – Tintina fault system marks the north margin of Zone 3, and the Shaw Creek fault its south margin. Crustal resistivity was based on average of TACT MT preliminary 1D interpretations.

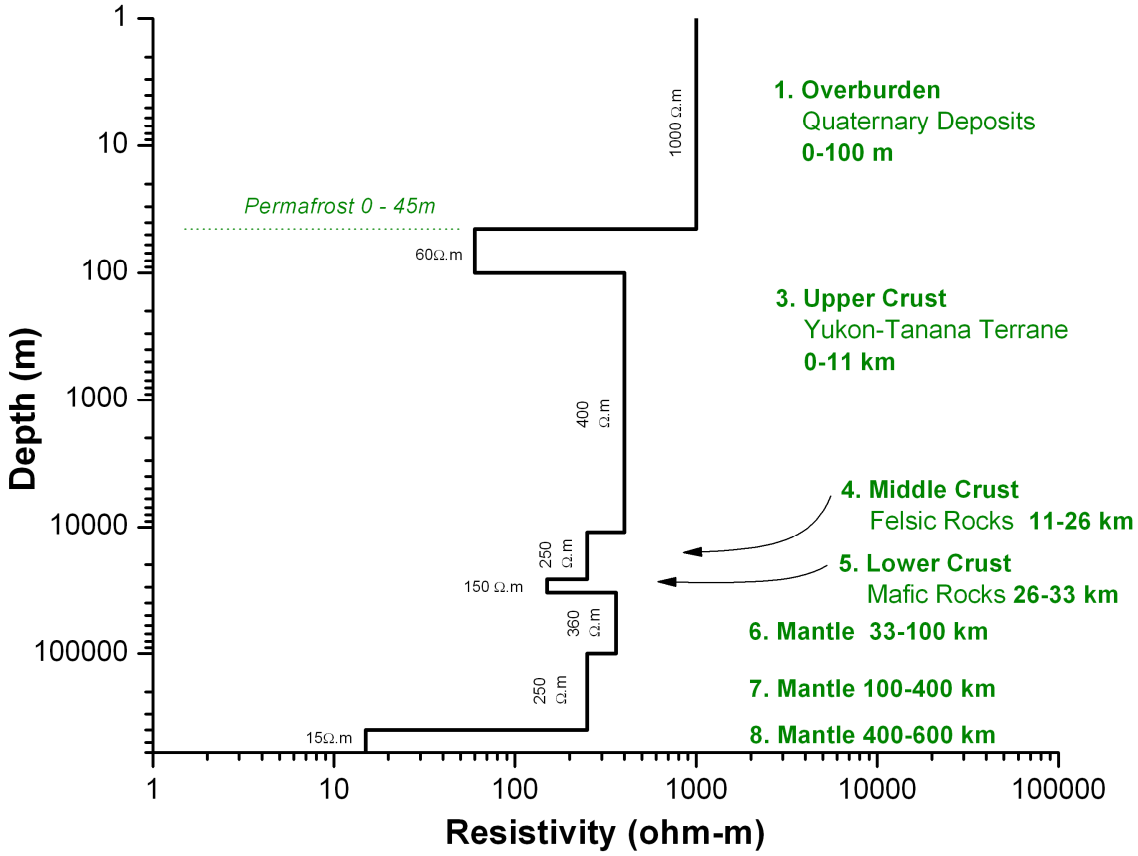

Figure is to be read in conjunction with accompanying table. Resistivity values and depths have been interpreted from published geological reports and maps, and may differ from actual conditions measured by a geophysical survey and/or borehole.

Figure 3.14: 1D Earth resistivity model for Zone 4. Refer to Table A3.4 for additional details.

3.3.7 Zone 5 – Tok

Zone 5 extends 344 km from near Big Delta (AMP-520) to the Alaska-Yukon border (AMP-734 / YKP-0), across the continuation of the Yukon-Tanana Uplands and in the Tanana river valley. Sporadic and/or isolated permafrost (discontinuous elsewhere) occurs along Tanana River valley which parallels much of the pipeline route and highway with depths ranging from about 10 to 60 m. Overburden exhibits rapid changes from modern flood-plain alluvium, alluvial fans to glacial outwash and moraines. Bedrock is strongly deformed metasediments with some younger volcanic rock, and extensive masses of intrusive rock; belonging either to ancestral North America or the Yukon-Tanana Terrane. The Shaw Creek fault marks the north margin of Zone 5. Upper crustal resistivity was obtained from examination of a contour plot of stitched TACT MT preliminary 1D interpretations. Crustal resistivity was based on average of TACT MT preliminary 1D interpretations. High resistivity of upper crust is attributed to presence of intrusive igneous rock.

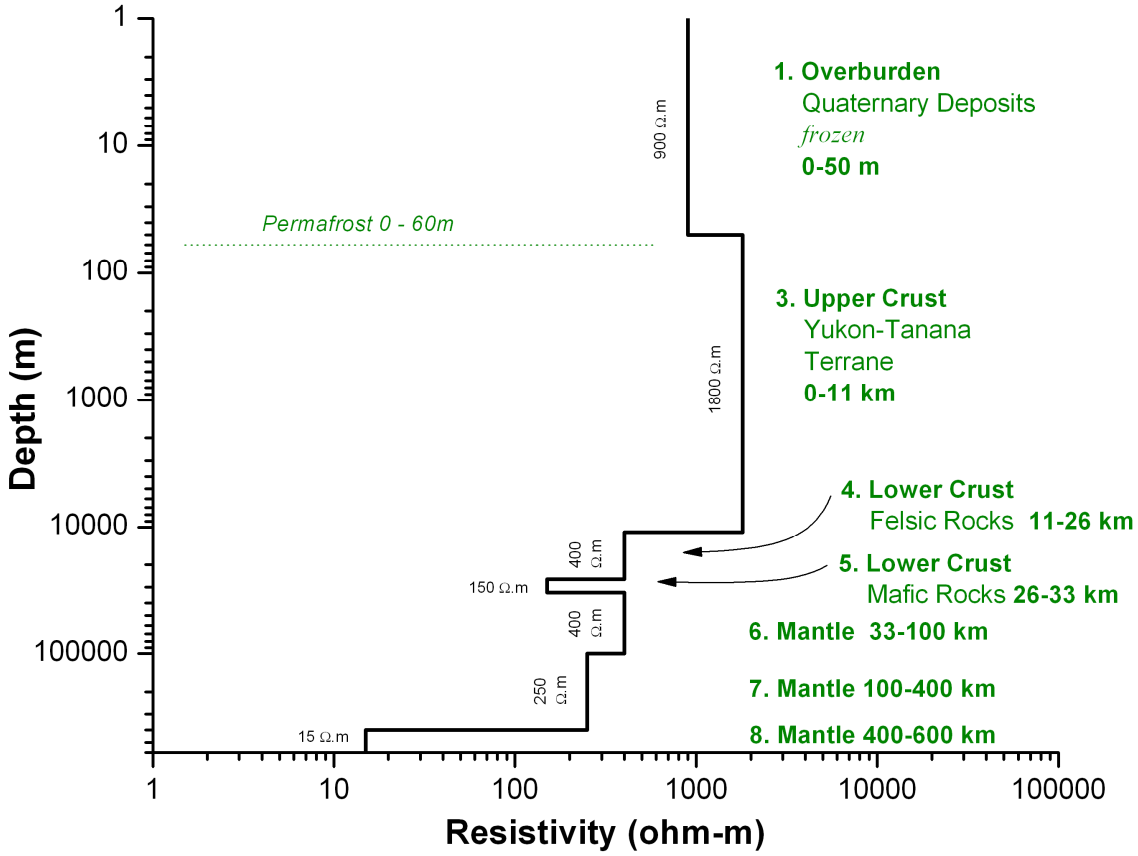

Figure is to be read in conjunction with accompanying table. Resistivity values and depths have been interpreted from published geological reports and maps, and may differ from actual conditions measured by a geophysical survey and/or borehole.

Figure 3.15: 1D Earth resistivity model for Zone 5. Refer to Table A3.5 for additional details.

3.3.8 Zone 6 – Whitehorse

Zone 6 extends 862 km from the Alaska-Yukon border (YKP-0) to Watson Lake / Lower Post area (BKP-30), across the Yukon Plateau, part of the Cassiar Mountains and into the Laird Plateau. Sporadic-discontinuous permafrost reaches a depth of about 10m. Overburden is variable. Bedrock consists of assemblages of meta-sediments, meta-volcanics, with considerable intrusive rock in the Whitehorse area; belonging to various terranes (largest being the Yukon-Tanana Terrane) that make up the Intermontane Superterrane. The Denali fault runs parallel to part of the pipeline route, with the Teslin Fault crossing the route, and the Tintina fault being the south margin of Zone 6. Crustal resistivity was obtained from regional combined seismic and MT crustal transects across the centre of the zone. High resistivity of the upper crustal rocks is consistent with presence of mafic/felsic rocks, interlayered with clastic sedimentary and carbonate rocks, and intrusive igneous rock (Wennberg and Ferguson, 2002). High resistivity of upper mantle possibly due to low-density rock and heat content (Ledo et al, 2004).

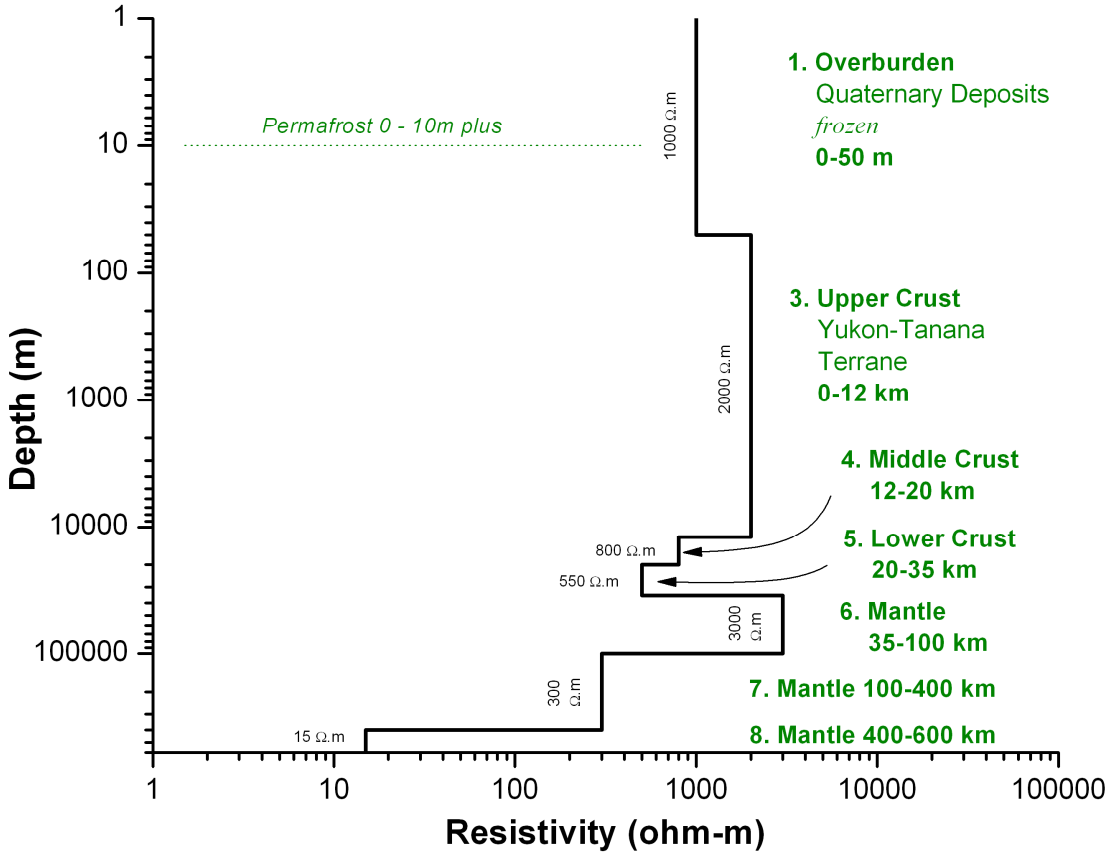

Figure is to be read in conjunction with accompanying table. Resistivity values and depths have been interpreted from published geological reports and maps, and may differ from actual conditions measured by a geophysical survey and/or borehole.

Figure 3.16: 1D Earth resistivity model for Zone 6. Refer to Table A3.6 for additional details.

3.3.9 Zone 7 – Northeastern BC

Zone 7 extends 350 km from the Watson Lake / Lower Post area (BKP-30) to Steamboat (BKP-380), across the Laird Plain. Sporadic-discontinuous permafrost can exist at depths of less than 10 m. Overburden is predominately till veneer and blanket with glaciolucustrine sand and gravel. Bedrock consists of thrust-faulted weakly metamorphosed sediments; belonging to the ancestral North American tectonic realm. The Tintina fault occurs at the north margin of Zone 7. Upper crustal resistivity was obtained from a regional MT crustal transect along the length of the zone. Diminished resistivity of the upper crustal rocks has been attributed to presence of carbonaceous shales (Ledo et al, 2004).

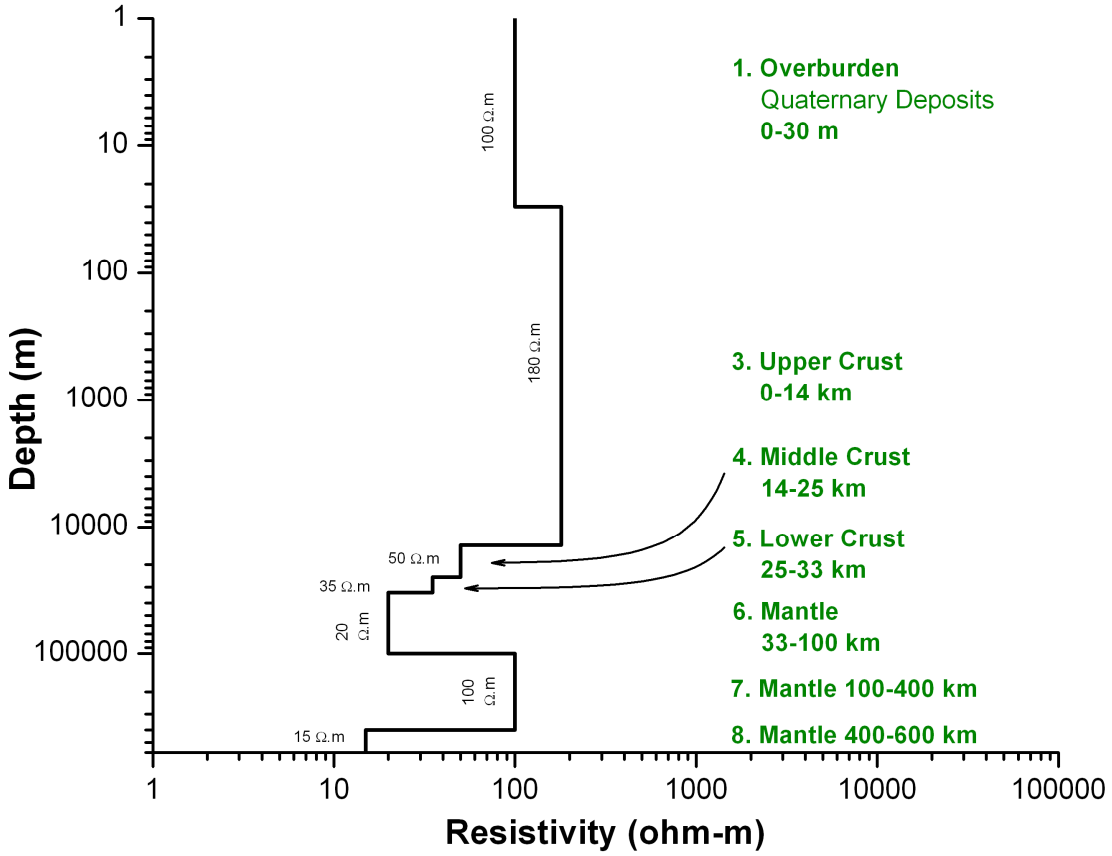

Figure is to be read in conjunction with accompanying table. Resistivity values and depths have been interpreted from published geological reports and maps, and may differ from actual conditions measured by a geophysical survey and/or borehole.

Figure 3.17: 1D Earth resistivity model for Zone 7. Refer to Table A3.7 for additional details.

3.3.10 Zone 8 – Boundary Lake

Zone 8 extends 343 km across part of the Fort Nelson Lowland and into the Alberta Plateau, from the Steamboat area (BKP-380) to the end of the pipeline route at Boundary Lake (BKP-722) on the Alberta-BC provincial border. Sporadic-discontinuous to isolated patches of permafrost occurs in the northern half of Zone 8. Overburden is predominately till veneer and blanket with glaciolucustrine sand and gravel in the main river valleys. Bedrock consists of the gently dipping to moderately folded 4 km thick Western Canada Sedimentary Basin that overlies a complex crystalline Precambrian basement which includes anomalous conductive zones and the Great Slave Lake Shear Zone. Crustal resistivity was obtained from a recent assessment of MT responses in northwestern Alberta (Turkoglu et al, 2009). The exceptionally low resistivity of upper crustal rocks in the Boundary Lake area is likely due to the presence of the 700m thick Cretaceous Manville Group, a highly carbonaceous shale which is electrically conductive (Boerner et al, 2000). Low resistivity measured in the lower crust layer could be due to organic material and carbonates transported to depth in an ancient fossil subduction zone and converted to electrically conductive graphite (Turkoglu et al, 2009).

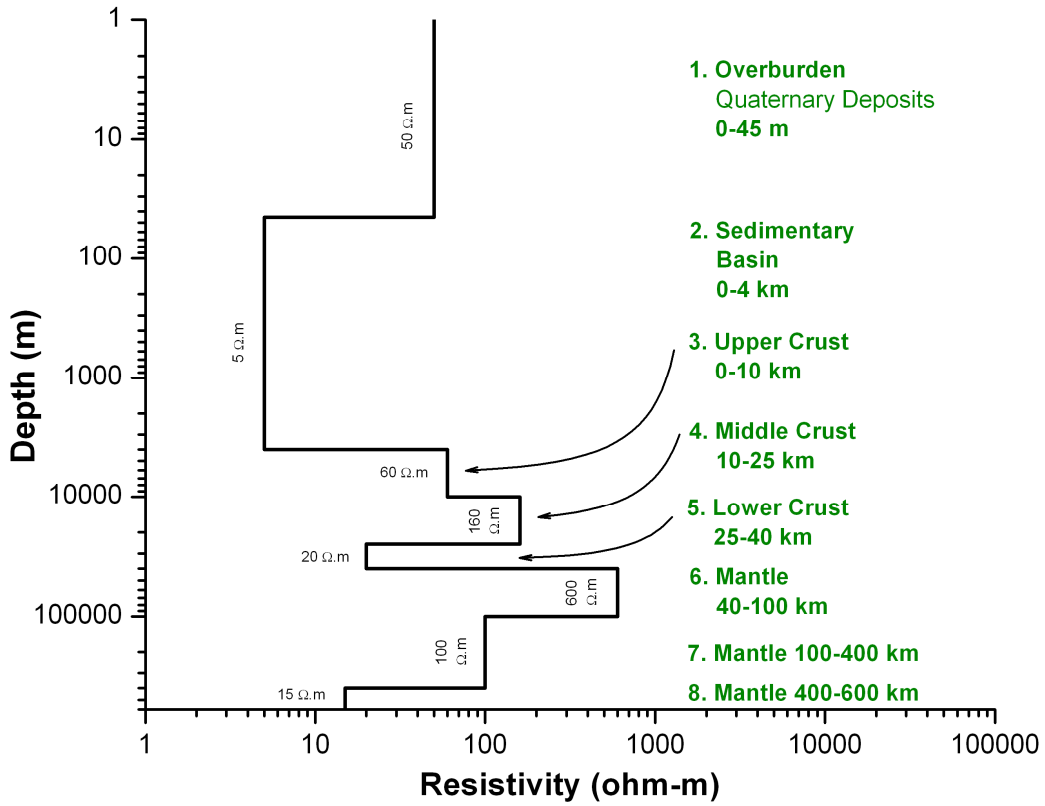

Figure is to be read in conjunction with accompanying table. Resistivity values and depths have been interpreted from published geological reports and maps, and may differ from actual conditions measured by a geophysical survey and/or borehole.

Figure 3.18: 1D Earth resistivity model for Zone 8. Refer to Table A3.8 for additional details.

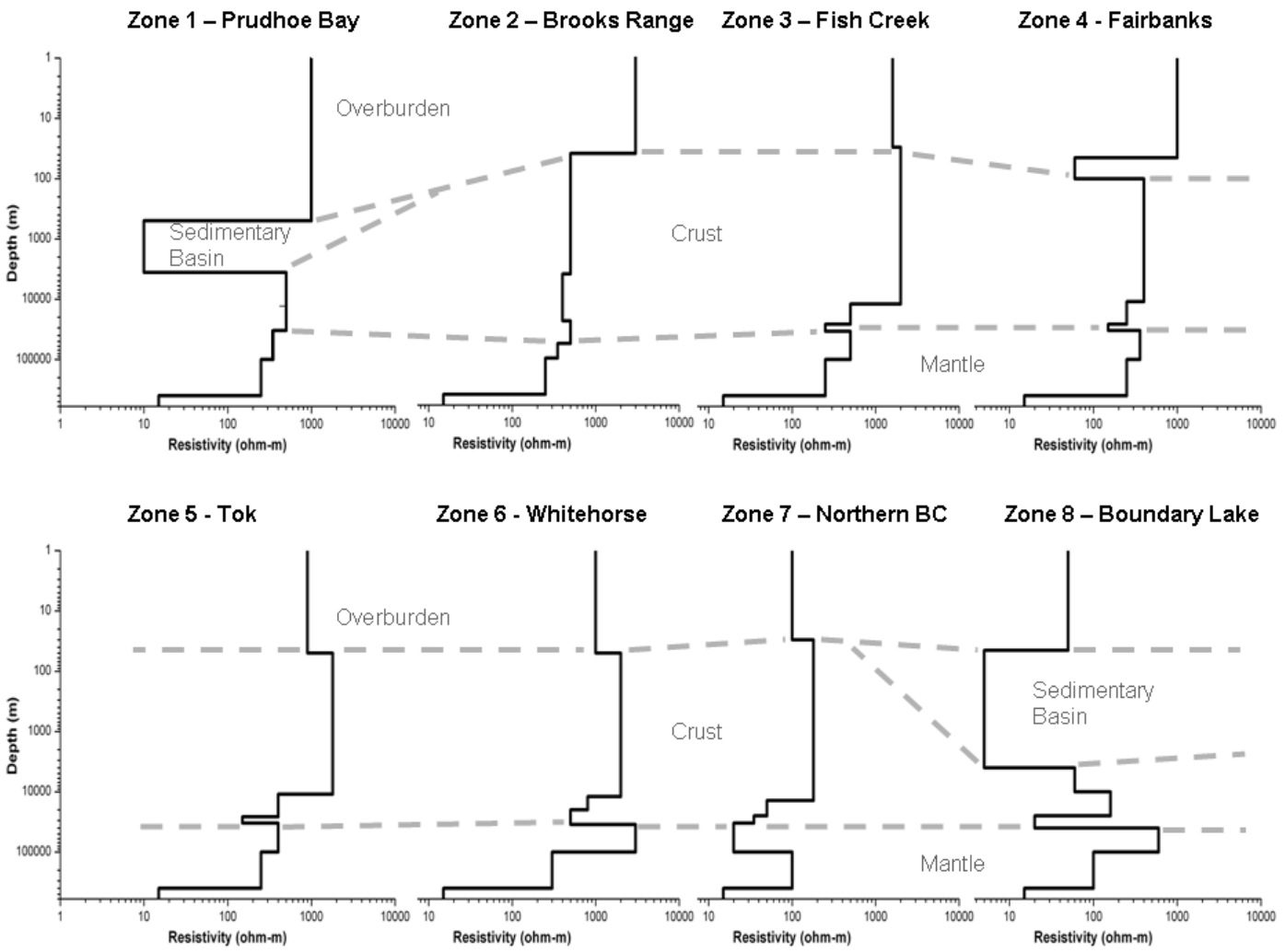

Figure 3.19. Compilation of the eight 1D Earth resistivity models along the proposed pipeline route.

References

Alberta Geological Survey, 2009. Geology of Alberta Interactive Map (on-line) <http://www.ags.gov.ab.ca> [accessed November, 2009].

Associated Mining Consultants Ltd., 2004. Report on the application of electrical and electromagnetic techniques in the design and construction of northern pipelines; Geological Survey of Canada, Open File Report.

Atlas of Canada, 2009. Permafrost. < http://atlas.nrcan.gc.ca/site/english/maps/environment/land/permafrost> [accessed November, 2009].

Beikman, H.M., 1980. Geologic map of Alaska, U.S. Geological Survey, Special Map, 2 sheets, scale 1:2,500,000.

Best, M.E., Leveson, V.M., Ferbey, T. and McConnell, D., Airborne electromagnetic mapping for buried Quaternary sands and gravels in northeast British Columbia, Canada, Journal of Environmental and Engineering Geophysics, v.11, no.1, p.17-26.

Boerner, D.E., Kurtz, R.D., Craven, J.A., Ross, G.M. and Jones, F.W., 2000. A synthesis of electromagnetic studies in the Lithoprobe Alberta Basement Transect: constraints on Paleoproterozoic indentation tectonics, Can. J. Earth Sci, v.37, p.1509-1534.

Bouzidi, Y., Schmitt, D.R., Burwash, R.A., and Kanasewich, E. R., 2002. Depth migration of deep seismic reflection profiles: crustal thickness variation in Alberta, Can. J. Earth Sci, v.39, p.331-350.

Brown J., and Kreig, R.A., 1983. 1983, Guidebook to permafrost and related features along the Elliott and Dalton Highways, Fox to Prudhoe Bay, Alaska, Alaska Division of Geological & Geophysical Surveys, Guidebook 4, 230 p.

Burn, C., 2005. Future permafrost response to climate change: lessons from ground temperature measurements in Takhini Valley, southern Yukon Territory, Rapid Landscape change and Human Response in the Arctic and Sub-Arctic, June 15-18, 2005, Whitehorse, Yukon, Abstracts http://atlas-conferences.com/c/a/p/x/56.htm [accessed November, 2009].

Burns, L.E., Fugro Airborne Surveys Corp., and Stevens Exploration Management Corp., 2006., 40,000 coplanar apparent resistivity of the Alaska Highway corridor, east-central Alaska, parts of Big Delta and Mt. Hayes quadrangles: Alaska Division of Geological & Geophysical Surveys Geophysical Report 2006-6-3A, 1 sheet, scale 1:63,360.

Burns, L.E., Fugro Airborne Surveys Corp., and Stevens Exploration Management Corp., 2006., 400 coplanar apparent resistivity of the Alaska Highway corridor, east-central Alaska, parts of Mt. Hayes Quadrangle: Alaska Division of Geological & Geophysical Surveys Geophysical Report 2006-6-6B, 1 sheet, scale 1:63,360.

Campbell, D. L.; Sampson, J. A.; Wise, R. A.; Williams, J. M., 2001. Magnetotelluric and audiomagnetotelluric data collected in Alaska by the U. S. Geological Survey, 1985-1992, version 1, U.S. Geological Survey Open-File Report 2001-053, 1 computer optical disk.

Campbell, W.H., 1978. Induction of auroral zone electric currents within the Alaska pipeline, Pure and Applied Geophysics, v.116, no.6, p.1143-1173.

Carrara, P.E., 2004. Surficial geologic map of the Tanacross B-5 Quadrangle, east-central Alaska, 1 sheet, scale 1:63,360.
(available on-line <http://pubs.er.usgs.gov/usgspubs/sim/sim2856>
[accessed November 2009].

Carrara, P.E., 2006. Surficial geologic map of the Tanacross B-4 Quadrangle, east-central Alaska, Scientific Investigations Map 2935, 1 sheet, scale 1:63,360.
(available on-line only <http://pubs.er.usgs.gov/usgspubs/sim/sim2935>
[accessed November 2009].

Clowes, R.M., Hammer, P.T.C., Fernandez-Viejo, G. and Welford, J.K., 2005. Lithospheric structure in northwestern Canada from Lithoprobe seismic refraction and related studies: a synthesis, Can. J. Earth Sci., v.42, p.1277-1293.

Collett, T. S., Bird, K. J., Kvenvolden, K. A., and Magoon, L. B., 1988. Geologic interrelations relative to gas hydrates within the North Slope of Alaska, U.S. Geological Survey, Open File Report 88-389, 150 p.

Dobrin, M.H., and Savit, C.H., 1988. Introduction to geophysical prospecting, 4th ed; McGraw-Hill Company, New York, 867 p.

Ferguson, I.J. 2008. Web page, Faculty and their research, Dept. of Geological Sciences, University of Manitoba. Retrieved Sept. 2008.
<http://www.umanitoba.ca/geoscience/people/faculty/ferguson/iferguson.htm>
[accessed May 29, 2009].

Ferguson, I. J., and Odwar, H.D., 1997. Review of conductivity soundings in Canada. Appendix 3, v.3; *in* Geomagnetically induced currents: Geomagnetic Hazard Assessment Phase II, Final Report, (contributing authors) D.H. Boteler, S. Boutilier, D. Swatek, Q. Bui-Van, R. Leonard, B. Hughes, L. Hajagos, I.J. Ferguson, and H.D. Odwar, Geological Survey of Canada and Canadian Electricity Association, 357 T 848A, p.A3-1-A3-121.

Ferguson, I. J., and Odwar, H.D., 1998. Conductivity structure of Canada, v.1; *in* Geomagnetically induced currents: Geomagnetic Hazard Assessment Phase II, Final Report, (contributing authors) D.H. Boteler, S. Boutilier and A.K. Wong, D. Swatek, Q. Bui-Van, R.

Ferrians, Jr., O.J., 1965. Permafrost map of Alaska, U.S. Geological Survey, Miscellaneous Geologic Investigations Map I-445, scale 1, 2,500,000.

Fisher, M.A., Pellerin, L., Ratchkovski, N.A., Nokleberg, W.J., Pellerin, L. and Glen, J.M.G., 2004, Geophysical data reveal the crustal structure of the Alaska Range orogen within the aftershock zone of the M7.9 Denali Fault earthquake, Bull. Seismological Soc. Of America, v.94, No.6B, p.5107-5131.

Fisher, M.A., Pellerin, L., Nokleberg, W.J., Ratchkovski, N.A, Glen, J.M.G., 2007, Crustal structure of the Alaska Range orogen and Denali fault along the Richardson Highway, *in* K.D. Ridgeway, J.M. Trop, J.M.G. Glen, and J.M. O'Neil (eds.), Tectonic Growth of a Collisional Continental margin: Crustal Evolution of Southern Alaska, Geological Society of America Special Paper 431, p.43-53.

Fuis, G.S., Moore, T.E., Plafker, G., Brocher, T.M., Fisher, M.A., Mooney, W.D., Nokleberg, W.J., Page, R.A., Beaudoin, B.C., Christensen, N.I., Levander, A.R., Lutter, W.J., Saltus, R.W., and Ruppert, N.A., 2008. Trans-Alaska Crustal Transect and continental evolution involving subduction underplaying and synchronous foreland closing, Geology, v.36, no.3, p.267-270.

Fulton, R.J., 1995. Surficial materials of Canada, Geological Survey of Canada, "A" Series Map 1880A, scale 1:5,000,000.

Grantz, A. Moore, T.E., and Roeske, S., 1991. A-3 Gulf of Alaska to Arctic Ocean: Boulder, Colorado, Geological society of America, Centennial Continental/Ocean Transect no. 15, 3 sheets with text, scale 1:500,000.

Hackbarth, D.D., 1978. Hydrogeological map of the Grande Prairie area, Alberta, NTS 83M, Map 125, Alberta Geological Survey, scale 1: 250,000.

Hartman, G.M.D. and Clague, J.J., 2008. Geology of northeastern British Columbia and northwestern Alberta; diamonds, shallow gas, gravel and glaciers, Can. J. Earth Sci., v.45, no.5, p.549-564.

Jones, A.G., 1992. Electrical conductivity of the continental lower crust, in Chapter 3, Continental Lower Crust, Developments in Geotectonics 23, Elsevier, (ed.) D.M. fountain, R. Arculus, and R.W. Kay, p.81-143.

Jones, A.G., 1999. Imaging the continental upper mantle using electromagnetic methods, Lithos, v.48, p.57-80.

Jones, A.G., Ledo, J., Ferguson, I.J., Farquharson, C., Garcia, X., Grant, N., McNeice, G., Spratt, J., Wennberg, G., Wolynec, L., and Wu, X., 2005. The electrical resistivity structure of Archean to Tertiary lithosphere along 3200 km of SNORCLE profiles, northwestern Canada, Can. J. Sci. v.42, p.1257-1275.

Kachadoorian, R., 1971a. Preliminary engineering geologic maps of the proposed Trans-Alaska pipeline route, Wiseman and Chandaler quadrangles, U.S. Geological Survey, Open-File Report 71-164, scale 250,000.

Kachadoorian, R., 1971b. Preliminary engineering geologic maps of the proposed Trans-Alaska pipeline route, Bettles and Beaver quadrangles, U.S. Geological Survey, Open-File Report 71-165, scale 250,000.

Kachadoorian, R., 1971c. Preliminary engineering geologic maps of the proposed Trans-Alaska pipeline route, Livengood and Tanana quadrangles, U.S. Geological Survey, Open-File Report 71-166, scale 250,000.

Keller, M. A. and Bird, K.J., 2003. Petroleum source potential of the Lower Cretaceous mudstone succession of the NPRA and Colville Delta area, North Slope Alaska, based on sonic and resistivity logs, U.S. Geological Survey, Open-File Report 03-325, poster < http://pubs.er.usgs.gov/usgspubs/ofr/ofr03325> [accessed May 29, 2009]

Klassen, R.W., 1997. Surficial Geology, Coal River [West Half], Yukon Territory, Geological Survey of Canada, Preliminary Map 13-1982, scale 1:250,000.

Klassen, R.W. and Morison, S.R., 1981. Surficial geology, Watson Lake, Yukon Territory, Geological Survey of Canada, Preliminary Map 21-1981, scale 1:250,000.

Kreig, R.A., and Reger, R.D., 1982, Air-photo analysis and summary of landform soil properties along the route of the trans-Alaska pipeline system, Alaska Division of Geological & Geophysical Surveys, Geologic Report 66, 149 p.

Kumar, N., Bird, K.J., Nelson, P.H., Grow, J.A. and Evans, K.R., 2002. A digital atlas of hydrocarbon accumulations within and adjacent to the National Petroleum Reserve-Alaska (NPRA), U.S. Geological Survey, Open-File Report 02-71, version 1.0., 80 p. < http://pubs.er.usgs.gov/usgspubs/ofr/ofr0271> [accessed May 29, 2009]

Ledo, J., Jones, A.G., Ferguson, I.J. and L. Wolynec, L. (2004), Lithospheric structure of the Yukon, northern Canadian Cordillera, obtained from magnetotelluric data, J. Geophys. Res., v.109, B04410, 15p..

Mackay, D.K., 1979. Electrical resistivity measurements in frozen ground, Mackenzie Delta area, Northwest Territories, in Hydrology of Deltas, Proceeding of the Bucharest Symposium, Vol.2, p.363-375.

Magoon, L.B., Bird, K.J., Claypool, G.E., Weitzman, D.E., and Thompson, R. H., 1988. Organic geochemistry, hydrocarbon occurrence, and stratigraphy of government-drilled wells, North Slope, Alaska, *in* Chapter 19, Geology and Exploration of the National Petroleum Reserve in Alaska, 1974 to 1982, (ed.) G. Gryc, U.S. Professional Paper 1399, p. 483-488.

Mair, J.L., Hart, C.J.R., and Stephens, J.R., 2006. Deformation history of the northwestern Selwyn Basin, Yukon, Canada: implications for orogen evolution and mid-Cretaceous magmatism, GSA Bulletin, v.118, no.3/4, p.304-323.

Miller, J.A. and Whitehead, R.L., 1999. Ground water atlas of the United States: Segment 13, Alaska, Hawaii, Puerto Rico, and the U.S. Virgin Islands, Hydrologic Atlas Report Number 730-N, US Geological Survey, 36p. <http://pubs.er.usgs.gov/usgspubs/ha/ha730N> [accessed November 2009]

Moore, T.E., Wallace, W.K., Bird, K.J., Karl, S.M., Mull, C.G., and Dillon, J.T., 1994. Generalized geologic map and sections for Northern Alaska, Plate 6, various scales; *in* The Geology of Alaska, (ed.) G. Plafker and H.C. Berg, Geological Society of America, The Geology of North America, v. G-1, plate 6, various scales.

Morison, S.R. and Klassen, R.W., 1991. Surficial geology, Whitehorse, Yukon Territory, Geological Survey of Canada, Preliminary Map 12-1990, scale 1:100,000.

Morison, S.R. and Klassen, R.W., 1997. Surficial geology, Teslin, Yukon Territory, Geological Survey of Canada, "A" Series Map 1891A, scale 1:125,000.

Mull, C.G., and Adams, K.E., 1989, Bedrock geology of the eastern Koyukuk Basin, central Brooks Range, and east central Arctic Slope along the Dalton Highway, Yukon River to Prudhoe Bay, Alaska: Alaska Division of Geological & Geophysical Surveys Guidebook 7 vol. 2, 167 p., 1 sheet, scale 1:2,851,200.

Mussett, A.E., and Khan, M.A., 2000. Looking into the Earth; An Introduction to Geological Geophysics, Cambridge Univ. Press, Cambridge, UK, 470 pp.

Nelson, J. and Colpron, M., 2007. Tectonics and Metallogeny of the British Columbia, Yukon and Alaskan Cordillera, 1.8 Ga to Present, *in* Mineral Deposits of Canada: A Synthesis of Major Deposit-types, District Metallogeny, the Evolution of Geological Provinces, and Exploration Methods, W.D. Goodfellow (ed.), Special Publication 5, Mineral Deposits Division, Geological Association of Canada, p.755-792 <http://gsc.nrcan.gc.ca/mindep/synth_prov/cord/index_e.php> [accessed November 2009].

Nelson, P.H., and Kibler, J.E., 2001. Well logs and core data from selected cored intervals, National Petroleum Reserve, Alaska, U.S. Geological Survey, Open File Report 01-167. (well logs available on-line at <http://pubs.er.usgs.gov/ >) [accessed May 29, 2009].

Palacky, G.J., 1988. Resistivity characteristics of geologic targets, *in* electromagnetic Methods in Applied Geophysics-Theory, Volume 1, M.N. Nabighian (ed.), Society of Exploration Geophysicists, Tulsa, Oklahoma, p.53-129.

Plafker, G., and Berg, H.C., 1994. Overview of the geology and tectonic evolution of Alaska, *in* Chapter 33, The Geology of Alaska, (ed.) G. Plafker and H.C. Berg, Geological Society of America, The Geology of North America, p.989-1021.

Parkhomenko, E. I. & Keller, G.V., 1967 Electrical Properties of Rocks*, translated from Russian and edited by George V. Keller* Plenum Press, New York.

Plover, P.W.J., 1996. Graphite and electrical conductivity in the lower continental crust: a review, Phy. Chem. Eunh, v.21, no.4, p.279-287.

Rawlinson, S.E., 1983, Guidebook to permafrost and related features at Prudhoe Bay, Alaska Division of Geological & Geophysical Surveys Guidebook 5, 150 p.

Reger, R.D., and Solie, D.N., 2008. Reconnaissance interpretation of permafrost, Alaska Highway corridor, Delta Junction to Dot Lake, Alaska: Alaska Division of Geological & Geophysical Surveys, Preliminary Interpretive Report 2008-3C, 10 p., 2 sheets, scale 1:63,360.

Ross, G.M., and Eaton, D.W., 2002. Proterozoic tectonic accretion and growth of western Laurentia: results from Lithoprobe studies in northern Alberta, Can. J. Earth Sci., v.39, p.313-329.

Scott, W.J., Sellmann, P.V., and Hunter, J.A., 1990. Geophysics in the study of permafrost, in S.H. Ward (ed.), Geotechnical and Environmental Geophysics, Vol.1: Review and Tutorial, Society of Exploration Geophysicists, p.355-384.

Sheriff, R.E., 2002. Encyclopedic dictionary of applied geophysics, 4th ed, Society of Exploration Geophysics, 429 pp.

Simpson, F., and Bahr, K., 2005. Practical Magnetotellurics, Cambridge University Press, 254. p.

Stanley, W.D., Labson, V.F., Nokleberg, W.J., Csejtey, Jr., B., and Fisher, M.A., 1990. the Denali fault system and Alaska Range of Alaska: evidence for underplayed Mesozoic flinch from magneto telluric surveys, Geological Society of America Bulletin. v.102, p.160-173.

Till A.B., Desmoulins, J.A., Moore, T.E., Black, H.A., and Sawyer, B.R., 2008. Bedrock geologic map of the southern Brooks Range, Alaska, and accompanying condone data, U.S. Geological Survey, Open-file Report 2008-1149, 88 p., 2 sheets, sheet 1-scale 1:500,000, sheet 2-scale 1:600,000.

Trommelen, M. and Levson, V., 2008. Quaternary stratigraphy of the Prophet River, northeastern British Columbia, Can. J. Earth Sci., v.45, no.5, p.565-575.

Turkoglu, E., Unworthy, M. and Pane, D., 2009. Deep electrical structure of northern Alberta (Canada): implications for diamond exploration, Can. J. Earth Sci, v.46, p.139-154.

Villeneuve, M.E., Ross, G.M., Thermal, R.J., Miles, M., Parrish, R.R., and Broome, J., 1993. Tectonic subdivision and U-Pb geochronology of the crystalline basement of the Alberta Basin, western Canada, Geological Survey of Canada, Bulletin 447, 86 p.

Weber, F.R., 1971. Preliminary engineering geologic maps of the proposed Trans-Alaska pipeline route, Fairbanks and Big Delta quadrangles, U.S. Geological Survey, Open-File Report 71-318, scale 250,000.

Welford, J.K., Clowes, R.M., Ellis, R.M., Spence, G.D., Asudeh, I., and Hajnal, Z., 2001. Lithospheric structure across the craton-Cordilleran transition of northeastern British Columbia, Can. J. Earth Sci., v.38, p.1169-1189.

Wu, X., 2001. Determination of near-surface, crustal and lithospheric structures in the Canadian Precambrian Shield using time-domain electromagnetic and magnetotelluric methods, Ph.D. thesis, University of Manitoba, Winnipeg, Manitoba, 541 p.

Wu, X., Ferguson, I., and Jones, A., 2002. Geological interpretation of electrical resistivity models along the SNORCLE corridors 1 and 1A, *in* Slave-Northern Cordillera Lithospheric Evolution (SNORCLE) and Cordilleran Tectonics Workshop, Report of the 2002 Combined Meeting, February 21-24, 2002, Pacific Geoscience Centre, Lithoprobe Report No.82, p.153-163.

Wu, X., Ferguson, I.J., and Jones, A.G., 2005. Geoelectric structure of the Proterozoic Wopmay Orogen and adjacent terranes, Northwest Territories, Canada, Can. J. Sci. v.42, p.955-981.

www.geo.arizona.edu/geo5xx/geo527/BrooksRange/geology.htm, Geology of the Brooks Range, [accessed November, 2009].

Yukon Geological Survey, 2002. Geoprocess file summary report, Whitehorse map area, N.T.S. 105D <http://ygsftp.gov.yk.ca/publications/openfile/2002/of2002_8d_geoprocess_file/documents/map_specific/105d.pdf> [accessed November, 2009].

Appendix Tables A3.1 – A3.8 (1D Earth Resistivity Models)

Additions to the Figures 3.11 – 3.18, Chapter 3 Review of Earth Resistivity Models

Table A3.1: 1D Earth resistivity model for Zone 1-**PRUDHOE BAY**

Layer	Resistivity (Ωm) Avg	Range	Determination, Confidence	Resistivity Reference	Comments
1. Overburden • unconsolidated stratified sandy-gravel (Quaternary Gubik Formation) (~ 100 m thick) ***frozen depth*** ~ 500m	1000	1000 to 2000 (well log)	well logs (North Slope) A	Collett et al (1988)	• depth from cross-section (Rawlinson, 1983, Fig.2) • permafrost depth from well log *Arco Prudhoe ST-1;* 660m max at North Slope coast (Rawlinson 1983; Brown and Krieg, 1983, p.206; Collett et al, 1988, p.20) • >1000 Ωm for frozen overburden and uppermost sandstone formation (Collett et al, 1988)
	---	350-1000 (surface EM)			
2. Sedimentary Basin • shale, siltstone, sandstone, (North Slope Subterrane, Arctic Alaska Terrane) (0.1 km – 3.6)	10	5-15 upper	well logs (North Slope) A	Nelson and Kibler (2001); Kumar et al (2002); Keller and Bird (2003); Magoon et al (1988)	• basin thickens to 8km, southward to Brooks Range • basin divisible into 7 sub-layers with average resistivity of ~ 5 Ωm in upper half, and 20-200 Ωm in bottom half of basin • resistivity extrapolated from wells 50-120 km away • average resistivity as mid-point of range from well logs
	---	20-200 lower			
3. Upper Crust • Basement Complex (weakly metamorphosed sediments, ± intrusives) (3.6 – 13 km)	500	20-30 or 100-1000	well logs (North Slope) A	Nelson and Kibler (2001)	• Steep dipping argillite, siltstone, sandstone, local interbedded limestone and cherty conglomerate (Moore et al, 1994) • Resistivity extrapolated from wells 50-120 km away • Average resistivity taken as midpoint of upper range
4. Middle - Lower Crust (13 – 33 km)	500	25-1000	MT survey (SNORCLE) B	Jones et al (2005, Fig.7)	• average resistivity taken as mid-point of range from SNORCLE transect – Corridor 2, for ancestral North America
	100	20-100	Compilation (regional) C	Ferguson and Odwar (1998, p.42) for range, northern BC	
	---	10-300	Compilation (global) C	Simpson and Bahr (2005, p.11), mid-lower continental crust	

Table A3.1: **PRUDHOE BAY** continued

5. Mantle (33 – 100 km)	350 40-650	MT survey (SNORCLE) B	Jones et al (2005, Fig.6)	• depth from Fuis et al (2008) and Grantz et al (1991) crustal cross-sections • average resistivity taken as mid-point of range from SNORCLE transect-regional profile
	300 ---	Compilation (regional) C	Ferguson and Odwar (1998, p.42) for range, northern BC	
	1000 15 - 2000	Compilation (global) C	Simpson & Bahr (2005, p.11) for range, upper continental mantle	
6. Mantle (100 – 400 km)	250 ----	MT survey (SNORCLE) B	Jones et al (2005, Fig.6)	• average resistivity taken from dominant resistivity on SNORCLE transect-regional profile
	100 ---	Compilation (regional) C	Ferguson and Odwar (1998, p.42) for range, northern BC	
7. Mantle (400 - 600 km)	~15 15-40	MT survey (SNORCLE) B	Jones et al (2005, Fig.6)	• average resistivity taken as lower end of range from SNORCLE transect-regional profile
	~ 5 2.6-6.6	Compilation (regional) C	Jones (1999, Fig. 9)	• range for western North America; average resistivity as mid-point of range

Table A3.2: 1D Earth resistivity model for Zone 2-**BROOKS RANGE**

Layer	**Resistivity (Ωm)** Avg Range	**Determination, Confidence**	**Resistivity Reference**	**Comments**
1. Overburden • unconsolidated gravel, sand and silt, and till (Quaternary deposits) 15 - 40 m ***frozen depth*** ~ 15 – 70 to 200 m	Unfrozen gravel 1000 500-3000 *Frozen gravel* 3000 800-10000 Unfrozen silty sand 600 300-1000 *Frozen silty sand* 2000 1000-3000 Unfrozen till ~ 100 *Frozen till* ~ 300 Quaternary Deposits 1500 50-3230	Compilation (regional) C - as above - - as above – - as above – - as above – - as above - MT survey (TACT) A	Assoc. Mining (2004) for range; average is mid-point - as above - - as above – - as above – Scott et al (1990) - as above – Campbell et al (2001)	• 15m minimum depth from boreholes along TAPS (Kreig & Reger 1982, p.73) • valley floor has ~ 8m old alluvium overlain by ~16m modern alluvium, with ~ 16m thick alluvial fans and colluvium on valley sides with overlapping alluvium (Brown & Kreig, 1983, p.147) • permafrost 15m at Coldfoot (Kreig and Reger, 1982), 70m in drillhole 75 km west (Ferrians, 1965), possible 200m at north edge Brooks Range (Kreig and Reger, 1982) • assigned 1500 Ωm average based on TACT MT soundings
2. Sedimentary Basin (absent)	--- ---	---	---	---
3a. Upper Crust (0 – 4 km) • Hammond Subterrane 0-3.5 km	500 15-720	MT survey (TACT) A	Campbell et al (2001)	• Subterrane and depth from Fuis et al (2008) crustal cross section • weakly metamorphosed sedimentary rocks; quartzite, phyllite, schist, marble, carbonate schist, metabasalt, tuff, amphibolite. Devonian to Proterozoic age (Mull, 1989) • range and average resistivity from TACT MT soundings
• Endicott Mountains Subterrane (3.5-4 km)	400 15-720 ~ 200 40->1000	MT survey (TACT) A Well logs (North Slope) B	Campbell et al (2001) Magoon et al (1988, plate 19-16) Nelson and Kibler (2001)	• metasedimentary rocks; dolostone, metalimestone, marble, shale, conglomerate. Devonian to Proterozoic age (Till et al (2008) • same subterrane near Prudhoe Bay • assigned average resistivity based on mid-point of TACT MT soundings and lower end of well log resistivities

… Table continued on next page

Table A3.2: **BROOKS RANGE** continued

3b. Upper Crust • Basement Complex: metasedimentary, metavolcanic and plutonic rocks (4 – 24 km)	500 15-720 500 20-30 100-1000	MT survey (TACT) A well logs (North Slope) B	Campbell et al (2001) Nelson and Kibler (2001)	• 24 km depth from Fuis et al (2008), incorporates the Cenozoic duplex zone • Layer equivalent to Basement Complex in Zone 1 • well logs show variable resistivity ranges, from • wells situated 100-300 km from pipeline route; average resistivity taken as mid-point of range • average resistivity taken as upper point of range • assigned average resistivity on basis of TACT MT soundings
4. Middle-Lower Crust (24 – 57 km)	500 25-1000	MT survey (SNORCLE) B	Jones et al (2005, Fig.7)	• depth from Fuis et al (2008) and Grantz et al (1991) crustal cross-sections • doubling of crustal thickness due North Slope lithosphere indenting ancestral North America plate • average resistivity taken as mid-point of range from SNORCLE transect – Corridor 2, for ancestral North America
	100 20-100	Compilation (regional) C	Ferguson and Odwar (1998, p.42) for range, northern BC	
	--- 10-300	Compilation (global) C	Simpson and Bahr (2005, p.11), mid-lower continental crust	
5. Mantle (57 – 100 km)	350 40-650	MT survey (SNORCLE) B	Jones et al (2005, Fig.6)	• depth from Fuis et al (2008) and Grantz et al (1991) crustal cross-sections • average resistivity taken as mid-point of range from SNORCLE transect-regional profile
	300 ---	Compilation (regional) C	Ferguson and Odwar (1998, p.42) for range, northern BC	
	1000 15 - 2000	Compilation (global) C	Simpson & Bahr (2005, p.11) for range, upper continental mantle	
6. Mantle (100 – 400 km)	250 40 - 650	MT survey (SNORCLE) B	Jones et al (2005, Fig.6)	• average resistivity taken from dominant resistivity on SNORCLE transect-regional profile
	~ 100 ---	MT survey B	Jones et al (2005, p.1266) for range, SNORCLE transect	
	100 ---	Compilation (regional) C	Ferguson and Odwar (1998, p.42) for range, northern BC	
7. Mantle (400 - 600 km)	~15 15-40	MT survey (SNORCLE) B	Jones et al (2005, Fig.6)	• average resistivity taken as lower end of range from SNORCLE transect-regional profile
	~ 5 2.6-6.6	Compilation (regional) C	Jones (1999, Fig. 9)	• range for western North America; average resistivity as mid-point of range

Table A3.3: 1D Earth resistivity model for Zone 3-**FISH CREEK**

Layer	**Resistivity (Ωm)** Avg Range	**Determination, Confidence**	**Resistivity Reference**	**Comments**
1. Overburden • unconsolidated colluvium, windblown silt, terrace sands & gravels, till (Quaternary deposits) 15 - 30 m ***frozen depth*** ~ 15- 120 m	Unfrozen gravel 1000 500-3000 *Frozen gravel* 3000 800-10000 Unfrozen silty sand 600 300-1000 *Frozen silty sand* 2000 1000-3000 Unfrozen till ~ 100 *Frozen till* ~ 300 Quaternary Deposits 1500 550-1600	Compilation (regional) C - as above - - as above – - as above – - as above – - as above - MT survey (TACT) A	Assoc. Mining (2004) for range; average is mid-point - as above - - as above – - as above – Scott et al (1990) - as above – Campbell et al (2001)	• unknown thickness for Kettle Moraine Complex till, at north end of zone (Tramway Flats lowland); terrace sands/gravels up to 23m thick • colluvium is dominant along slopes and covers much of zone, up to 15m thick • silt covers southern-third of zone, up to 30m thick (Kachadoorian, 1971a,b) • northern end of zone (Tramway Flats lowlands) mostly underlain by permafrost up to 120m thick (Ferrians, 1965) • massive ice wedges and lenses (up to 17m thick) common in frozen silt in southern half of zone • average resistivity taken as upper end of MT measurements
2. Sedimentary Basin (absent)	--- ---	---	---	---
3. Upper Crust • Basement Complex: metasedimentary, plutonic and metavolcanic rocks (Tozitna and Ruby Terranes) (0 – 12 km)	1800 --- 450 250 –650 (overall range) 3050 1600 - 4500 (plutonic rock)	MT survey (TACT) A	Campbell et al (2001)	• depth from Fuis et al (2008) crustal cross-section • predominately Ruby Terrane metasediments (phyllite, schist, marble, quartzite, calc-schist, amphibolite) with extensive granite gneiss intrusions, and Tozitna Terrane mafic volcanics
		• includes lesser metasedimentary terranes; Angayucham, Slate Creek, Prospect Creek, Livengood, Manley, White Mountain and Wickersham • variable resistivities from preliminary 1D models from TACT MT soundings, strongly anisotropic • possible zone of higher resistivity 6-8km depth, average 2500 Ωm • assigned resistivity of 1800 Ωm, by taking average of non-plutonic rock (450) and plutonic rock (3500) from MT soundings, higher resistivity at depth and presence of intrusives		

… Table continued on next page

Table A3.3: **FISH CREEK** continued

4. Middle Crust • Felsic rocks (12 – 26 km)	--- 500	10-100 lower curve 120-820 upper curve	MT survey (TACT) A	Campbell et al (2001)	• depth from Fuis et al (2008) crustal cross-section • extremely variable resistivities from preliminary 1D models from TACT MT soundings, strongly anisotropic • assigned average resistivity of 500 Ωm on basis of MT soundings indicating higher resistivity possibly perpendicular to pipeline route
	100	20-100	Compilation (regional) C	Ferguson and Odwar (1998, p.48) for range, northern BC	
	120	10-300	Compilation (global) C	Simpson & Bahr (2005, p.11) for range, mid-lower continental crust	
5. Lower Crust • Mafic rocks (26 – 34 km)	--- ---	10 - 100 2000 - 8000	MT survey (TACT) A	Campbell et al (2001)	• depth from Fuis et al (2008) crustal cross-section • extremely variable resistivities from preliminary 1D models from TACT MT soundings, strongly anisotropic • assigned higher end of global range resistivity 250 Ωm on basis of MT sounding indicating higher resistivity
	---	20-100	Compilation (regional) C	Ferguson and Odwar (1998, p.48) for range, northern BC	
	---	10-300	Compilation (global) C	Simpson & Bahr (2005, p.11) for range, mid-lower continental crust	
6. Mantle (34 – 100 km)	830 mean 500 median ---	15-2200	MT survey (TACT) A	Campbell et al (2001)	• depth from Fuis et al (2008) crustal cross-section • Averaged resistivity ranges at 40 and 100 km depths from SNORCLE transect in Whitehorse area • assigned median resistivity 500 Ωm on basis of MT soundings indicating higher resistivity
	1000 500	~100-3000 (40 km) ~30-300 (100 km)	MT survey (SNORCLE) B	Jones et al (2005), Fig. 4)	
	300	---	Compilation (regional) C	Ferguson and Odwar (1998, p.42) for range, northern BC	
	1000	15 - 2000	Compilation (global) C	Simpson & Bahr (2005, p.11) for range, upper continental mantle	
7. Mantle (100 – 400 km)	250	40 - 650	MT survey (SNORCLE) B	Jones et al (2005, Fig.6)	• average resistivity taken from dominant resistivity on SNORCLE transect-regional profile
	100	---	Compilation (regional) C	Ferguson and Odwar (1998, p.42) for range, northern BC	
8. Mantle (400 - 600 km)	~15	15-40	MT survey (SNORCLE) B	Jones et al (2005, Fig.6)	• average resistivity taken as lower end of range from SNORCLE transect-regional profile
	~ 5	2.6-6.6	Compilation (regional) C	Jones (1999, Fig. 9)	• range for western North America; average resistivity as mid-point of range

Table A3.4: 1D Earth resistivity model for Zone 4-**FAIRBANKS**

Layer	**Resistivity (Ωm)** Avg Range	**Determination, Confidence**	**Resistivity Reference**	**Comments**
1. Overburden • windblown silt, alluvium, colluvium, dune sand, glaciofluvial pebble-gravel (Quaternary deposits) 15 - 100 m (minimum) ***frozen depth*** 0 - 45 m	Unfrozen silt [a] --- 4-60 [b] --- 40-60 *Frozen silt* [a] --- 1000-1200 [b] --- 200 Unfrozen silty sand [b] --- 300-1000 *Frozen silty sand* [b] --- 1000-3000 Unfrozen gravel [b] --- 500-3000 *Frozen gravel* [b] 3000 avg 800-10000 rge 1430 --- --- 700-1000	Compilation (regional) C AMT survey (TACT) A Airborne EM A	[a] Mackay (1970), [b] Assoc. Mining (2004) Campbell et al (2001) Burns et al (2006a, b), for range	• bedrock hill slopes generally permafrost free, covered by wind-blown loess; lowland slopes, creek valleys and river floodplains typically underlain by permafrost, ice rich (Brown and Kreig, 1983) • windblown silt predominant in northern-third of zone, up to 30m thick; colluvium on slopes, up to 15 m thick (Kachadoorian, 1971c) • central-third of zone covered mainly by wind-blown silt, up to 60m thick; coarse alluvium along Tanana River, 60-200m thick; with lesser colluvium, up to 3m thick (Weber, 1971a) • southern-third of zone covered by frozen silt, up to 90m thick, and dune sand, up to 60m thick (Weber, 1971a)
		• lowlands (Tanana River valley, southeastward of Fairbanks underlain by numerous isolated masses of permafrost, up to 45m thick (Ferrians, 1965) • single TACT-AMT sounding at northern end of zone shows high resistivity of 1430 Ωm to 55m depth • assigned maximum permafrost depth 45m, and resistivity of 1000 Ωm - low range of frozen overburden – on basis of airborne survey, compilation studies and possible confirmation by AMT sounding • assigned resistivity of 60 Ωm for unfrozen silt in underlying lowlands		
2. Sedimentary Basin (absent)	--- ---	---	---	---

… Table continued on next page

Table A3.4: **FAIRBANKS** continued

3. Upper Crust • Basement Complex: strongly deformed continental metasedimentary rocks (schists, gneiss) ancestral North America, ± Yukon-Tanana Terrane) (0 – 11 km)	--- 350 – 500 (upper 500m) 400 100 - 2300 (overall range)	MT survey (TACT) A	Campbell et al (2001)	• depth from Fuis et al (2008) crustal cross-section, thickening southwestward, 11km average thickness • Paleozoic and/or Precambrian metamorphic rocks – predominately clastic metasediments including schist and gneiss of many different compositions (Beikman, 1980); subordinate younger intrusives
	--- 60-300 (0-5 km depth)	MT survey (Line C) A	Stanley et al (1990)	
	30 3-100	MT survey B	Fisher et al (2004, Fig.2)	
		• variable resistivities from preliminary 1D models from TACT MT soundings; overall lower resistivity north of Shaw Creek Fault at AMP-520; higher resistivities may be indicative of intrusive bodies at depth • Stanley's (1990) MT survey near south end of zone, three widely varying ranges: 0-5 km, 60-300 Ωm; 5-8km, 8-30 Ωm; 8-10km, 1-3 Ωm • Fisher et al (2004) identified low resistive bodies beneath and adjacent to Denali Fault, located 50km south of pipeline, overall 30 Ωm, uncertain if low resistivity extends beneath pipeline • Assigned average resistivity of 400 Ωm on basis of averaged MT sounding values		
4. Middle Crust • Felsic rocks (11 – 26 km)	250 90 - 630	MT survey (TACT) A	Campbell et al (2001)	• depth from Fuis et al (2008) crustal cross-section, thickening southwestward, 15km average thickness • Stanley's (1990) MT survey near south end of zone; resistivity may not be representative (Fisher et al 2007) • assigned average resistivity of 250 Ωm on basis of TACT-MT soundings and high-end range from Simpson & Barr
	--- 1-3 (11-22km) --- 60-300 (22-40km)	MT survey B	Stanley et al (1990)	
	--- 20-100	Compilation (regional) C	Ferguson and Odwar (1998, p.48) for range, northern BC	
	120 10-300	Compilation (global) C	Simpson & Bahr (2005, p.11) for range, mid-lower continental crust	
5. Lower Crust • Mafic rocks (26 – 33 km)	~ 150 30 - 450	MT survey (TACT) A	Campbell et al (2001)	• depth from Fuis et al (2008) crustal cross-section, thickening southwestward, 7km average thickness • assigned average resistivity of 150 Ωm on basis of TACT-MT soundings and low-end range from Simpson & Barr
	--- 60 - 300	MT survey B	Stanley et al (1990)	
	--- 20-100	Compilation (regional) C	Ferguson and Odwar (1998, p.48) for range, northern BC	
	--- 10-300	Compilation (global) C	Simpson & Bahr (2005, p.11) for range, mid-lower continental crust	

… Table continued on next page

Table A3.4: **FAIRBANKS** continued

6. Mantle (33 – 100 km)	350 40-650	MT survey (SNORCLE) B	Jones et al (2005, Fig.6)	• average resistivity taken from dominant resistivity on SNORCLE transect-regional profile
	300 ---	Compilation (regional) C	Ferguson and Odwar (1998, p.42) for range, northern BC	
	1000 15 - 2000	Compilation (global) C	Simpson & Bahr (2005, p.11) for range, upper continental mantle	
7. Mantle (100 – 400 km)	250 40 - 650	MT survey (SNORCLE) B	Jones et al (2005, Fig.6)	• average resistivity taken from dominant resistivity on SNORCLE transect-regional profile
	100 ---	Compilation (regional) C	Ferguson and Odwar (1998, p.42) for range, northern BC	
8. Mantle (400 - 600 km)	~15 15-40	MT survey (SNORCLE) B	Jones et al (2005, Fig.6)	• average resistivity taken as lower end of range from SNORCLE transect-regional profile
	~ 5 2.6-6.6	Compilation (regional) C	Jones (1999, Fig. 9)	• range for western North America; average resistivity as mid-point of range

Table A3.5: 1D Earth resistivity model for Zone 5-**TOK**

Layer	**Resistivity (Ωm)** Avg Range	**Determination, Confidence**	**Resistivity Reference**	**Comments**
1. Overburden • unconsolidated, stratified pebble-gravel, some sand and silt (Quaternary deposits) 30 - 50 m (minimum) ***frozen depth*** 0 ~ 60 m	Unfrozen silt [a] --- 4-60 [b] --- 40-60 *Frozen silt* [a] --- 1000-1200 [b] --- 200 Unfrozen silty sand [b] --- 300-1000 *Frozen silty sand* [b] --- 1000-3000 Unfrozen gravel [b] --- 500-3000 *Frozen gravel* [b] 3000 avg 800-10000 rge 900 700-1000	Compilation (regional) C Airborne EM A	[a] Mackay (1970), [b] Assoc. Mining (2004) Burns et al (2006a,b), for range	• northwest end of zone underlain by glaciofluvial deposits (stratified outwash gravels with some sand); sporadically frozen (10-50% permafrost) with low to moderate ice content (Reger and Solie, 2008) • west-central part of zone underlain by mix of river and creek alluvium (predominant), glaciofluvial deposits and colluvium; discontinuously frozen (50 – 90% permafrost) with low to moderate ice content (Reger and Solie, 2008) • east-central half of zone underlain by alluvial fans, some colluvium, floodplain alluvium in the upper Tanana River valley, and at extreme southeast end is windblown sand. Minimum thickness of deposits varies from 30 to 50 m (Carrara, 2007)
		• permafrost minimum depth 6m (Reger and Solie, 2008); drill holes indicate depths of 37m near Tok (Reger and Solie, 2008), and 27-63m at Northway Junction area (Ferrians, 1965) • numerous isolated masses of permafrost underlie the Alaska Highway • assigned resistivity based on mid-point of airborne EM survey		
2. Sedimentary Basin (absent)	--- ---	---	---	---

… Table continued on next page

Table A3.5: **TOK** continued

3. Upper Crust • Basement Complex: strongly deformed continental metasedimentary (schists & gneiss), plutonic and volcanic rocks (Yukon-Tanana Terrane) (0 – 11 km)	--- 350 – 500 (upper 500m) 1800 1000 - 8700 (overall range)	MT survey (TACT) A	Campbell et al (2001)	• extrapolated depth from Fuis et al (2008) crustal cross-section, 11km average thickness; MT survey (Stanley et al, 1990) shows dramatic resistivity contrast at 11 km depth • Paleozoic and/or Precambrian metamorphic rocks – predominately clastic metasediments including schist and gneiss of many different compositions (Beikman, 1980); extensive Paleozoic and Mesozoic felsic intrusives (granite to granodiorite) occupy about half of zone; younger Tertiary and Paleozoic volcanic rocks (basalts) within the intrusives
	--- 1000-10000 (0-11 km depth)	MT survey (Line D) A	Stanley et al (1990), for range	
	30 3-100	MT survey B	Fisher et al (2004, Fig.2)	
	--- ~600-6000	MT survey (SNORCLE) B	Jones et al (2005), Fig. 4)	
		• variable resistivities from preliminary 1D models from TACT MT soundings • Stanley's (1990) MT survey -Line D - crosses central portion of zone • Fisher et al (2004) identified low resistive bodies beneath and adjacent to Denali Fault, located 50km south of pipeline, overall 30 Ωm, uncertain if low resistivity extends beneath pipeline • SNORCLE MT survey shows averaged resistivity at 5 km depth in Whitehorse area • Assigned average resistivity of 1800 Ωm on basis of overall averaged MT sounding values, reflecting extensive exposure of intrusive rocks		
4. Middle Crust • Felsic rocks (11 – 26 km)	400 90 - 740	MT survey (TACT) A	Campbell et al (2001)	• extrapolated depth from Fuis et al (2008) crustal cross-section, 15km average thickness • Stanley's (1990) MT survey across central part of zone; resistivity may not be representative (Fisher et al 2007) • SNORCLE MT survey shows averaged resistivity at 20 km depth in Whitehorse area • assigned average resistivity of 400 Ωm on basis of TACT-MT soundings and higher resistivities mapped in Whitehorse area
	--- 1-3 (11-22km)	MT survey (Line D) A	Stanley et al (1990)	
	--- ~300-3000	MT survey (SNORCLE) B	Jones et al (2005), Fig. 4)	
	--- 20-100	Compilation (regional) C	Ferguson and Odwar (1998, p.48) for range, northern BC	
	120 10-300	Compilation (global) C	Simpson & Bahr (2005, p.11) for range, mid-lower continental crust	

… Table continued on next page

Table A3.5: **TOK** continued

5. Lower Crust • Mafic rocks (26 – 33 km)	**~ 150** 30 - 200	MT survey (TACT) A	Campbell et al (2001)	• extrapolated depth from Fuis et al (2008) crustal cross-section, 7km average thickness • SNORCLE MT survey shows resistive mid-lower crust and upper mantle beneath Whitehorse area • assigned average resistivity of 150 Ωm on basis of TACT-MT soundings and low-end ranges from Stanley, and Simpson & Barr
	--- 60 - 300	MT survey (Line D) A	Stanley et al (1990)	
	--- ~5000-10000+	MT survey (SNORCLE) B	Ledo et al (2004, Fig.4)	
	--- 20-100	Compilation (regional) C	Ferguson and Odwar (1998, p.48) for range, northern BC	
	--- 10-300	Compilation (global) C	Simpson & Bahr (2005, p.11) for range, mid-lower continental crust	
6. Mantle (33 – 100 km)	~ 400 340-530	MT survey (TACT) A	Campbell et al (2001)	• limited TACT-MT soundings that penetrate to mantle depth • SNORCLE MT survey (Fig.4) shows averaged resistivity at 40 km and 100 km depths in Whitehorse area, and dominant resistivity on regional profile (Fig.6) • assigned average resistivity ~400 Ωm on basis of mid-point of TACT-MT soundings, and higher resistivities indicated from SNORCLE-MT survey
	--- ~100-3000 (40 km) --- ~100-300 (100 km)	MT survey (SNORCLE) B	Jones et al (2005), Fig. 4)	
	350 40-650	MT survey (SNORCLE) B	Jones et al (2005, Fig.6)	
	300 ---	Compilation (regional) C	Ferguson and Odwar (1998, p.42) for range, northern BC	
	1000 15 - 2000	Compilation (global) C	Simpson & Bahr (2005, p.11) for range, upper continental mantle	
7. Mantle (100 – 400 km)	250 40 - 650	MT survey (SNORCLE) B	Jones et al (2005, Fig.6)	• average resistivity taken from dominant resistivity on SNORCLE transect-regional profile
	100 ---	Compilation (regional) C	Ferguson and Odwar (1998, p.42) for range, northern BC	
8. Mantle (400 - 600 km)	~15 15-40	MT survey (SNORCLE) B	Jones et al (2005, Fig.6)	• average resistivity taken as lower end of range from SNORCLE transect-regional profile
	~ 5 2.6-6.6	Compilation (regional) C	Jones (1999, Fig. 9)	• America; average resistivity as mid-point of range

Table A3.6: 1D Earth resistivity model for Zone 6-**WHITEHORSE**

Layer	**Resistivity (Ωm)** Avg Range	**Determination, Confidence**	**Resistivity Reference**	**Comments**
1. Overburden • unconsolidated, sand and gravel, silt and clay (Quaternary deposits) ≤ 5 – 30 to 50 m (minimum) ***frozen depth*** 0 ~ ≤ 10 m	Unfrozen silt [a] --- 4-60 [b] --- 40-60 *Frozen silt* [a] --- 1000-1200 [b] --- 200 Unfrozen silty sand [b] --- 300-1000 *Frozen silty sand* [b] --- 1000-3000 Unfrozen gravel [b] --- 500-3000 *Frozen gravel* [b] 3000 avg 800-10000 rge	Compilation (regional) C	[a] Mackay (1970), [b] Assoc. Mining (2004)	• underlain by sporadic; permafrost depths less than 10m (Atlas of Canada) to occasional thicker 16 m in Whitehorse area (Burn, 2005) • northern end of zone has alluvial plains and fans 35-60m thick; outwash plains up to 60m thick, till up to 50m (map 6-1978) • central and southern part of zone, outside of the Takhini River valley, majority of route crosses till blanket (less than 30 thick) to till veneer (less 1m thick) on bedrock. Glaciolacustrine deposits (clay, silt and sand; 5-10m thick) cover river and creek channel floors and lower slopes of large valleys (Yukon Geol. Surv., 2002; Morison and Klassen, 1991).
		Where crosses or follows river valley bottoms is underlain by alluvium (stratified gravel, sand, silt) of variable thickness (Morison and Klassen, 1997). Outwash plains containing gravel, sand and silt, 5-20 m thick also along the route. Up to 75m thick silt and clay deposits (from glacial lake Champagne) underlie the Takhini river valley (Yukon Geol. Surv., 2002) • assigned resistivity of 1000 Ωm for frozen silt, covering major portion of route in Whitehorse area		
2. Sedimentary Basin (absent)	--- ---	---	---	---
3. Upper Crust • metamorphosed volcanic and sedimentary rock, extensive intrusive rock (Nisling, Kooteney, Stikine, Cache Creek, Slide Mountain, Dorsey & Cassier Terranes) (0 – 12 km)	2000 1000-6000 (Corridor 3) 1800 600-6000 (5 km depth)	MT survey (SNORCLE) A MT survey (SNORCLE) A	Jones et al (2005), Fig. 7) Jones et al (2005), Fig. 4)	• crustal depth from Clowes et al (2005, Fig.4) • SNORCLE-Corridor 3 gives coarse resolution of crust, showing wide resistivity range (300-10000 Ωm), with dominant range being 1000-3000Ωm; averaged resistivity at 5km depth also shows wide range with dominant range being 600-3000 Ωm • Assigned average resistivity of 2000 Ωm as mid-point of dominant ranges, also reflecting presence of intrusive rocks

… Table continued on next page

Table A3.6: **WHITEHORSE** continued

4. Middle Crust (12 ~ 20 km)	--- 3000-10000+ (Corridor 3)	MT survey (SNORCLE) A	Jones et al (2005), Fig. 7)	• crustal depth from Clowes et al (2005, Fig.4) • SNORCLE-Corridor 3 shows resistive mid-lower crust and upper mantle beneath Whitehorse area • averaged resistivity at 20km depth also shows wide range with dominant range being 600-1000 Ωm • assigned average resistivity of 800 Ωm as mid-point of dominant range at 20 km depth
	800 100-3000 (20 km depth)	MT survey (SNORCLE) A	Jones et al (2005), Fig. 4)	
	--- 20-100	Compilation (regional) C	Ferguson and Odwar (1998, p.48) for range, northern BC	
	120 10-300	Compilation (global) C	Simpson & Bahr (2005, p.11) for range, mid-lower continental crust	
5. Lower Crust (~ 20 ~ 35 km)	--- 1000-10000+	MT survey (SNORCLE) A	Jones et al (2005), Fig. 7)	• crust/ mantle depth from Clowes et al (2005, Fig.4) and Ledo et al (2004, Fig.7) • averaged resistivity at 40km depth also shows wide range with dominant range being 100-1000 Ωm • assigned average resistivity of 550 Ωm as mid-point of dominant range at 40 km depth
	550 10-3000 (40 km depth)	MT survey (SNORCLE) A	Jones et al (2005), Fig. 4)	
	--- 20-100	Compilation (regional) C	Ferguson and Odwar (1998, p.48) for range, northern BC	
	--- 10-300	Compilation (global) C	Simpson & Bahr (2005, p.11) for range, mid-lower continental crust	
6. Mantle (~35 – 100 km)	--- 1000-10000+	MT survey (SNORCLE) A	Jones et al (2005), Fig. 7)	• SNORCLE Corridor 3 shows very high resistivity beneath Whitehorse area • assigned average resistivity 3000 Ωm on basis of high-end resistivity at 40 and 100 km depths
	--- 10-3000 (40 km depth) --- 100-3000 --- 30-300 (100 km depth)	MT survey (SNORCLE) A	Jones et al (2005), Fig. 4)	
	300 ---	Compilation (regional) C	Ferguson and Odwar (1998, p.42) for range, northern BC	
	1000 15 - 2000	Compilation (global) C	Simpson & Bahr (2005, p.11) for range, upper continental mantle	
7. Mantle (100 – 400 km)	300 30-600 (100 km depth)	MT survey (SNORCLE) A	Jones et al (2005), Fig. 4)	• assigned average resistivity 300 Ωm on basis of mid-point of averaged resistivity range at 100 km depth
	375 40-700 (regional profile)	MT survey (SNORCLE) A	Jones et al (2005), Fig. 6), for range	
	100 ---	Compilation (regional) C	Ferguson and Odwar (1998, p.42) for range, northern BC	
8. Mantle (400 - 600 km)	~15 15-40	MT survey (SNORCLE) B	Jones et al (2005, Fig.6)	• average resistivity taken as lower end of range from SNORCLE transect-regional profile
	~ 5 2.6-6.6	Compilation (regional) C	Jones (1999, Fig. 9)	• range for western North America; average resistivity as mid-point of range

Table A3.7: 1D Earth resistivity model for Zone 7-**NORTHEASTERN BC**

Layer	**Resistivity (Ωm)** Avg Range	**Determination, Confidence**	**Resistivity Reference**	**Comments**
1. Overburden • Gravel, sand and silt, till (Quaternary deposits) 5 – 30 m ***frozen depth*** 0 – ≤ 10 m	Unfrozen sand and gravel [a]--- 70-100 Unfrozen silty sand [b]--- 300-1000 Unfrozen Till [a]--- 5-15 [c]--- 20-100 [d] 100 ---	[a] Airborne EM B (northeast BC) [b] Compilation (regional) C [c] Compilation C (Saskatchewan) [d] Compilation C	[a] Best et al (2006) [b] Assoc. Mining (2004) [c] Palacky (1980, p.101) [d] Scott et al (1990)	• sporadic discontinuous permafrost (10-50%) (Atlas of Canada, 2009) • northwestern half of zone commonly underlain by glaciofluvial deposits (5-20m thick outwash plains, 5-50m thick terraces, 5-20m thick modern alluvium) consisting of gravel, sand and silt (Klassen and Morison, 1981; Klassen, 1997)
		• southeastern half commonly underlain by a thick and continuous till blanket (≤ 30m thick), with areas of till veneer; glaciofluvial deposits (5-20m thick outwash plains, 5-50m thick terraces, 5-20m alluvium) of sand and gravel in river valleys • predominately a thick and continuous till blanket, with areas of till veneer; glaciofluvial deposits of sand and gravel in river valleys (Fulton, 1995) • assigned resistivity of 100 Ωm on basis majority of route follows river valleys infilled with unfrozen sand and gravel		
2. Sedimentary Basin (absent)	--- ---	---	---	---
3. Upper Crust • limestone, shale, siltstone, sandstone, dolostone (Rocky Mountain Fold Belt) (0 – ~14 km)	--- +10000 (Corridor 2)	MT survey (SNORCLE) A	Jones et al (2005, Fig. 7)	• approximate, varying crustal depth (10-18 m) from Welford et al (2001, Fig.12); took mid-point for profile depth • upper 2km portion is sediments of the Rocky Mountain Fold Belt, of the Ancestral North America craton margin; a strongly deformed and thrust-faulted package of sandstone,
	--- 10-45 (regional profile)	MT survey (SNORCLE) A	Jones et al (2005, Fig. 6)	
	180 60-300 (5 km depth)	MT survey (SNORCLE) A	Jones et al (2005, Fig. 4)	
		shale and carbonate rocks, sometimes weakly metamorphosed (Mair et al, 2006) • SNORCLE-Corridor 2 gives coarse resolution of crust, showing varying and high resistivity SE of Tintina Fault • averaged resistivity at 5 km depth becomes less resistive SE toward Fort Nelson • assigned average resistivity 180 Ωm as mid-point of resistivity at 5 km depth		

… Table continued on next page

Table A3.7: **NORTHEASTERN BC** continued

4. Middle Crust (~14 – ~ 25 km)	--- 60-10000+ (Corridor 2)	MT survey (SNORCLE) A	Jones et al (2005, Fig. 7)	• approximate crustal depth from Welford et al (2001, Fig.12); took mid-point for profile depth • SNORCLE-Corridor 2 shows coarse resolution of crust, with considerable variation of resistivity • assigned average resistivity 50 Ωm as mid-point of dominant range (10-100 Ωm) at 20 km depth
	--- 10-300 (20 km depth)	MT survey (SNORCLE) A	Jones et al (2005, Fig. 4)	
	--- 20-100	Compilation (regional) C	Ferguson and Odwar (1998, p.48) for range, northern BC	
	--- 10-300	Compilation (global) C	Simpson & Bahr (2005, p.11) for range, mid-lower continental crust	
5. Lower Crust (~ 25 – ~ 33 km)	--- 10000+ (corridor 2)	MT survey (SNORCLE) A	Jones et al (2005,, Fig. 7)	• average crust/ mantle depth from Clowes et al (2005, Fig.4) • assigned average resistivity 35 Ωm as mid-point of range on regional profile
	--- 10-65 (regional profile)	MT survey (SNORCLE) A	Jones et al (2005, Fig. 6)	
	--- 20-100	Compilation (regional) C	Ferguson and Odwar (1998, p.48) for range, northern BC	
	--- 10-300	Compilation (global) C	Simpson & Bahr (2005, p.11) for range, mid-lower continental crust	
6. Mantle (~33 – 100 km)	5 3-30 (Corridor 2)	MT survey (SNORCLE) A	Jones et al (2005), Fig. 7)	• SNORCLE Corridor 2 shows very low resistivity east of Watson Lake to Laird River area • averaged resistivity at 40 and 100 km depths, chosen from mid-point of dominant ranges • assigned average resistivity of 20 Ωm as an average of mid-points of ranges
	--- 15-100 (regional profile)	MT survey (SNORCLE) A	Jones et al (2005), Fig. 7)	
	20 10-100 (40 km depth) 35 10-60 (100 km depth)	MT survey (SNORCLE) A	Jones et al (2005), Fig. 4)	
	300 ---	Compilation (regional) C	Ferguson and Odwar (1998, p.42) for range, northern BC	
	1000 15 - 2000	Compilation (global) C	Simpson & Bahr (2005, p.11) for range, upper continental mantle	
7. Mantle (100 – 400 km)	--- 15-250 (regional profile)	MT survey (SNORCLE) A	Jones et al (2005), Fig.6)	• assigned average resistivity 100 Ωm on basis of averaging mid-points SNORCLE ranges and regional compilation values
	--- 10-60 (100 km depth)	MT survey (SNORCLE) A	Jones et al (2005), Fig.6)	
	100 ---	Compilation (regional) C	Ferguson and Odwar (1998, p.42) for range, northern BC	
8. Mantle (400 – 600 km)	~15 15-40	MT survey (SNORCLE) B	Jones et al (2005, Fig.6)	• average resistivity taken as lower end of range from SNORCLE transect-regional profile, for Proterozoic mantle • range for western North America; average resistivity as mid-point of range
	~ 5 2.6-6.6	Compilation (regional) C	Jones (1999, Fig. 9)	

Table A3.8: 1D Earth resistivity model for Zone 8 - **BOUNDARY LAKE**

Layer	Resistivity (Ωm) Avg Range	Determination, Confidence	Resistivity Reference	Comments
1. Overburden • till, silt and clay (Quaternary deposits) 15 - 60 m	Sand and gravel (unfrozen) [a]--- 70-100 Till (unfrozen) [a]--- 5-15 [c]--- 20-100 [d] 100 --- Clay (unfrozen) [b]--- 10-45 Silt (unfrozen) [a]--- 4-60 [b]--- 40-60	[a] Airborne EM B (northeast BC) [b] Compilation (regional) C [c] Compilation C (Saskatchewan) [d] Compilation C	[a] Best et al (2006) [b] Assoc. Mining (2004) [c] Palacky (1980, p.101) [d] Scott et al (1990)	• no permafrost • predominately a thick and continuous till blanket, with areas of till veneer, and glaciolacustrine / lacustrine deposits of silt and clay in river valleys (Fulton, 1995) • till thicknesses varies 20-60m (Trommelen and Levson, 2009; Hartman and Clague, 2008); 15 - 45 m thick in Alberta provincial boundary area (Hackbath, 1978) • assigned resistivity 50 Ωm on basis of mid-point resistivities of unfrozen till measurements, for typical depth of 45m
2. Sedimentary Basin • upper half, clastic dominant: shale, siltstone, sandstone, some limestone • lower half, carbonate dominate: limestone, shale (0 km – 3 to 4 km)	5 1-20 (averaged resistivity, 1.7 km depth)	MT survey A	Turkoglu et al (2009, Fig.8)	• Western Canada Sedimentary Basin (Interior Platform) thickens westward • exposed sedimentary bedrock is Kaskapau Formation: Cretaceous, shale with thin ironstone beds, and in lower portion is interbedded with quartzitic sandstone and mudstone (Ab. Geol. Surv., 2009) • 5 Ωm average resistivity of WCSB, based on induction logs from drill holes
	--- 10 – 15	MT survey (Corridor 1) B (1D interpretation)	Wu et al (2005, Fig.7)	
	5 ---	Compilation (Alberta) C	Boerner et al (2000, Fig.9)	
	100 Edmonton 300 Northern BC	Compilation (regional) C	Ferguson and Odwar (1998; p.41-42)	
		penetrating to Precambrian basement (Boerner et al, 2000) • SNORCLE Corridor 1 located 500 km N of Boundary Lake zone • assigned average resistivity 5 Ωm on basis of MT surveys by Turkoglu and Boerner		
3. Upper Crust • Basement Complex: volcanic and sedimentary rock, extensive intrusive rock (Ksituan, Kiskatinaw, Nova, Fort Simpson terranes) (4 – 10km)	135 20-250 (overall range) 60 --- (dominant)	MT survey A (3D interpretation)	Turkoglu et al (2009, Fig.8)	• very approximate 10 km crustal depth interpreted from Welford et al (2001, Fig.12) • assigned 60 Ωm on basis of dominant resistivity in area of Boundary Lake
	--- 2.5 – 60 (overall range) --- 7.5 – 30 (dominant range)	MT Survey (ABT) A (2D interpretation)	Boerner et al (2000, Fig. 15)	
	165 30 - 300	MT Survey (Corridor 1) B (1D interpretation)	Wu et al (2005, Fig.7)	

… Table continued on next page

Table A3.8: **BOUNDARY LAKE** continued

4. Middle Crust (~15 – ~ 25 km)	160 20 - 300 (20.5 km depth)	MT survey A (3D interpretation)	Turkoglu et al (2009, Fig.8)	• very approximate 15 km crustal thickness interpreted from Welford et al (2001, Fig.12) • assigned average resistivity 160 Ωm as mid-point of dominant range at 20 km depth
	600 200-1000	MT survey A (2D interpretation)	Turkoglu et al (2009, Fig.7)	
	1000 ---	MT Survey (ABT) A (2D interpretation)	Boerner et al (2000, Fig. 15)	
	--- 200 - 400	MT Survey (Corridor 1) B (2D interpretation)	Wu et al (2005, Fig.10)	
	--- 20-100	Compilation (regional) C	Ferguson and Odwar (1998, p.48) for range, northern BC	
	--- 10-300	Compilation (global) C	Simpson & Bahr (2005, p.11) for range, mid-lower continental crust	
5. Lower Crust (~ 25 – ~ 40 km)	20 1 - 80 (41 km depth)	MT survey A (3D interpretation)	Turkoglu et al (2009, Fig.8)	• crust / mantle depth from Turkoglu et al (2009), Clowes et al (2005, Fig.4), and Bouzidi et al (2002, Fig.8) • assigned 20 Ωm layer resistivity on basis of most recent MT survey; low resistive zone follows pipeline route
	600 300-1000	MT survey A (2D interpretation)	Turkoglu et al (2009, Fig.7)	
	--- 600-1000	MT Survey (ABT) A (2D interpretation)	Boerner et al (2000, Fig. 15)	
	--- 200 - 400	MT Survey (Corridor 1) B (2D interpretation)	Wu et al (2005, Fig.10)	
	--- 20-100	Compilation (regional) C	Ferguson and Odwar (1998, p.48) for range, northern BC	
	--- 10-300	Compilation (global) C	Simpson & Bahr (2005, p.11) for range, mid-lower continental crust	
6. Mantle (~40 – 100 km)	200 30-600 (65 km depth) 600 --- (at pipe end)	MT survey A (3D interpretation)	Turkoglu et al (2009, Fig.8)	• assigned 600 Ωm layer resistivity on basis of most recent MT survey, 100 km depth at pipe end
	250 200-300	MT survey A (2D interpretation)	Turkoglu et al (2009, Fig.7)	
	600 300-1000 (40-50 km depth)	MT Survey (ABT) A (2D interpretation)	Boerner et al (2000, Fig. 15)	
	300 200 - 400	MT Survey (Corridor 1) B (2D interpretation)	Wu et al (2005, Fig.10)	
	300 ---	Compilation (regional) C	Ferguson and Odwar (1998, p.42) for range, northern BC	
	1000 15 - 2000	Compilation (global) C	Simpson & Bahr (2005, p.11) for range, upper continental mantle	

… Table continued on next page

Table A3.8: **BOUNDARY LAKE** continued

7. Mantle (100 – 400 km)	100 20-200 (200-250 km depth)	MT survey A (3D interpretation)	Turkoglu et al (2009, Fig.8)	• assigned 100 Ωm layer resistivity on basis of most recent 3D-MT survey
	--- 1 – 10 (175-250 km depth)	MT survey A (2D interpretation)	Turkoglu et al (2009, Fig.7)	
	100 ---	Compilation (regional) C	Ferguson and Odwar (1998, p.42) for range, northern BC	
8. Mantle (400 – 600 km)	~15 15-40	MT survey (SNORCLE) B	Jones et al (2005, Fig.6)	• average resistivity taken as lower end of range from SNORCLE transect-regional profile, for Proterozoic mantle • range for western North America; average resistivity as mid-point of range
	~ 5 2.6-6.6	Compilation (regional) C	Jones (1999, Fig. 9)	

NOTE:
1. Determination – geophysical method used to determine the resistivity, or compilation form variety of sources.
2. Confidence – judgment as to how representative is the resistivity value, based on following criteria;
   * A = best representative (measurements from site specific or a part of a regional MT survey near site)
   * B = likely representative (resistivity values extrapolated from measurements taken at some distance from the site; either well logs or regional MT survey)
   * C = possibly representative (measurements from general compilations, either regional or global, typically obtained from regional MT surveys)

ABBREVIATIONS

avg	average
BC	British Columbia
EM	electromagnetic
MT	magnetotelluric
rge	range
SNORCLE	Slave-Northern Cordillera Lithospheric Evolution
TACT	Trans-Alaska Crustal Transect
TAPS	Trans-Alaska Pipeline System
WCSB	Western Canada Sedimentary Basin

Chapter 4 Assessment of Telluric Activity

4.1. Introduction

The geomagnetic field fluctuations are accompanied by the geo-electric (telluric) field and telluric currents at the surface of the Earth and in the pipelines. These telluric currents disturb pipeline cathodic protection levels, creating pipe-to-soil potential (PSP) fluctuations with different amplitudes. These amplitudes directly depend on the telluric activity in the area of the pipeline. This chapter contains description of telluric activity in the area of the proposed Alaska pipeline route.

Two factors affect telluric activity in the particular area, one is the geomagnetic field variations and other is the deep ground resistivity structure. The basic theory of the relations between geomagnetic field and telluric currents is presented in Part 4. 2. This theory allows us to find the geo-electric (telluric) field at the Earth surface if the geomagnetic field and the Earth resistivity profile are known.

The theory was applied in order to calculate geo-electric (telluric) field variations in the pipeline area. Magnetic data from four Geomagnetic Observatories (Chapter 2) were used with surface impedances for the four different zones, derived from one-dimensional Earth resistivity models created on the basis of the geological surveys (Chapter 3). The data from the geomagnetic observatory at Sitka were not used in this process. Though the observatory lies in the proximity of the pipeline geographically, it has a lower geomagnetic latitude and so experiences much less geomagnetic activity than that in the area of the pipeline.Frequency characteristics of the surface impedance, as well as its influence on the geo-electric field, are discussed in Part 4.3.

In Part 4.4 we present examples of 1-minute electric field variations for days with different geomagnetic activity for the zones along the pipeline route.

To properly evaluate the effects of telluric activity on the scale of years, statistical study is required. For the statistical analysis of telluric activity in the pipeline area, we established two types of indices of telluric electric field: the hourly maximum of the absolute value of the electric field and the hourly standard deviation of the electric field. These telluric indices were calculated for a low latitude (Ottawa) and the areas (zones) along the pipeline. The statistical distribution of the hourly maximum amplitude index was then used to derive the different levels of telluric activity. The low latitude results were used to establish the normal quiet level, that occurring 95% of the year. For the other values of the telluric activity scale, the geo-electric field was calculated for eight different zones and these statistical distributions were used (Part 4.5).

From statistical geomagnetic results (Chapter 2) for nearly three complete solar cycles, the most active (2003) and the most quiet (1996) years for the Yellowknife magnetic observatory were chosen for electric field calculations and the production of plots of the telluric field indices for analysis (Part 4.6).

4.2. Theoretical Background

The electric fields produced by geomagnetic disturbances drive electric currents within the earth. These induced currents have the effect of shielding the interior of the earth from the geomagnetic disturbances. The decrease of the magnetic and electric fields within the earth is dependent both on frequency and the resistivity structure of the earth. At the frequencies of the geomagnetic field variations, the skin depths within the earth extend to hundreds of kilometers, and the resistivity of the earth down to these depths has to be taken into account in calculating the relationship between the electric and magnetic fields at the surface.

The variation of resistivity with depth within the earth can be modeled using multiple horizontal layers with different uniform conductivities as shown in Chapter 3, with the last layer as a uniform half-space. For the calculation of the geo-electric field an assumption also needs to be made about the spatial structure of the source of geomagnetic fluctuations. Here we assume the simplest case of a plane wave (a wave uniform in both the x and y directions) propagating down into the Earth.

We use the geomagnetic coordinate system with axis *x* north, *y* east, and *z* vertically downwards. For the frequency range of 1 sec - 24 hours and earth resistivities 1 - 1000 Ohm-m, displacement currents are small and can be neglected. Therefore, electric (*E*) and magnetic (*H*) fields in the frequency domain (ω) can be given by diffusion equations.

$$\frac{d^2E}{dz^2} = i\omega\mu\sigma E \tag{4.1}$$

$$\frac{d^2H}{dz^2} = i\omega\mu\sigma H \tag{4.2}$$

where z is the depth into the earth, σ is the conductivity and μ is the constant of permeability of free space ($4\pi\cdot10^{-7}$ H/m).

Solutions for each layer have the form

$$E = A(e^{-kz} + Re^{kz}) \tag{4.3}$$

$$H = A(\frac{e^{-kz}}{Z_0} - R\frac{e^{kz}}{Z_0}) \tag{4.4}$$

where A and R are the amplitude and reflection coefficient, $k = \sqrt{i\omega\mu\sigma}$ is the propagation constant, and

$$Z_0 = \frac{i\omega\mu}{k} = \sqrt{\frac{i\omega\mu}{\sigma}}$$

is the characteristic impedance (ratio of the electric and magnetic fields for the uniform medium).

In our case, the magnetic field at the surface of the earth (1st layer) is known from magnetic observations, and the electric field can be obtained from the ratio (impedance) of magnetic and electric fields

$$E_s = Z_s H_s \tag{4.5}$$

where Z_s is the impedance of the surface layer (1st layer) and E_s and H_s are surface geo-electric and geomagnetic fields.

The impedance at any layer can be found by applying the recursion relation for the impedance of an n-layered half-space (Weaver, 1994).

$$Z_n = i\omega\mu\left(\frac{1 - r_n e^{-2k_n l_n}}{k_n(1 + r_n e^{-2k_n l_n})}\right) \tag{4.6}$$

Where l_n and k_n are thickness and propagation constant of layer n,

$$r_n = \frac{1 - k_n \dfrac{Z_{n-1}}{i\omega\mu}}{1 + k_n \dfrac{Z_{n-1}}{i\omega\mu}} \tag{4.7}$$

and for the last layer

$$Z_N = \frac{i\omega\mu}{k_N} \tag{4.8}$$

To obtain geo-electric field at the earth's surface from known geomagnetic field data, the following sequence of operations (Figure 4.1) was performed:

1. Conversion of the geomagnetic data from time into frequency domain [using Fast Fourier Transformation (FFT)].
2. Multiplication by the surface impedance, obtained from one-dimensional resistivity profile of particular area.
3. Inverse transform of geo-electric data into time domain by using inverse FFT.

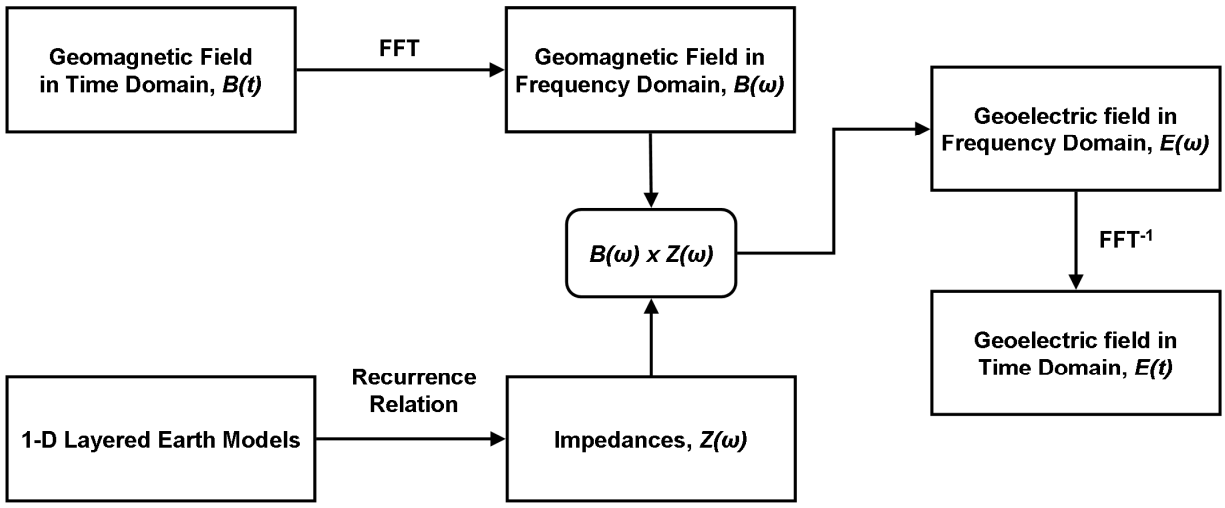

Figure 4.1. Calculation of the electric field from the geomagnetic field and layered earth model

The Fast Fourier Transform routine is available as built-in procedures in ORIGIN 6 and IDL, and available as FORTRAN code in *Numerical Recipes in Fortran 77* (Press et al, 1992).

4.3. Surface Impedance Models

The earth resistivity profiles for the different zones, described in Chapter 3, were used as input to the recursion relation (4.6) to produce surface impedance values for the eight zones along the pipeline route. This surface impedance represents the transfer function between geomagnetic variations and geo-electric (telluric) field at the Earth's surface, as $E(\omega) = Z(\omega) \times B(\omega)$.

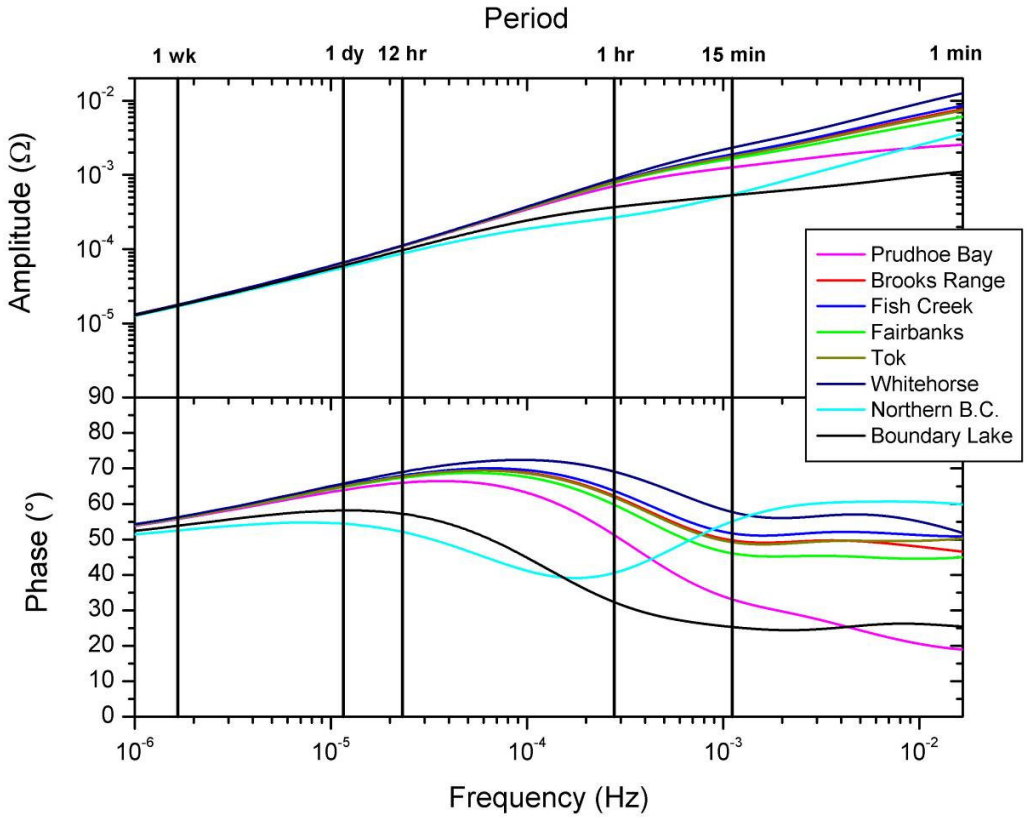

Figure 4.2. Surface impedances for the layered earth resistivity models

As shown in Figure 4.2, the surface impedances vary for the different zones, depending upon frequency as well as the conductivities of the different layers. This dependence can be explained in terms of the "skin depth" of conductors with respect to the electromagnetic waves. When electromagnetic waves propagate down through the Earth, they partially penetrate conductive layers and decay at different depths, depending on their frequency and the particular resistivity of the layer. In our study we are using 1 minute data, which defines the highest frequency we are concerned with as ~0.015 Hz . Variations with more than 12 hours period or about 0.01 mHz, characterize the lower part of studied frequency spectrum. Natural electromagnetic waves of this frequency range (0.01 Hz-0.01 mHz) penetrate deep into the Earth and are not affected by the surficial geology. Thus changes in the resistivity of a topmost layer, such as those due to permafrost (which penetrates to a maximum depth of approximately half a kilometer) do not affect the surface impedance at the frequencies we are concerned with.

The largest difference between the surface impedances can be seen in the amplitudes of Northern BC-Zone 7 and Boundary Lake-Zone 8 compared with the other areas. The amplitude of Prudhoe Bay-Zone 1 also differs from the other Alaskan zones for periods between 1 and 15 minutes. The lower amplitude of these impedances will result in attenuated geo-electric field variations compared with the other zones'. This will translate into different telluric fields produced by geomagnetic variations in this frequency range and as a result different pipe-to-soil variations at different sites along the pipeline.

The effect of different impedances can best be illustrated by calculating geo-electric field values from a sample of geomagnetic data using different the earth resitivity parameters and comparing the results. The same geomagnetic field values (Ottawa, 01/17/2004) were used in the electric field calculations using these parameters from all eight earth models. The sets of values most representative of all the plots are displayed below in Figure 4.3.

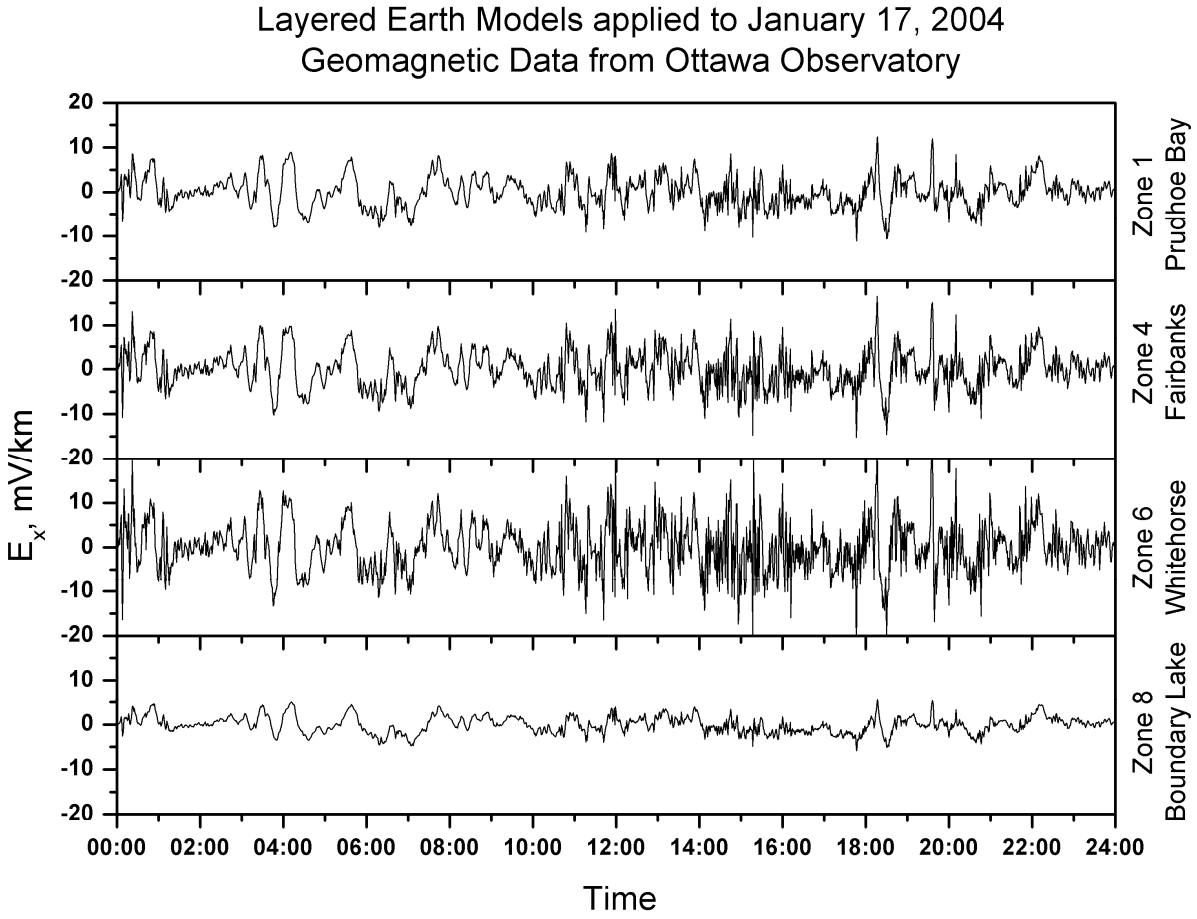

Figure 4.3. Electric field values for January 17, 2004 calculated using magnetic field data from Ottawa with different earth models

Zones 4 and 6 are characteristic of the central Alaskan zones - the high surface impedances result in large electric field values. Zone 1 is similar but slightly attenuated. Zone 8 is similar to Zone 7 - both have smaller electric fields due to their lesser surface impedances.

4.4. Daily Variations of the Geo-electric Field

From the investigation of geomagnetic activity in 2004, specific days were chosen as representative of the classes of activity. To choose these days, we applied the following procedure to the geomagnetic hourly range index from Yellowknife geomagnetic observatory data as the observatory corresponding to the broader auroral zone area.

When certain predefined hourly range limits of the geomagnetic activity occurred for the most of the day, this day has been chosen as representative. For example, there were some days with 24 HRX values below the 40 nT quiet limit, from which the day with the lowest HRX values was chosen. There were no days when HRX was greater than 600 nT for all 24 hours, so the day with largest number of this highest level of activity has been chosen.

The dates for the geo-electric field calculations thus chosen were the three consecutive days in November and two in January:

Active day with 300 nT < HRX < 600 nT:	January 16
Unsettled day with 40 nT < HRX < 300 nT:	January 17
Quiet day with HRX < 40 nT:	November 6
Special transitional from quiet to stormy day:	November 7
Stormy day with HRX>600 nT:	November 8

Geomagnetic data from the 4 observatories were used to calculate geo-electric field X (northward) and Y (eastward) components with 8 different earth models of surface impedances and layer depths, representing the zones along the pipeline route.

The respective sources of the geomagnetic data used in the telluric field calculations for each zone along the pipeline are the same as those which were used with the corresponding areas in the original calculations. The eight zones and the corresponding data used in the calculations are listed in Table 4.1.

Name	Number	Data Source
Prudhoe Bay	1	Barrow
Brooks Range	2	College
Fish Creek	3	College
Fairbanks	4	College
Tok	5	College
Whitehorse	6	College
Northern British Columbia	7	Yellowknife
Boundary Lake	8	Meanoook

Table 4.1. Summary of geomagnetic data used in telluric field calculations by pipeline zone

The results of the telluric field calculations are shown in Figures 4.4 - 4.13.

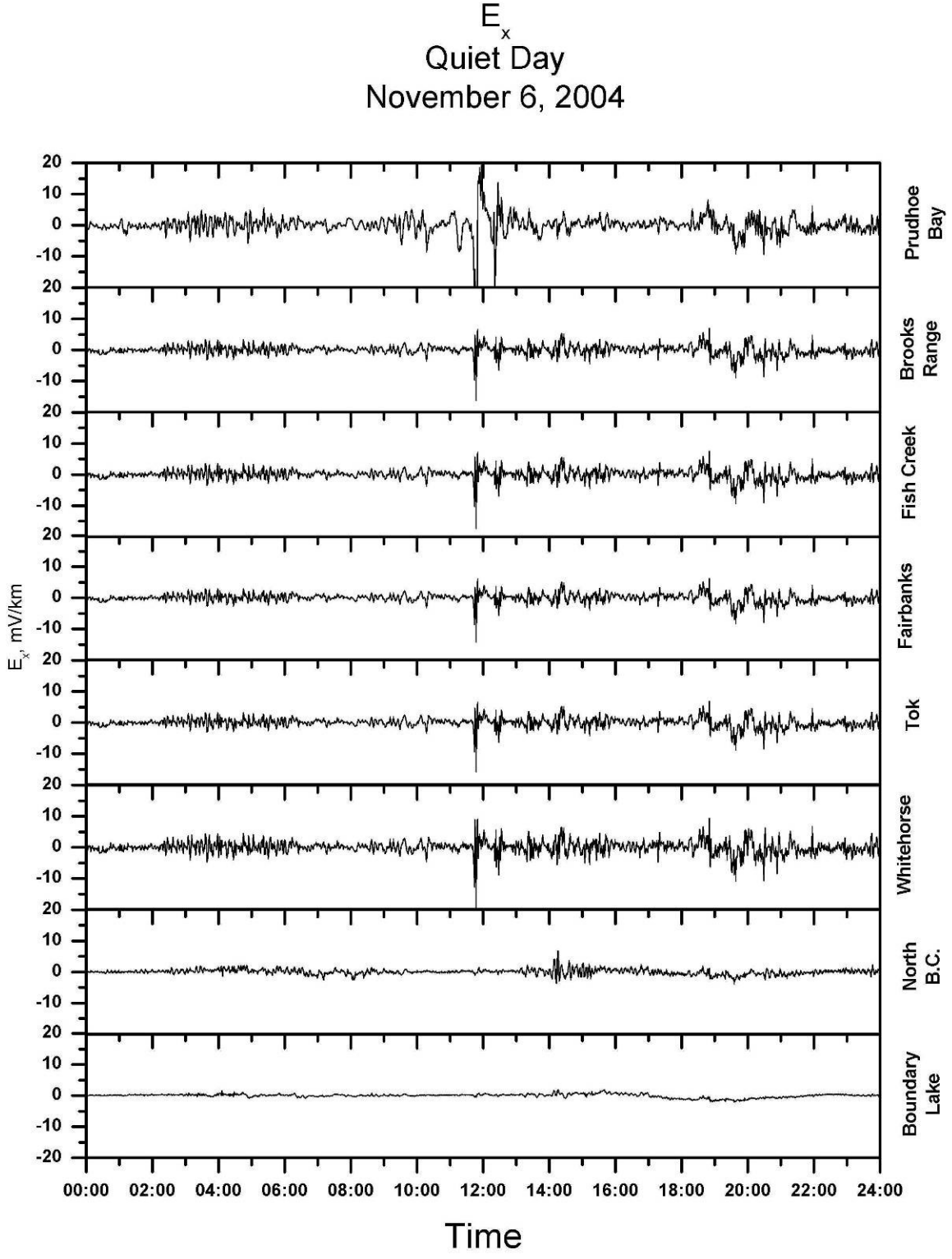

Figure 4.4. Northward electric field variations on a quiet day

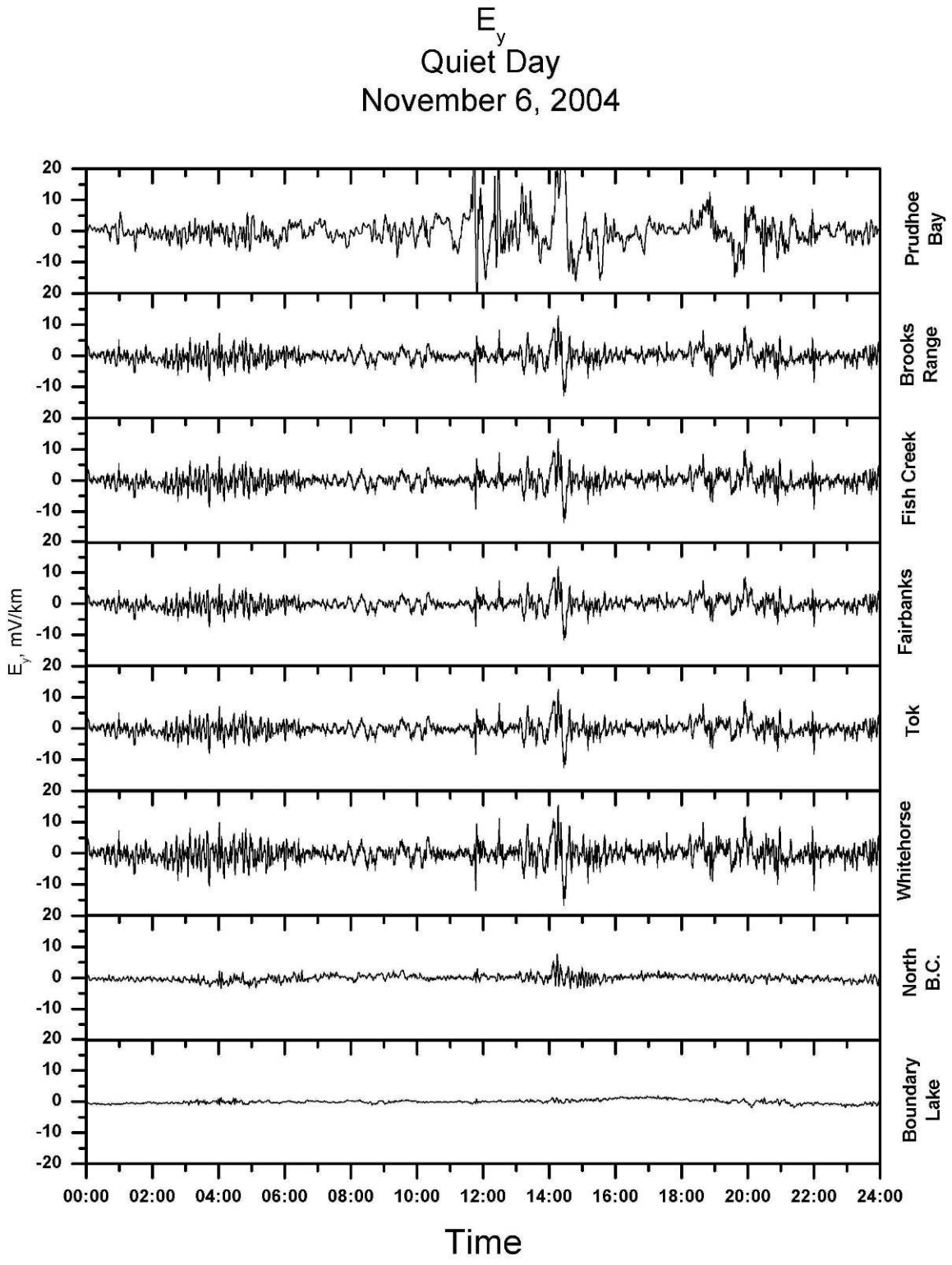

Figure 4.5. Eastward electric field variations on a quiet day

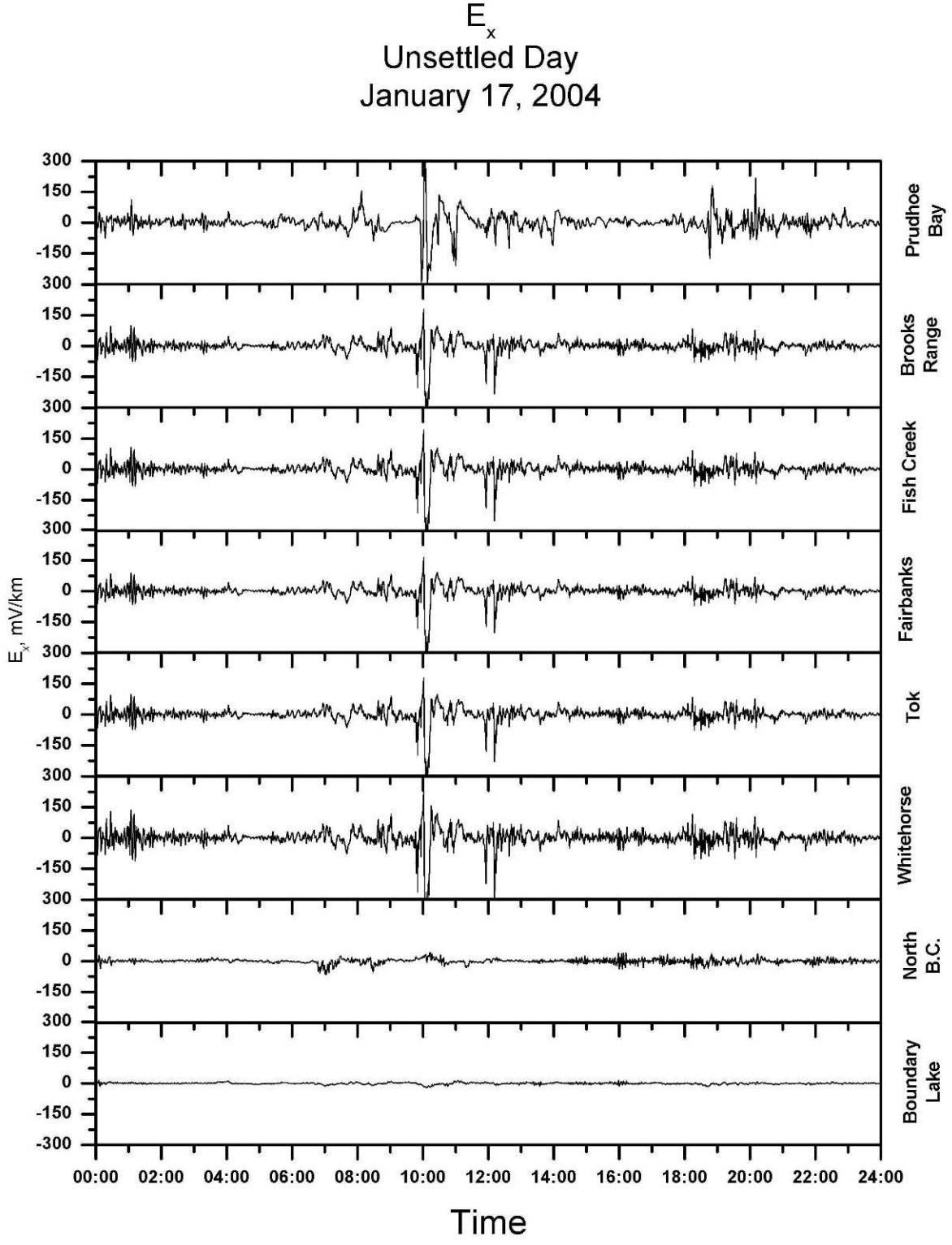

Figure 4.6. Northward electric field variations on an unsettled day

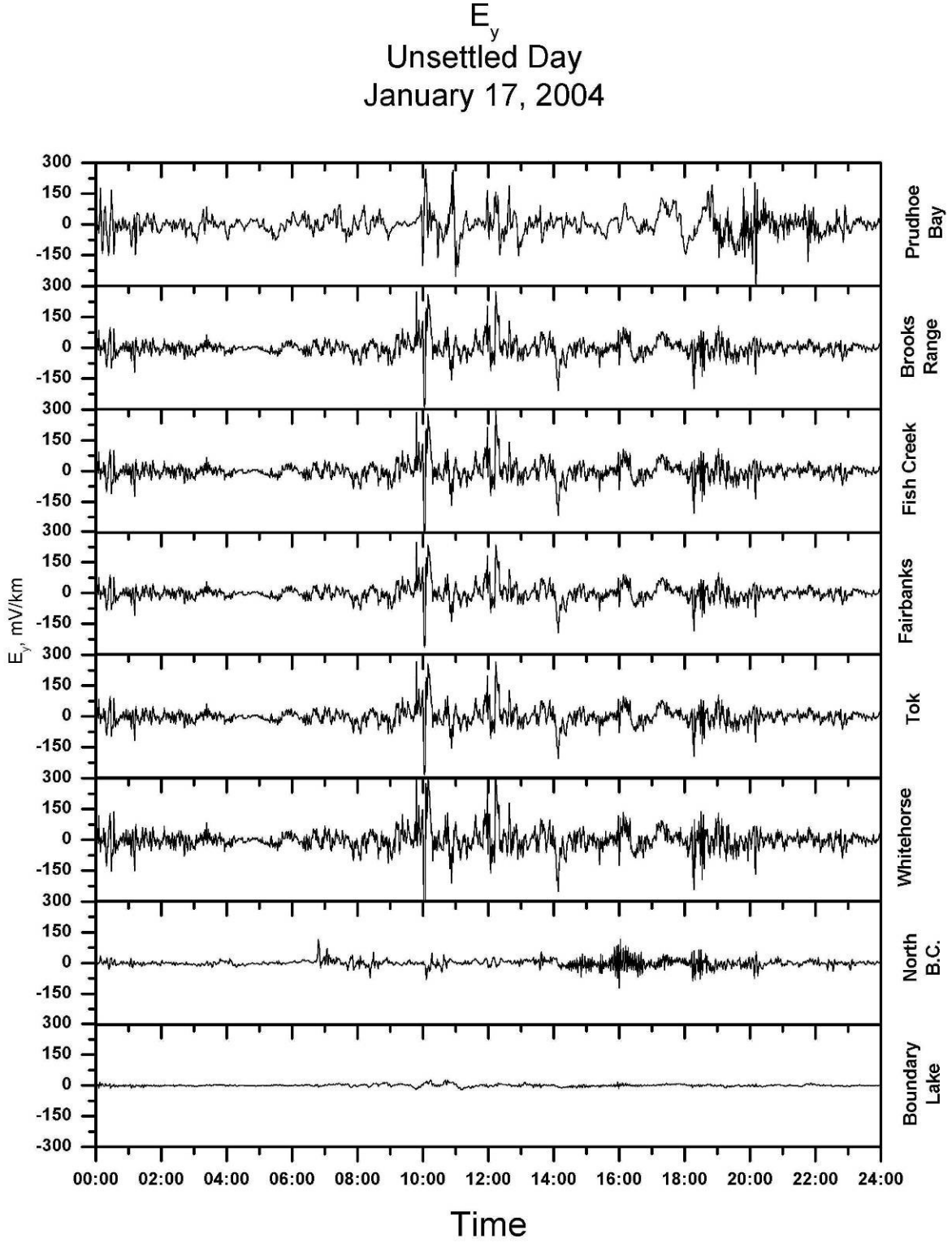

Figure 4.7. Eastward electric field variations on an unsettled day

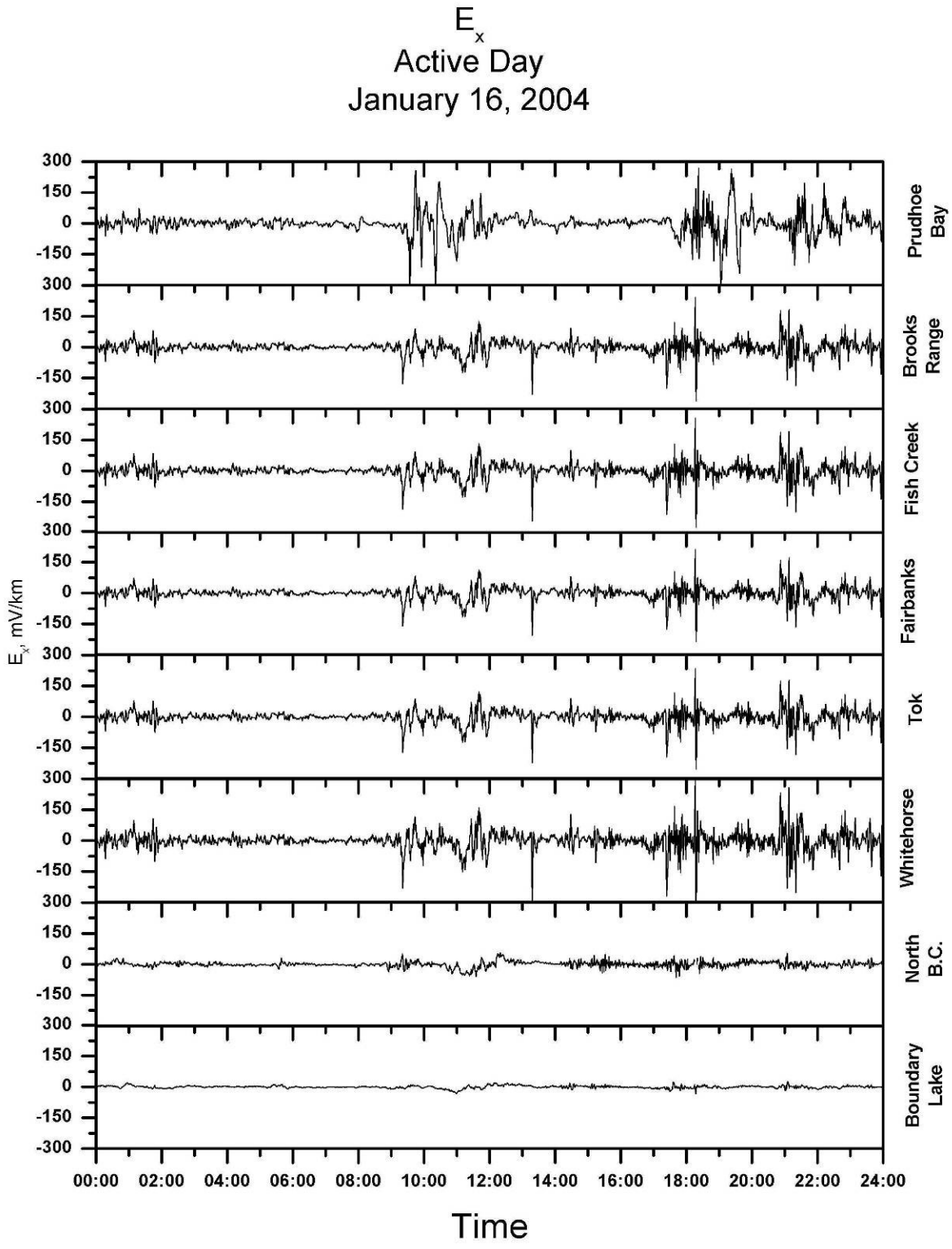

Figure 4.8. Northward electric field variations on an active day

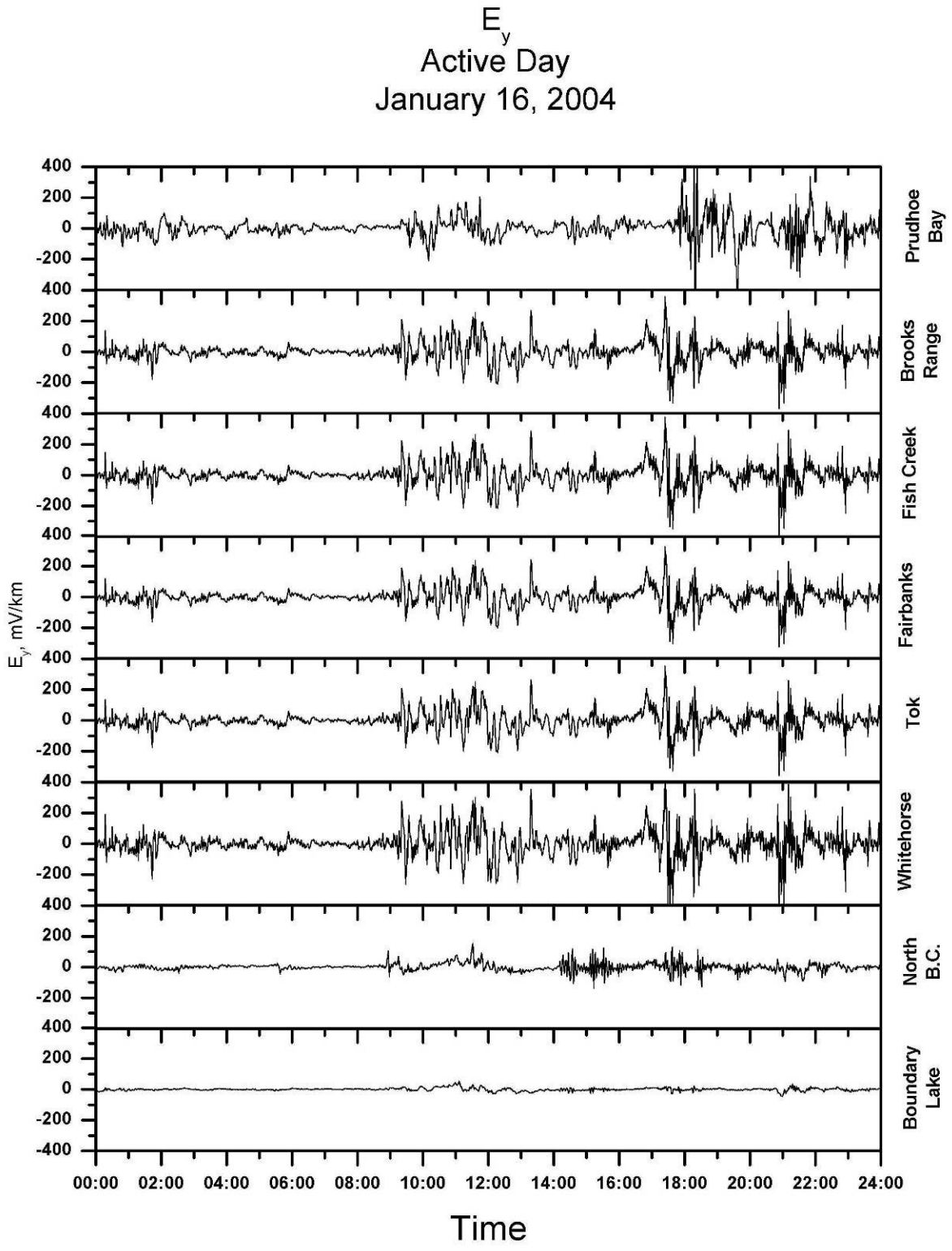

Figure 4.9. Eastward electric field variations on an active day

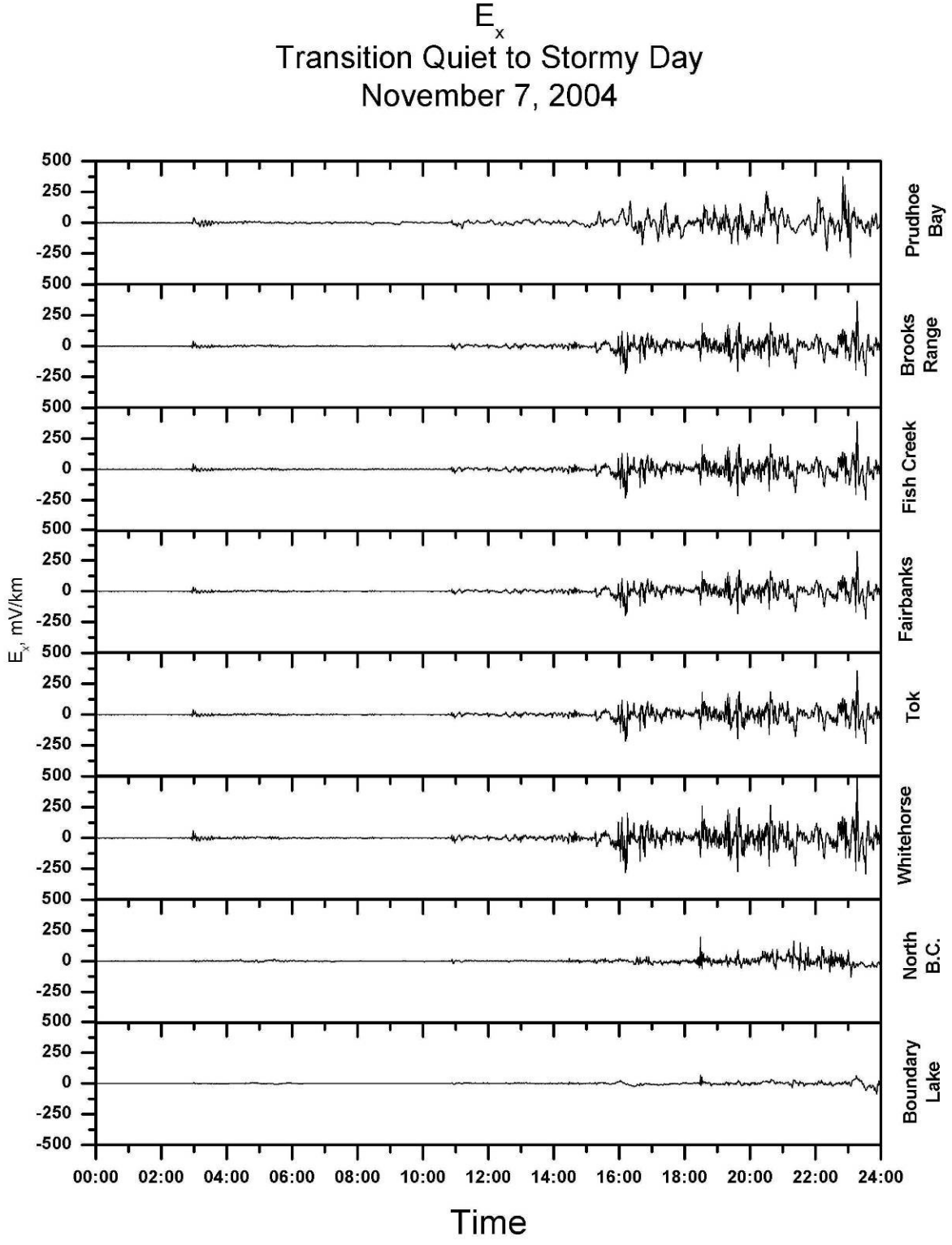

Figure 4.10. Northward electric field variations on a transition day

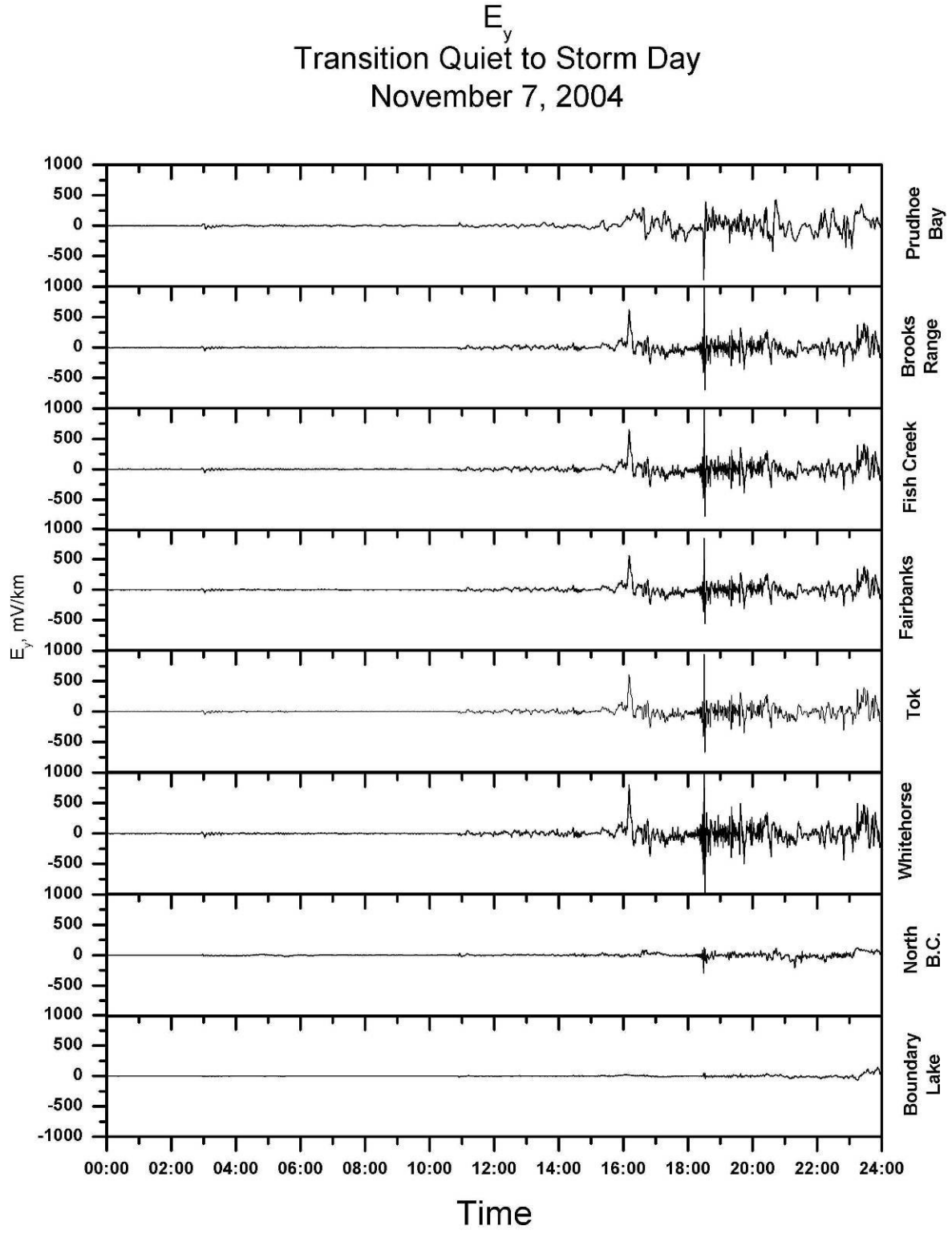

Figure 4.11. Eastward electric field variations on a transition day

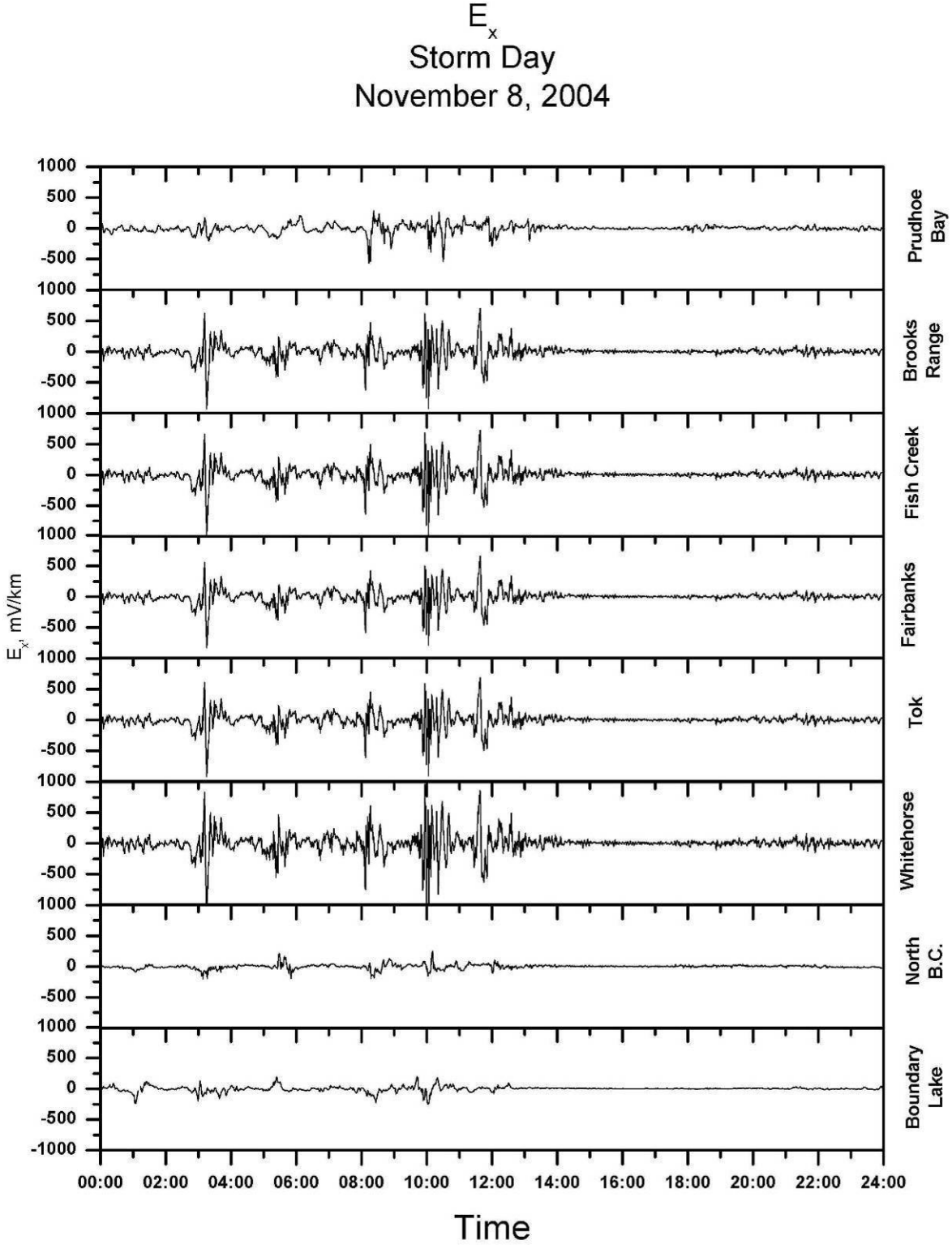

Figure 4.12. Northward electric field variations on a storm day

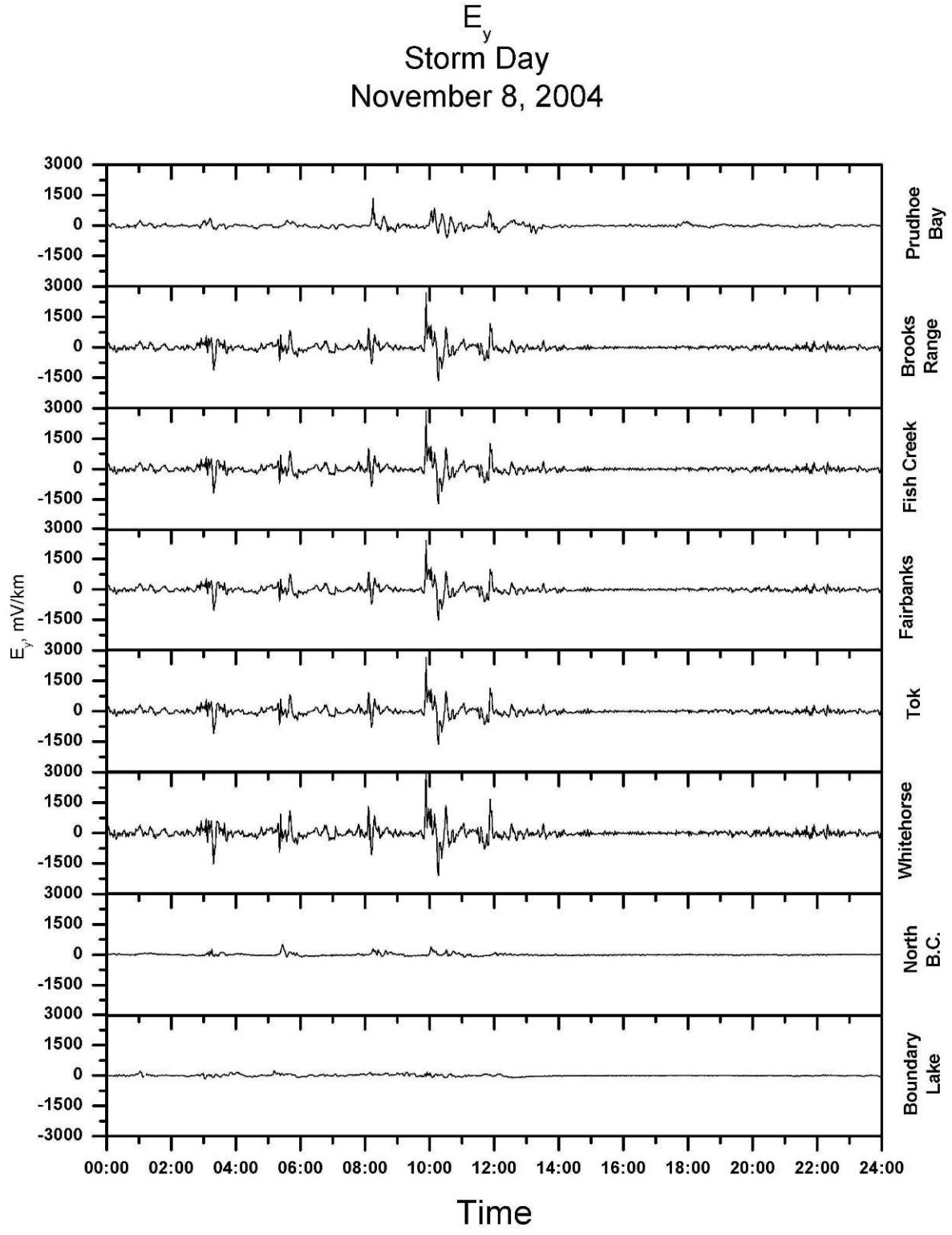

Figure 4.13. Eastward electric field variations on a storm day

It can be seen that the amplitude of geo-electric field fluctuations ranges from less than 20 mV/km on quiet day to above 3 V/km during an intense geomagnetic storm.

It should also be noted that though the electric field may possess similar characteristics for a given day, it can be quite different quantitatively. This is due not only to a differing geomagnetic field in each area but also the areas' respective earth resistivity models.

On quieter days it appears areas located in the auroral zone have more disturbed fields, as is evidenced by comparing Zone 1 and the other Alaskan areas with those of lower latitude in Figures 4.4 – 4.7.

The active and storm days (Figures 4.8 – 4.13) show Zones 2-6 having much greater telluric field variations due both to local geomagnetic field variations and also the earth resistivity characteristics.

The E_x and E_y components of the geo-electric field are later used to produce the variations of the geo-electric field in the direction of the pipeline and to serve as input to the pipeline model for PSP calculations.

4.5. Indices of Telluric Activity

In order to get a statistical description of the levels of telluric activity it is necessary to first establish descriptive indices, as was done previously in the analysis of geomagnetic activity.

To give the most general characteristics of telluric currents and geo-electric field, we establish two types of the indices. The first is a measure of extreme values: the maximum amplitude of the geo-electric field in one hour (Hourly Maximum Amplitude, HMA). The second index characterizes the distribution of the fluctuations in one hour: the hourly standard deviation of the geo-electric field (Hourly Standard Deviation, HSD).

As was done for geomagnetic activity, we establish telluric activity levels by examining the 95% occurrence levels for all the areas, as well as a low latitude area. Here we use the HMA of the y component of the geo-electric field, as this is produced by the geomagnetic field x component used for our geomagnetic index, HRX (the geomagnetic and geo-electric fields are orthogonal). We take the 95% occurrence rates for the HMA of E_y for our sample year, 2004, and use it to get the telluric activity indices (Figure 4.14).

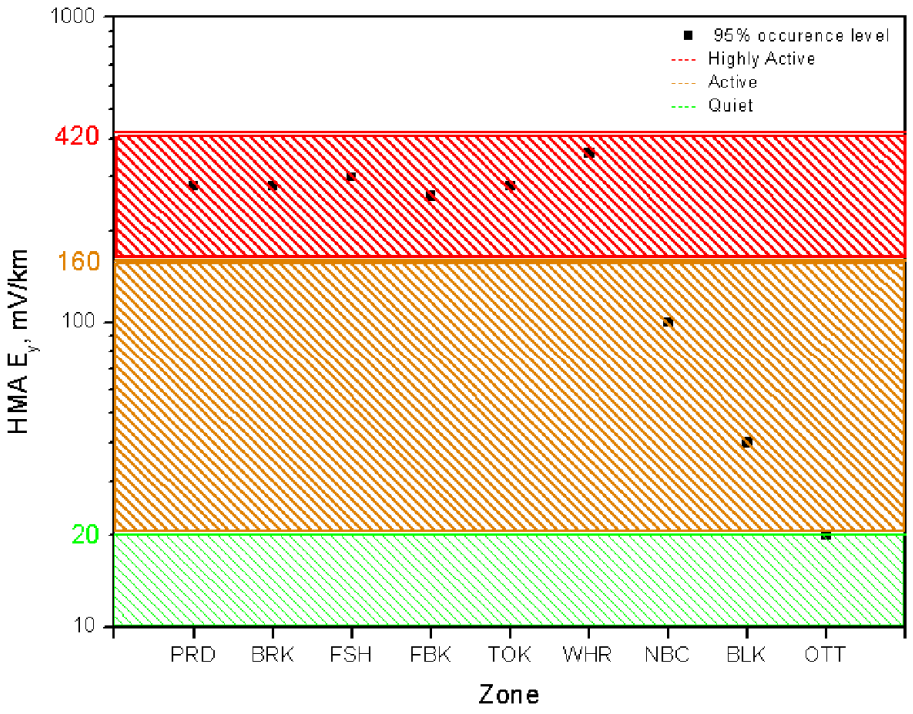

Figure 4.14. Activity indices derived from the 95% occurrence levels for E_y in 2004

It can be seen that the geo-electric activity levels are 20 mV/km (low activity), 160 mV/km (active) and 420 mV/km (highly active). Considering these 3 activity levels allows us to compare the zones across 30 years in terms telluric activity.

4.6 Statistical Properties of the Geo-electric Field Variations

Applying the derived levels to the calculated field values for the entire 30 year time period allows a statistical examination of the activity levels in each zone (Figure 4.15). We consider the number of hours that each activity level is exceeded as a percentage of the total number of hours for the whole time period. Here we consider the Hourly Maximum Amplitude (HMA) of E_y, the geoelectric field directed eastward.

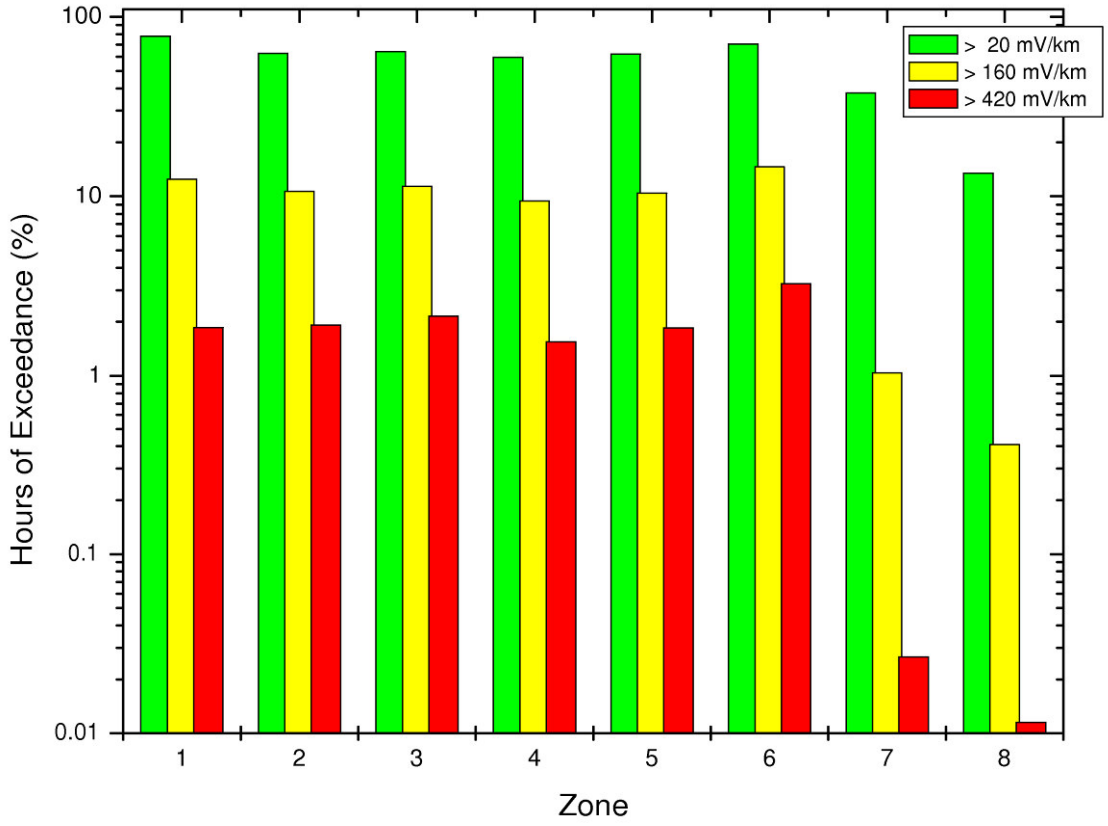

Figure 4.15. Percentage of hours exceeding activity indices for each zone for the entire time period (1975-2007)

Here we can see that the two southernmost zones are the least active, having the smallest percentages of hours exceeding all three of the activity indices. The activity in Zone 6 is the highest, exceeding 420 mV/km ~3% of the time.

The same values on a year-by-year basis are presented in Figure 4.16 on the following page. An examination of the plots again shows the southernmost zones having the smallest percentages of hours exceeding all three indices of activity. The remaining zones values appear similar over the time period, though the geo-electric activity in Zone 1 exceeds the quiet level more than in the other zones, almost constantly for all years. The telluric activity in Zones 2-6 is the highest, exceeding the highly active index for the greatest number of hours, with values ranging from 5-10% for many of the years.

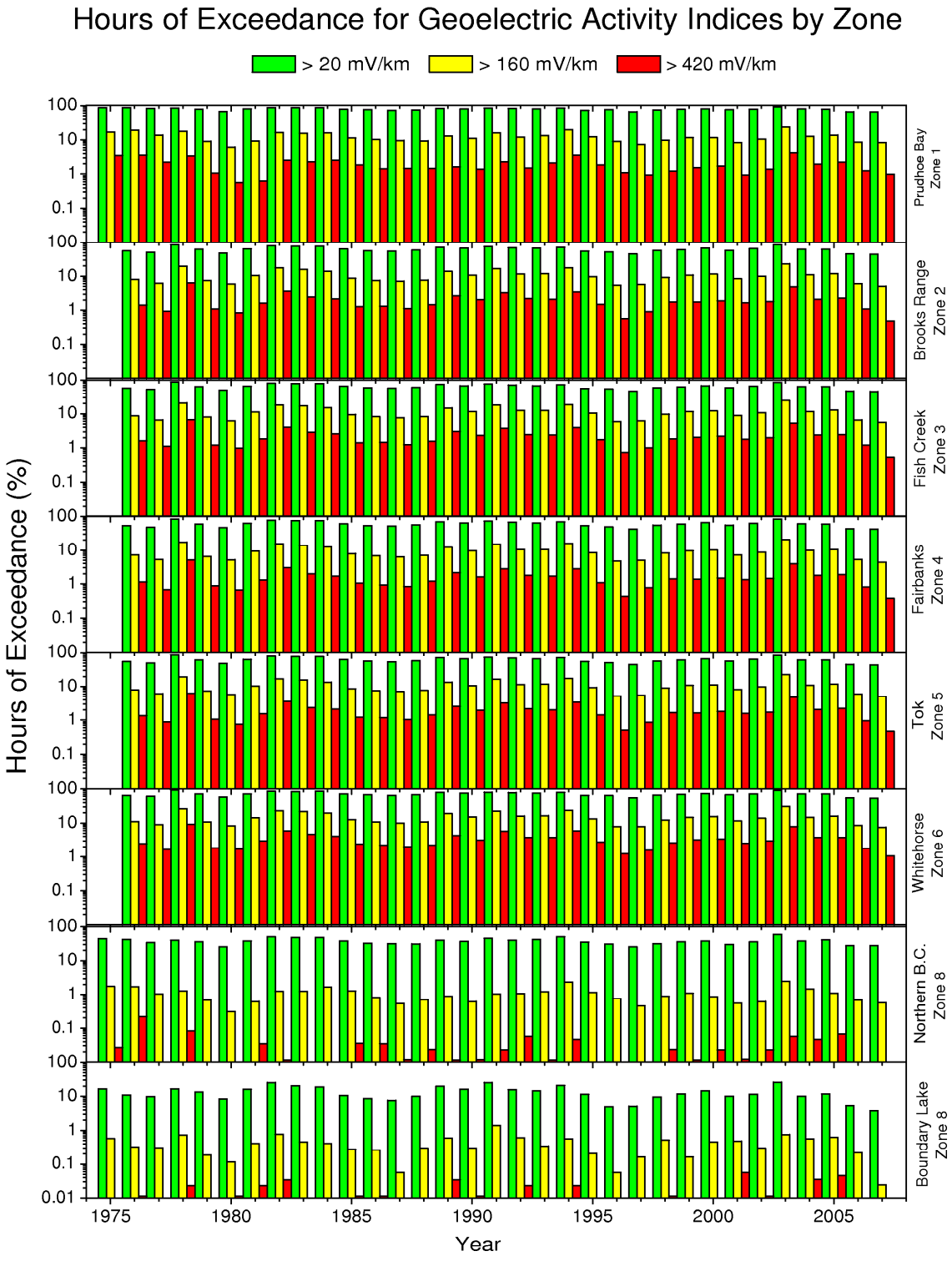

Figure 4.16. Percentage of hours exceeding geo-electric activity indices by year

4.7 Long-Term (Solar Cycle) Variations

Previous analysis of telluric activity dealt with the year 2004 as a representative year in terms of typical geomagnetic activity. Here we extend our analysis to the entire time period considered as well as the most active year (2003) and the year of the lowest activity (1996) as defined by our representative geomagnetic observatory of the auroral area, Yellowknife. These two years occur close to the last solar maximum and minimum, respectively.

Looking at Figure 4.17, it can be seen that Zone 6 experiences significantly greater telluric activity than the other zones, both in terms of maximum amplitudes and minute to minute variations. The southernmost zones experience the least amount of telluric activity and are clearly distinct from the others. Of the remaining zones, Zone 1 experiences the least levels of activity and variability.

This is also seen in Figures 4.18 - 4.19, which depict the hours of exceedance and number of hours of different geo-electric activity levels for the most and least active years. Note again that Zone 1's activity levels are large comparatively during the quiet year, but that the reverse is true during the most active year. Zone 6 experiences the largest maximum amplitudes and levels of variability for all cases, and Zones 7 & 8 the lowest.

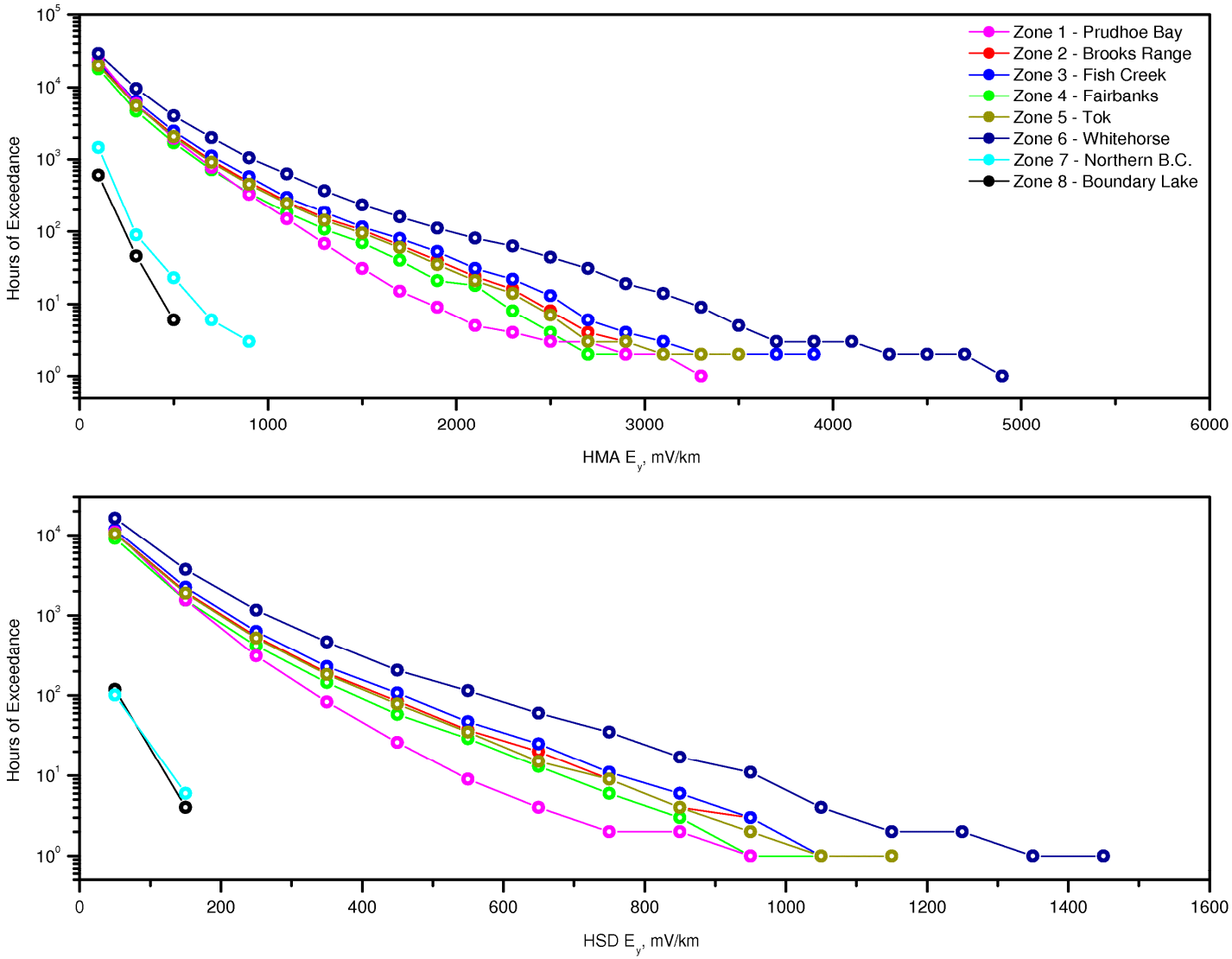

Figure 4.17. Statistical characteristics of the telluric activity indices HMA (top) and HSD (bottom) for the time period 1975-2007.

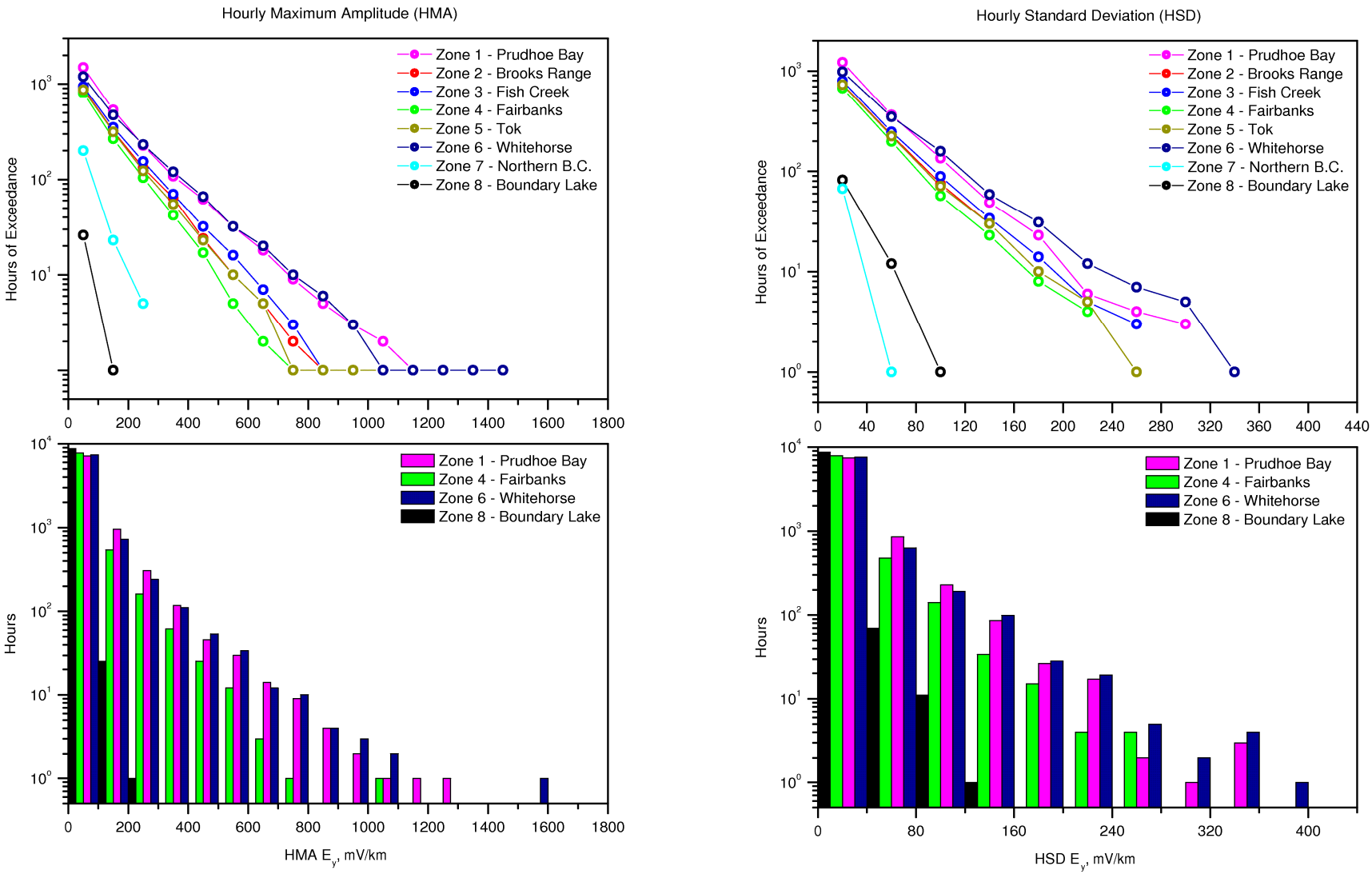

Figure 4.18. Exceedance of activity levels (top) and histograms of activity indices (bottom) for Solar MinimumYear 1996.

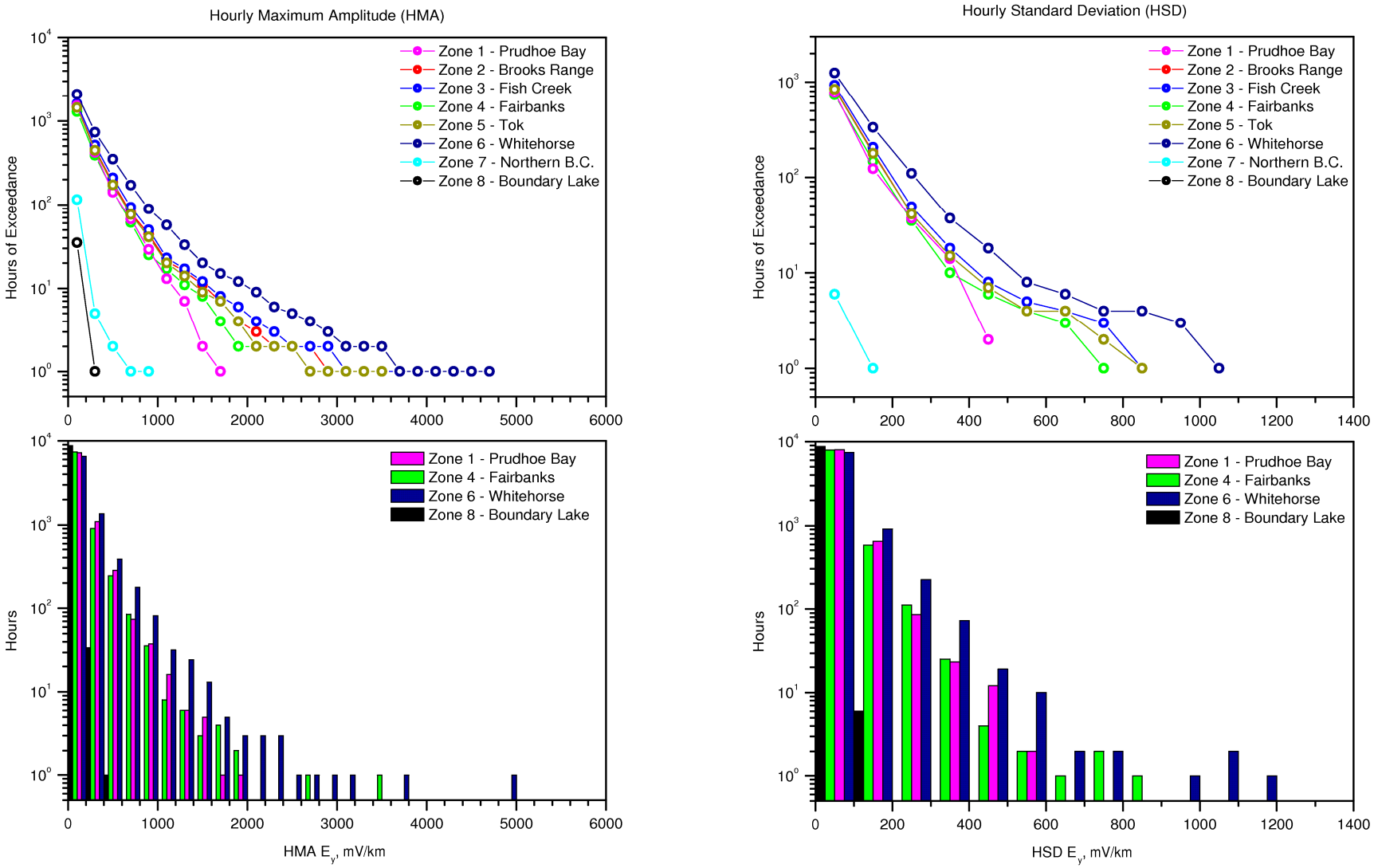

Figure 4.19. Exceedance of activity levels (top) and histograms of activity indices (bottom) for Solar Maximum Year 2003.

4.8. Possible Application to Cathodic Protection Design

After finishing the electromagnetic environment assessment, the next step should be the assessment of the PSP variations. Although it is not the purpose of the report, the simple example of how the statistical estimation of PSP variations can be made, is as follows.

The effect of electric fields induced in pipelines can be modelled using distributed-source transmission line (DSTL) theory [Boteler and Seager, 1998]. This was first used for modelling AC induction in pipelines and was subsequently applied to geomagnetic induction in pipelines. In the DSTL approach the pipeline is represented by a transmission line with series impedance, *Z*, given by the resistance of the pipeline steel and a parallel conductance, *Y*, given by the conductance through the pipeline coating. The induced electric field is represented by voltage sources distributed along the transmission line (Figure 4.20). The modelling can include multiple pipeline sections connected together. Each pipeline section can have different material characteristics, pipeline direction and size of electric field. This enables model claculations to be made for realistic pipelines including features such as bends, insulating flanges and ground connections.

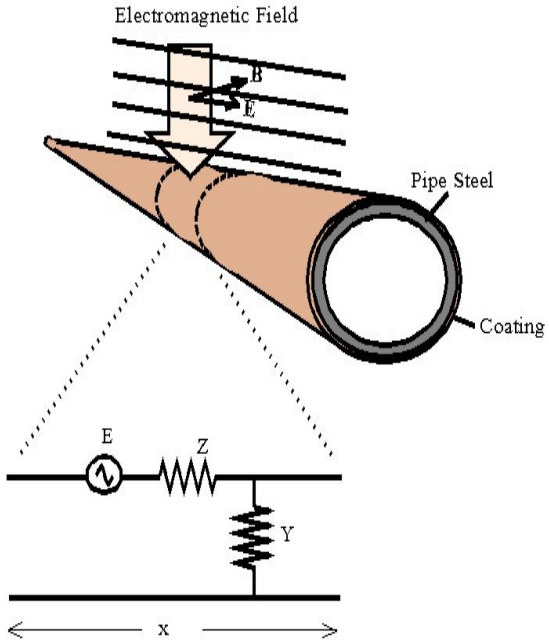

Figure 4.20 Transmission line model of pipeline including distributed voltage sources representing induced electric field.

Expression of the PSP variations for the section of the pipeline with uniform induced electric field has the form [Trichtchenko and Boteler, 2002]

$$PSP = \frac{E_p}{\gamma}(A_p e^{-\gamma(x-x_1)} - B_p e^{-\gamma(x_2-x)}) \qquad (4.9)$$

where x_1 and x_2 are the positions of the ends of the specific section of pipeline, A_p and B_p are constants dependent on the boundary conditions at the ends of the pipeline, where

$Z_c = \sqrt{Z/Y}$

is the characteristic impedance, γ is the propagation constant along the pipeline, defined as

$\gamma = \sqrt{ZY}$

Y is the parallel admittance (coating conductance to ground) and Z is series impedance per unit length (resistance of the pipeline steel).

Assuming the pipeline is "electrically long", i.e. longer than $1/\gamma$, and is running in the east-west direction (i.e. $E_p=E_y$), the terminating impedances are the same at both ends and equals Z_T, for

any end of the pipeline (at $x=x_1$ or $x=x_2$), formula (4.9) can be re-written as:

$$PSP_T = \frac{E_y Z_T}{\gamma(Z_c + Z_T)} \tag{4.10}$$

Using values for pipelines parameters as $1/\gamma$=60 km, Z_c=1.67 Ohms, Z_T =0.1 Ohms, (4.10) will become

$$PSP_T(mV) = 3.4(km) \cdot E_y(mV/km) \tag{4.11}$$

Thus, now Fig 4.15 can present the statistics of the hourly maximum PSP with following changes: the low level of telluric activity of 20 mV/km is equivalent to hourly maximum PSP of 0.068 V; medium level of 160mV/km is equivalent to 0.544 V and high level of 420 mV/km is equivalent to1.428 V.

It can be now estimated, that if pipeline has a life time is 60 years, then in "active" zone PSP will exceed 544 mV during10% of this time, i.e. 6 years.

4.7. Conclusions

This report shows the example of the electromagnetic environment assessment for northern area, particular for Alaska Highway region. The analysis of more than 30 years of data from geomagnetic observatories in Alaska and Northern Canada shows that geomagnetic activity in the area of proposed pipeline is 80% higher than in southern locations. Thus, estimation of telluric activity in the area has been done to further clarify the effects the effects which might be not significant in lower latitudes. In order to do that, telluric activity indices and levels were statistically established. Results of analysis show that as in the case of the geomagnetic activity, 80% of the time telluric activity in the pipeline area is above "normal" level. In regard to PSP evaluations, the simplified approach shows how developed assessment can be used for estimation of PSP variations for design considerations.

Proper estimation of the telluric current effects on pipelines corrosion protection system will improve the design considerations for new pipelines in the Northern areas and operations of the corrosion protection systems for existing pipelines.

References:

1. Boteler, D. H. and Seager, W.H., Telluric Currents: A meeting of Theory and Observations, Corrosion, 54, 751-755, 1998
2. L. Trichtchenko, D.H. Boteler, "Modeling of Geomagnetic Induction in Pipelines", Annales Geophysicae, 20 (2002), pp. 1063-1072.
3. Press, W.H., Vetterling, W.T., Teukolsky, S.A., & Flannery B.P. (1992). *Numerical Recipes in Fortran 77: The Art of Scientific Computing (2nd ed.)*. New York: Cambridge University Press.
4. Weaver, J.T., (1994). *Mathematical Methods for Geo-electromagnetic Induction.* Toronto: John Wiley & Sons Inc.